RHO/MRTF PATHWAY SIGNALING AND SMALL-MOLECULE INHIBITOR DEVELOPMENT IN SYSTEMIC SCLEROSIS AND METASTATIC MELANOMA

by

Andrew J. Haak

A dissertation submitted in partial fulfillment
of the requirements for the degree of
Doctor of Philosophy
(Pharmacology)
in the University of Michigan
2015

Doctoral Committee:

Professor Richard R. Neubig, Co-Chair
Professor Paul F. Hollenberg, Co-Chair
Professor Scott D. Larsen
Professor Elizabeth Lawlor
Professor John Tesmer

To my mother and father, for always supporting me

ACKNOWLEDGMENTS

I would like to first acknowledge and thank my mentor, Dr. Rick Neubig for his insight and guidance and for allowing creativity to drive the direction of my research. I would also like to thank the other members of my committee, Drs. Paul Hollenberg, Scott Larsen, Beth Lawlor, and John Tesmer, for their mentorship and support. Specifically, I would like to acknowledge Dr. Hollenberg for stepping into the role of co-chair of my thesis committee. For training and skills I developed during my rotations in their labs, I would like to thank Dr. John Tesmer and Dr. Beth Lawlor. So much of my work was dependent on close collaboration from many labs. I would like to thank Dr. Scott Larsen and members of his lab specifically, Jessica Bell and Kim Hutchings for designing and synthesizing CCG-203971, along with hundreds of other analogs, which didn't make it into the spotlight. Through this collaboration, I have gained a perspective and respect for medicinal chemistry. I would like to thank Dr. Beth Lawlor and members of her lab specifically, Merlin Airik and Melanie Krook for their role in the melanoma work, especially the *in vivo* metastasis study. I would also like to thank Dr. Monique Verhaegen for her support and supplying us with the metastatic melanoma cells. I would like to thank the scleroderma research group from The University of Michigan department of Rheumatology including, Drs. David Fox, Dinesh Khanna, Eliza Tsou, as well as Phillip Campbell, Jeffrey Ruth, and Asif Amin, for supplying cells, carrying out *in vivo* experiments, and their insight into fibrosis. I would also like to thank Dr. Peter Higgins and members of his lab, Laura Johnson and Eva Rodansky for their work in intestinal fibrosis.

I would like to thank Dr. Stephanie Watts (Michigan State University, East Lansing, MI) for her training and reagents in immunohistochemistry, which brought light to our melanoma metastasis study. I would like to thank former and current members of the Neubig lab for their friendship and support over the years, including Benita Sjogren, Sue Wade, Raelene Van Noord, Levi Blazer, Andrew Storaska, Jason Kehrl, Sergio Parra, Erika Lisabeth, Hoa Phan, Sean Misek, Sam Olson, and Jeff Leipprandt. I would like to thank the Michigan State Assay Development & Drug Repurposing Core (ADDRC), especially Dr. Thomas Dexheimer for initial work in developing high-throughput phenotype assays. I would like to thank the friends I made while working at both the University of Michigan Department of Pharmacology and Michigan State University Department of Pharmacology and Toxocology, without camaraderie, science would just be work.

I would like to thank my parents, Harlan and Pam Haak, for their constant support and encouragement not just during graduate school, but my whole life. I would also like to thank my brother, Dan Haak for keeping me grounded, even when science and results from experiments feel like the center of the universe. Lastly, I would like to thank my wife, Karla Frohmader for inspiring my creativity and always believing in me.

TABLE OF CONTENTS

DEDICATION……..……..ii

ACKNOWLEDGEMENTS…….……iii

LIST OF FIGURES……..……..viii

LIST OF ABBREVIATIONS…….…….xi

CHAPTER I 1

INTRODUCTION 1

Fibroblast to myofibroblast: A Target Transition for Treating Tissue Fibrosis 1

Profibrotic Signaling Pathways Converge onto Rho GTPases 5

MRTF/SRF Transcription in Cancer Metastasis 13

Targeting Rho GTPase/MRTF-Regulated Gene Transcription 15

My Work 17

References 20

CHAPTER II 29

THE ROLE OF CTGF AND ET-1 IN TGF-BETA STIMULATED ACTIN STRESS FIBERS AND RHO-KINASE DEPENDENT TRANSCRIPTION OF PROFIBROTIC GENES ACTA2 AND COL1A2 29

Abstract 29

Introduction 31

Materials and Methods 34

Results 37

Discussion 54

References 59

CHAPTER III 63

TARGETING THE MYOFIBROBLAST GENETIC SWITCH: INHIBITORS OF MRTF/SRF-REGULATED GENE TRANSCRIPTION PREVENT FIBROSIS IN A MURINE MODEL OF SKIN INJURY 63

Abstract 63

Introduction 64

Materials and Methods 67

Results 71

Discussion 82

References 85

CHAPTER IV 90

PHARMACOLOGICAL INHIBITION OF MYOCARDIN-RELATED TRANSCRIPTION FACTOR PATHWAY BLOCKS LUNG METASTASIS OF RHOC OVEREXPRESSING MELANOMA 90

Abstract 90

Introduction 92

Materials and Methods 94

Results 100

Discussion 113

References 117

CHAPTER V 123

CONCLUSIONS AND FUTURE DIRECTIONS 123

References 132

LIST OF FIGURES

Figure. 1-1. The fibroblast to myofibroblast transition requires MRTF/SRF gene transcription... 4

Figure. 1-2. Rho GTPase signaling pathway represent a convergence point for targeting fibrosis. 6

Figure 2-1. TGFβ stimulated F-actin stress fibers are dependent on Rho-kinase and de novo protein synthesis..... 38

Figure 2-2. LPA stimulated stress fibers are independent of *de novo* protein synthesis. 40

Figure 2-3. TGFβ activates delayed MRTF/SRF regulated transcription. 42

Figure 2-4. Kinetic profile of profibrotic gene transcription following TGFβ and LPA treatment. 45

Figure. 2-5. Rho kinase inhibitor blocks TGFβ-induced delayed expression of MRTF target genes COL1A2 and ACT2..... 48

Figure. 2-6. LPA synthesis and signaling following TGFβ..... 49

Figure. 2-7. CTGF and ET-1 stimulate actin stress fibers and MRTF/SRF activity. 50

Figure. 2-8. CTGF and ET-1 signaling is essential for TGFβ induced F-actin stress fibers and MRTF/SRF gene transcription. 52

Figure. 2-9. CTGF neutralizing antibody and endothelin antagonist CI 1020 do not inhibit MRTF/SRF activity in the absence of TGFβ. 53

Figure. 2-10. Current model of TGFβ stimulation of the Rho/MRTF pathway. 58

Figure 3-1. TGFβ and LPA activate MRTF/SRF and pro-fibrotic gene expression in 3T3 fibroblasts via a Rho/MRTF-dependent manner. 73

Figure. 3-2. The Rho/MRTF pathway inhibitor CCG-203971 prevents pro-fibrotic gene expression. 74

Figure. 3-3. SSc patient dermal fibroblasts show increased expression of fibrosis markers/MRTF target genes which are inhibited by CCG-203971. 75

Figure. 3-4. Scleroderma dermal fibroblasts proliferate faster than normal cells and this is inhibited by CCG-203971. 77

Figure. 3-5. CCG-203971 modulates myofibroblast transition of dermal fibroblasts. 78

Figure. 3-6. CCG-203971 prevents bleomycin-induced fibrosis *in vivo*. 81

Figure 4-1. Using cell-based models of metastasis the melanoma cells separate into aggressive and nonaggressive groups. 101

Figure. 4-2. Melanoma cell line panel migration and proliferation. 102

Figure. 4-3. Aggressive melanomas selectively overexpress RhoC but not RhoA. 104

Figure. 4-4. MRTF-A localization and activity is increased with F-actin stress fiber formation in aggressive melanoma cells. 106

Figure. 4-5. Regulation of MRTF-A localization in serum-starved melanomas is determined by actin dynamics. 107

Figure. 4-6. CCG-203971 regulates cellular localization and blocks MRTF target gene expression. 109

Figure. 4-7. CCG-203971 inhibits cellular migration and invasion. 110

Figure. 4-8. Rho/MRTF pathway effect on experimental lung metastasis 112

LIST OF ABBREVIATIONS

ATP: adenosine triphosphate

ATX: autotaxin

cDNA: complementary DNA

CHX: cycloheximide

CTGF: connective tissue growth factor

CYR61: cysteine-rich angiogenic inducer 61

DMEM: Dulbecco's modified eagle medium

DMSO: dimethyl sulfoxide

ECM: extracellular matrix

ET-1: endothelin-1

FAK: focal adhesion kinase

FBS: fetal bovine serum

GDP: guanosine diphosphate

GEF: guanine nucleotide exchange factor

GFP: green fluorescent protein

GPCR: G-protein coupled receptor

GTP: guanosine triphosphate

IBC: inflammatory breast cancer

ILD: interstitial lung disease

IPF: idiopathic pulmonary fibrosis

LPA: lysophosphatidic acid

LPAR: lysophosphatidic acid receptor

MAPK: mitogen-activated protein kinase

mDia1: mouse diaphanous-related formin-1

MICAL-2: microtubule associated monoxygenase, calponin and LIM domain containing 2

mRNA: messenger RNA

MRTF: myocardin-related transcription factor

MYPT1: myosin phosphatase target subunit 1

PBS: phosphate-buffered saline

PDGF: platelet-derived growth factor

PFD: pirfenidone

qPCR: quantitative polymerase chain reaction

ROCK: Rho-associated, coiled-coil-containing protein kinase

RT: room temperature

SAR: structure-activity relationship

SEM: standard error of the mean

SRE: serum response element

SRF: serum response factor

SSc: systemic sclerosis

TGFβ: transforming growth factor beta

TGFβRI: transforming growth factor beta receptor type I

TGFβRII: transforming growth factor beta receptor type II

VEGF: vascular endothelial growth factor

α-SMA: alpha-smooth muscle actin

CHAPTER I

INTRODUCTION

Fibroblast to Myofibroblast: A Target Transition for Treating Tissue Fibrosis

Fibrosis is defined by excess deposition of extra-cellular matrix (ECM) for which the most commonly, identified components are collagen and fibronectin. This progressive injury often results in organ failure and death, targeting nearly any tissue in the body. Although specific diseases such as scleroderma (SSc), idiopathic pulmonary fibrosis (IPF) and Crohn's disease are relatively rare, when combined with the detrimental contribution of fibrosis in renal, liver, and cardiac disease, fibrotic diseases account for 45% of all deaths in the United States (1). Many of these diseases are categorized as autoimmune diseases and are a manifestation of both environmental and genetic triggers (2). Although there are many cell types that contribute to pathological fibrosis including invading immune cells, damaged epithelial layers, and dysfunctional endothelium, local tissue myofibroblasts are the recognized cellular conductors of fibrosis. This activated form of a fibroblast is induced by local conditions including mechanical stress, growth factors, adhesion proteins and cytokines. These highly contractile cells classically express alpha smooth muscle actin (α-SMA) and display increased migration and proliferation. During normal physiological events, fibroblasts become activated into myofibroblasts to promote wound healing; after epithelialization has occurred they are lost through apoptosis. In the case of scleroderma and IPF however, this specialized cell type has become resistant to apoptosis and

continues to stimulate fibrogenesis, even in the absence of an identifiable injury (3,4). Over the past decades, specific receptor systems which combinatorially induce myofibroblast transition have been identified (1). These include lysophosphatidic acid (LPA), endothelin 1 (ET-1), connective tissue growth factor (CTGF), transforming growth factor beta (TGFβ), and others. However only more recently has a downstream genetic program that regulates and maintains this stimulation been defined.

Rho GTPases are a sub-family of small GTP-binding proteins within the Ras super-family, which modulate the actin cytoskeleton. The best-studied members within this subfamily are Rac, Cdc42, and RhoA/C. Although each of these affect the cytoskeleton, their specific control of regions and cytoskeletal sub-structures classifies their biological role. Rac GTPases coordinate actin changes at the leading edge-projection called the lamellipodium. Further projections, which extend beyond the lamellipodia, called filopodia, are organized by Cdc42 (5). RhoA and RhoC are homologous proteins which regulate highly ordered actin filaments called stress fibers (6). Although these two proteins can display subtle differences in biological activity, they share similar characteristics. For the work presented here, unless otherwise specified "Rho" refers to both RhoA and RhoC. These small GTPases are often referred to as "molecular switches" where their activation is regulated through Rho guanine nucleotide exchange factors (GEFs) which directly bind Rho proteins allowing for exchange of GDP for GTP (7). In the GTP-bound, active state they are able to interact with downstream effector proteins. Two main effector proteins for Rho signaling are Rho-associated, coiled-coil containing protein kinase (ROCK) (8,9) and mouse diaphanous-related formin-1 (mDia1) (10). Mechanistically, mDia1 induces nucleation of F-actin filaments while ROCK phosphorylation modulates F-actin

stabilization though multiple downstream targets including myosin light chain phosphatase (MYPT1).

Recent analyses of the Rho GTPase signaling cascade have appreciated changes in gene expression induced by Rho activity and the serum response factor (SRF) transcription factor. A key regulatory mechanism of SRF-mediated gene transcription includes the myocardin related transcription co-factors (MRTFA/B) which are regulated by Rho. The N-terminal region of MRTFs contains a unique nuclear localization sequence (NLS) which is enveloped by G-actin binding motifs, RPxxxEL (RPEL) (11,12). When there is a surplus of G-actin monomers within the cytoplasm, the RPEL motifs bind to MRTF sequestering it away from the nucleus. Rho activation results in F-actin stress fiber formation, reducing the abundance of G-actin and exposing the nuclear localization sequence of MRTF. Trafficking MRTF into the nucleus is regulated through direct interaction with importin α/β nuclear import mechanisms (13). Nuclear accumulation of MRTF allows for interaction with SRF and induction of gene expression. Importantly, multiple target genes for MRTF/SRF are known drivers of fibrosis (14-18). Additionally, SRF-mediated gene transcription has been shown to be essential for myofibroblast differentiation (Fig.1-1) (19-21). As the identity of additional microenvironment triggers that activate myofibroblasts continues to increase, it raises the question as to which receptor future therapies should attempt to target.

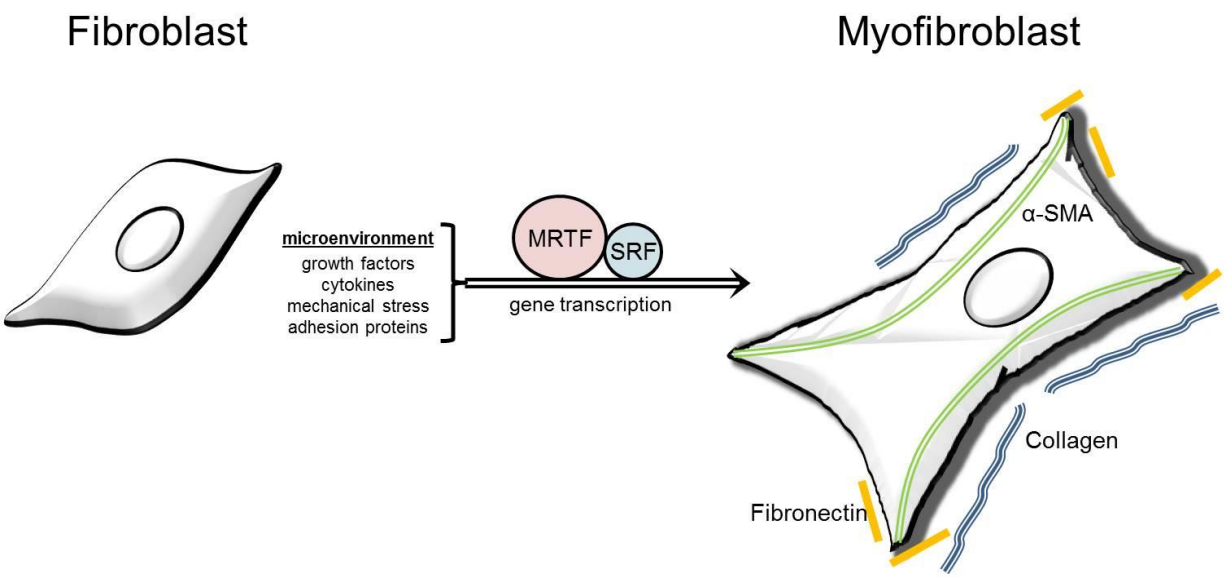

Figure. 1-1. The fibroblast to myofibroblast transition requires MRTF/SRF gene transcription.

Alpha- smooth muscle actin expressing myofibroblasts are responsible for the excess deposition of extracellular matrix components observed in pathological fibrosis. Most notably, collagen and fibronectin play important roles in the contractile and fibrous tissue. A variety of microenvironment conditions including growth factors, cytokines, mechanical stress and adhesion proteins combine to propagate the stimulatory response into MRTF/SRF regulated gene transcription and transition into a myofibroblast state. (Reproduced with permission from The American Journal of Physiology- Cell Physiology, for full citation see (22))

Profibrotic Signaling Pathways Converge onto Rho GTPases

In the past several decades, the specific microenvironment triggers, which stimulate fibroblast to myofibroblast transformation, have been partly resolved. These vary from pro-inflammatory cytokines such as transforming growth factor beta (TGFβ), to G-protein coupled receptor (GPCR) ligands like LPA, to components of the extracellular matrix such as CTGF or even the mechanical rigidity of the surrounding tissue itself (22-26). There is strong preclinical evidence suggesting that many of these pathways may provide opportunities for novel therapeutics. Less promising however, several clinical trials that target these individual pathways failed due to minimal efficacy. The focus here will be on how these multiple signaling systems appear to converge onto Rho GTPase and MRTF (Fig. 1-2). This evidence supports our overall approach to target downstream of the receptor, at the merging step in these varied pathways.

Inflammatory Cytokine TGFβ

In fibrotic disorders like scleroderma and IPF, multiple inflammatory cytokines are released into the affected tissue by invading immune cells, compromised epithelial and endothelial cells, or stimulated myofibroblasts (27-29). Transforming growth factor β (TGFβ) is the central profibrogenic cytokine that is an indispensible player in connective tissue homeostasis and is considered the "master cytokine" in fibrosis (30). The TGFβ superfamily comprises TGFβ1, 2, and 3 which are synthesized by a wide variety of cell types. Among them TGFβ1 is the most abundant and is the prototype of this family. TGFβ signaling occurs when TGFβ receptor II, which is constitutively active, trans-phosphorylates and forms a complex with the TGFβ-bound TGFβ receptor I.

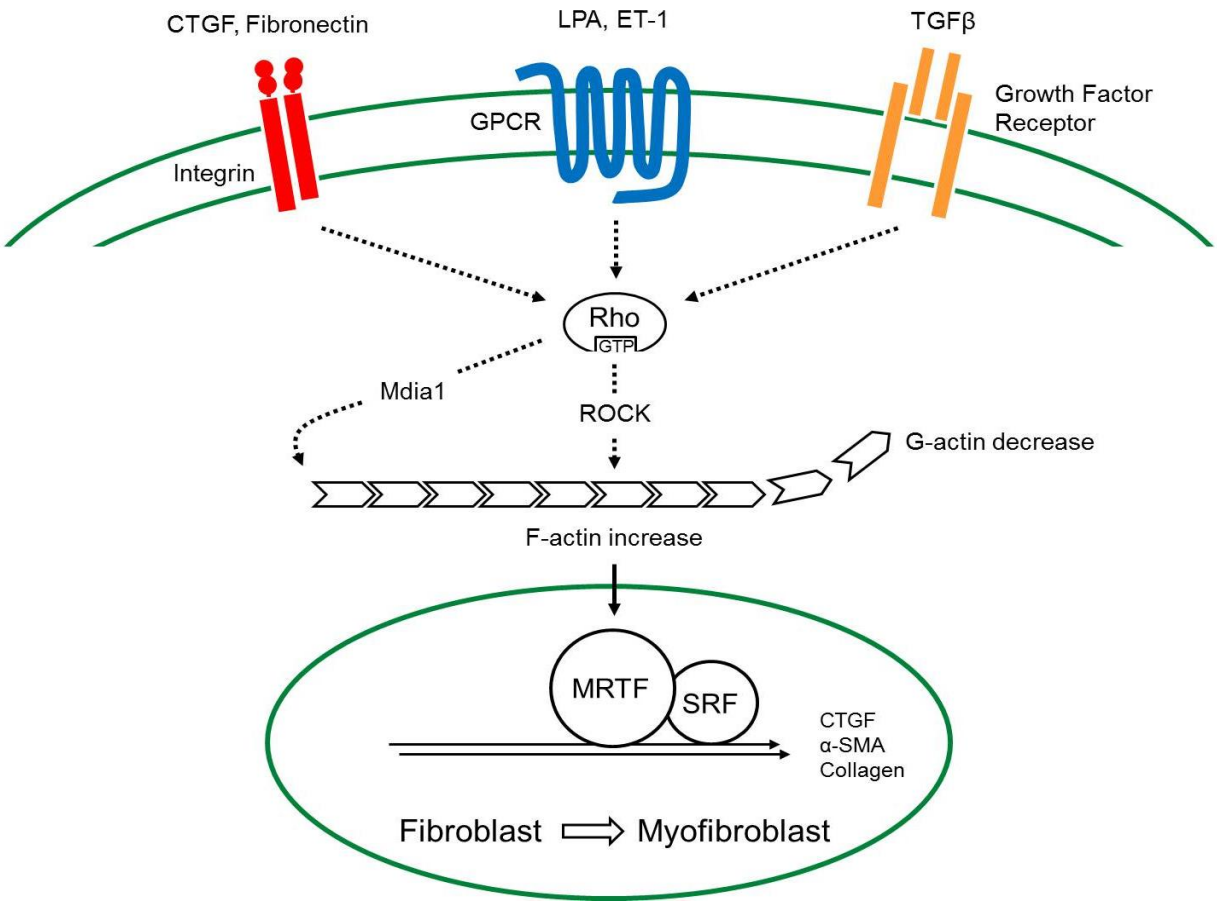

Figure. 1-2. Rho GTPase signaling pathway represent a convergence point for targeting fibrosis.

Many current drugs being developed for fibrotic diseases are targeting specific receptors known to be involved stimulating fibroblasts into myofibroblasts. Interestingly many of these specific receptor systems converge onto Rho small GTPase signaling. GTP bound active Rho can interact with downstream effector proteins, most notibly ROCK kinase and mDia1 which together initiate and stabilize actin stress fibers. This increase in F-actin and resulting decrease in G-actin monomers frees MRTF to translocate into the nucleus where it cooperates with SRF to induce gene transcription. Many MRTF/SRF target genes are known drivers of fibrosis including CTGF, α-SMA, and collagen; together this activation of gene transcription induces and maintains the activation of fibroblasts to myofibroblasts. (Reproduced with permission from The American Journal of Physiology- Cell Physiology, for full citation see (22))

Activated TGFβ receptor phosphorylates serine residues of cytoplasmic R-SMAD, a complex of SMAD2 and SMAD3. The two heterodimerize and bind to the co-SMAD, SMAD4, and the whole complex translocates across the nuclear membrane to interact with SMAD binding elements, recruiting co-activators, co-repressors, or transcription factors to modulate gene expression (29).

The role of TGFβ in fibrogenesis was demonstrated by Schultz et al (31) who showed that angiotensin II induced cardiac fibrosis in wild type mice but not in TGFβ1 null animals. Similar results were obtained in SMAD3 knockout mice, which were protected from bleomycin-induced skin and lung fibrosis and dimetheylnitrosamine-induced liver fibrosis (32-34). In addition, SMAD4 deficient mice were protected from unilateral ureteral obstruction-induced renal fibrosis (35). Based on these results, neutralizing antibodies to TGFβ have been evaluated in several clinical trials. Despite promising early studies, trials of two anti-TGFβ antibodies (CAT-192, TGFβ1; CAT-152, TGFβ2>TGFβ3) did not show clinical improvements in early diffuse cutaneous scleroderma (36).

Importantly, it has also been observed that TGFβ stimulation leads to Rho activation, however, unlike GPCR mechanisms such as LPA and ET-1 which have been well studied, and are described below, the pathway leading from TGFβ receptor activation to Rho signaling remains mostly unresolved. The formation of stress fibers following GPCR ligand stimulation occurs very rapidly while TGFβ induced stress fiber formation is delayed to around 18-24 hours following stimulation (37). This raised the possibility of an indirect mechanism such as SMAD 2/3-dependent transcriptional regulation of other Rho activators (37). Known TGFβ/Smad target genes which could induce this activation of Rho include CTGF (38), ET-1 (39), sphingosine

kinase-1 (40), or RhoGEFs; NET1 and H1/Lfc (41-43). This gap in knowledge connecting TGFβ to Rho signaling becomes the basis for my work in Chapter II of this thesis.

GPCR Ligands

LPA and endothelin represent two families of profibrotic GPCR ligands. By acting through specific G-protein-coupled receptors, LPA, a phospholipid that is produced by the enzyme autotaxin, mediates many diverse cellular responses. There are currently 6 recognized receptors that signal in response to LPA, designated as LPA1-6 (44). Among them, a key role for LPA1 has been demonstrated in the development of tissue fibrosis in a variety of organ systems. LPA1 acts through three distinct families of G proteins: $G\alpha_{i/o}$, $G\alpha_{q/11}$, and $G\alpha_{12/13}$ (45,46). The involvement of LPA signaling in fibrosis has been demonstrated in various animal models of skin (47), lung (48), kidney (49), peritoneal fibrosis (50), and liver (51). Bleomycin-induced dermal fibrosis, characterized by increased dermal thickness and accumulation of collagen, is absent in LPA1 knockout mice (47). In addition, pharmacological antagonism of LPA1 significantly attenuates bleomycin-induced skin fibrosis in both prevention and therapeutic treatment regimens, as well as preventing bleomycin-induced pulmonary fibrosis (52). Several LPA receptor antagonists have entered clinical trials. The LPA1 antagonist AM152 (now termed BMS-986020) was safe and well-tolerated in healthy subjects (53) and is now in phase II trials to evaluate its safety and efficacy in IPF patients (ClinicalTrials.gov NCT01766817). An LPA1/3 dual antagonist, SAR100842, is currently in a phase II clinical trial to evaluate safety and tolerability in patients with early diffuse cutaneous SSc (ClinicalTrials.gov NCT01651143).

There are 3 isoforms of endothelins (ET), ET-1, 2, and 3. Among them, ET-1 is the predominant isoform in humans and it acts as a potent vasoconstrictor. It also participates in angiogenesis, cell survival, epithelial-to-mesenchymal transition (EMT), and tumor-related activities (54). ET-1 is produced by a number of cell types including endothelial cells, epithelial cells, smooth muscle cells, fibroblasts, macrophages, and cardiomyocytes, and its expression can be induced by various stimuli such as angiotensin II and TGFβ (55). ETs mediate their physiological effects by binding to two seven-transmembrane G protein-coupled receptors, ET_A and ET_B. The ET_A receptor is ET-1 selective while ET_B has equal affinity for all three ET isoforms. While ET_A appears to be profibrotic, ET_B has been shown to be anti-proliferative for myofibroblasts (56-58).

The role of ET-1 in fibrosis has been studied extensively. In healthy lung fibroblasts, ET-1 is able to induce ECM and α-SMA synthesis as well as contractile activity (59,60). The role of ET-1 in promoting fibrogenesis is further demonstrated using transgenic mice with overexpression of human ET-1 (61). These animals spontaneously develop progressive pulmonary fibrosis and lung inflammation. Blockade of both ET_A and ET_B receptors suppresses TGFβ- or bleomycin-induced fibrosis *in vivo* (62). ET-1 plays significant roles in the pathophysiology of various fibrosis diseases. ET-1 is overexpressed in SSc dermal fibroblasts (63) and expression of ET-1 in patient lung tissue correlates with disease severity in diffuse SSc patients (64). Enhanced ET-1 expression and binding is observed in lung fibroblasts obtained from SSc-interstitial lung disease (ILD) patients and blocking the ET-1 pathway significantly reduces α-SMA levels in these cells (60).

Concerning LPA and endothelin receptors, the G-protein mediated mechanisms leading to activation of Rho have been well mapped. Most notably, receptors which couple to $G_{12/13}$ proteins directly activate a family of three RhoGEFs: p115-RhoGEF, PDZ-RhoGEF, and leukemia-associated RhoGEF (65). These GEFs then directly interact with members of the Rho GTPase family, most notably RhoA and RhoC, inducing exchange of GDP for GTP. This facilitates interaction with downstream effector proteins, which are essential for profibrotic phenotypes. LPA and endothelin receptors can couple to both $G_{12/13}$ and $G_{q/11}$ (66,67). The formation of stress fibers and activation of ROCK following ET-1 stimulation in vitro is likely mediated through both $G_{12/13}$ and $G_{q/11}$ family mechanisms (68). Although $G_{12/13}$ subunits have classically been identified to activate Rho through the guanine exchange factors listed above, $G_{q/11}$ alpha subunits can also directly activate RhoA/C through stimulation of p63 RhoGEF (66,69).

Matricellular Protein CTGF

CTGF, also known as CCN2, is a matricellular protein that belongs to the ECM-associated signaling CCN family. It is involved in angiogenesis, tissue wound repair, ECM regulation, and cellular migration, adhesion, and proliferation (70). Under physiological conditions, CTGF is minimally expressed, but in fibrotic conditions, its expression is significantly elevated. CTGF functions by binding to various cell surface receptors, including integrins (71,72), cell surface heparan sulfate proteoglycans (72), low density lipoprotein receptor-related protein/alpha2-macroglobulin receptor (73), and the tyrosine kinase receptor TrkA (74). It also binds growth factors and ECM proteins such as vascular endothelial growth factor (VEGF) (75), TGFβ/bone morphogenetic proteins (76), and fibronectin (77). CTGF

expression is induced by a variety of extracellular stimuli such as TGFβ, PDGF, and ET-1, which all utilize a Rho/MRTF mechanism (78). CTGF appears to act as the downstream mediator of several of these pro-fibrogenic factors (78). In addition, it reciprocally induces a variety of cytokines such as TGFβ and VEGF, forming a positive feedback loop that induces more expression of CTGF. It also aids TGFβ in fibrogenesis and helps sustain fibrosis (79).

Overexpression of CTGF in fibroblasts promotes *in vivo* fibrosis in multiple organs while deletion of it in fibroblasts or smooth muscle cells greatly reduces bleomycin-induced skin fibrosis (80,81). In addition, inhibition of CTGF alleviates fibrosis in animal models of cardiac, liver, and kidney fibrosis (82-84). A humanized anti-CTGF antibody, FG-3019, has been evaluated in several clinical trials for diabetes and kidney disease and is well tolerated in these studies. Phase II trials of this approach in IPF (ClinicalTrial.gov NCT01890265) and liver fibrosis (ClinicalTrial.gov NCT01217632) are pending. STX-100, a monoclonal antibody targeting αvβ6 is also being evaluated in a phase II clinical trial for the treatment of patients with IPF (ClinicalTrial.gov NCT01371305).

CTGF may also function as a positive feedback mechanism in Rho signaling. In addition to being a transcriptional target of Rho/MRTF, CTGF has been shown to induce focal adhesion complexes and stress fibers through binding of integrin αvβ3 (85).

Cell Substrate Rigidity

Although traditional ligand-receptor signaling mechanisms have made up a bulk of cellular fibrosis research, mechanical signaling between the cell and its structural surroundings has also been recently identified as a driver of fibrogenesis. Along with being hyperproliferative

relative to normal fibroblasts, myofibroblasts are also highly contractile (86). Along with their excess deposition of ECM, myofibroblast contraction leads to the characteristic rigid tissue observed in IPF and scleroderma. Interestingly, the resulting stiff matrix environment also feeds back onto the myofibroblasts to further promote fibrogenesis (87,88). It has also been recognized that alterations in matrix stiffness modulate fibroblast morphology, proliferation, and cytokine signaling (89,90). This suggests that cell matrix stiffness could play a significant role in the initiation, progression, and stabilization of tissue fibrosis. To a large degree, integrins and focal adhesion complexes are the conductors for transmitting a signal from the ECM to the intracellular space (88). Integrins are heterodimeric transmembrane glycoproteins which consist of non–covalently associated α and β subunits. There are 18 α and 8 β subunits, with a total of 24 documented heterodimers with distinct specificities for different ECM components. A synthetic, small-molecule RGD peptidomimetic antagonist (CWHM 12), that potently inhibits αv-containing integrins, attenuates CCl_4-induced hepatic fibrosis (in both prevention and treatment models) (91). In addition to the αv integrins, other integrins also participate in promoting tissue fibrosis. Mice bearing specific depletion of fibroblast integrin β1 are resistant to bleomycin-induced skin fibrosis and have reduced collagen and α-SMA expression (92). Again, Rho GTPases are essential for stiff matrix and integrin induced fibrosis (93-95). Similar to TGFβ, integrin activation of Rho signaling has been described, but the exact mechanism has not been established. It is clear however, that fibronectin and CTGF stimulated integrin signaling results in a rapid formation of actin stress fibers and stimulation of the MAP kinase cascade, both of which required Rho activity (96).

MRTF/SRF Transcription in Cancer Metastasis

The classic identity of Rho GTPases revolves around their regulation of the actin cytoskeleton and cellular migration (97,98). Although the focus of my work has focused mostly on the role of Rho proteins in tissue fibrosis, much of the research on these signaling mediators has been related to their involvement in cancer initiation, progression, and especially metastasis (99-101). Melanoma is a malignant cancer of melanocytic cells that line the basal layer of the epidermis. Although melanoma is less common than other forms of skin cancer, it is much more dangerous, resulting in over 50,000 deaths globally each year (102). Melanoma is a prime example of how deaths arising from cancer are most commonly dependent on metastasis of the primary tumor to an alternative site in the body (103,104). Until very recently, therapeutic options for metastatic melanoma were very limited and lacked efficacy (105). Based on the prevalence of a common mutation observed in around 50% of human melanomas ($BRAF^{V600E}$), targeted therapeutics against mutant BRAF were designed, tested, and approved in 2011 (106). As research continues to push the efficacy of and reduce resistance to these targeted therapies, even under a best-case scenario these BRAF-targeted drugs will only benefit half of all melanoma patients. This presents a clear unmet, clinical need. Another complication with our current understanding of the genetic and phenotypic markers of melanoma is the lack of definition of determinants of aggressive metastatic melanoma relative to more benign and potentially responsive disease. In an effort to identify genes important for melanoma metastasis, Hynes et al, (107) compared gene expression patterns from highly metastatic B16F2 mouse melanoma cells to those of the parental non-invasive B16 cells. RhoC was found to be upregulated and essential for experimental metastasis (107). RhoC was also found to be overexpressed in aggressive inflammatory breast cancer (IBC) relative to non-IBC (108,109). To

functionally characterize the specific consequences of RhoC overexpression, researchers created genetic knockdowns of MRTF and SRF, in the metastatic B16F2 melanoma cells. In the absence of MRTF or SRF the metastatic potential of these cells was dramatically reduced in a mouse tail-vein injection study analyzing lung colonization (109). Interestingly, the *in vitro* proliferation and *in vivo* primary tumor growth were unaffected in the MRTF knockdowns cells but cellular migration and invasion were both reduced. These data suggest that the metastatic potential of Rho GTPases is actually driven by MRTF/SRF-regulated gene transcription rather than by a direct effect on the actin cytoskeleton itself. In my work here, I investigate activation of this pathway as a potential marker of aggressive, metastatic melanomas and also evaluate the efficacy of a small-molecule inhibitor of the Rho/MRTF pathway at blocking experimental metastasis.

Targeting Rho GTPase/MRTF-Regulated Gene Transcription

Although individual receptor systems like TGFβ and LPA are important to drive fibrosis, treating complex diseases like SSc and IPF may demand a multifaceted approach. Here we discuss the gene transcription mechanism (MRTF/SRF) downstream of Rho as an alternative target. The convergent role that Rho signaling plays in pathways downstream of LPA, ET-1, and TGFβ in fibrosis (Fig. 1-2), suggests that blocking this mechanism may provide greater efficacy. Despite the substantial body of work on Rho GTPases in cancer, its importance in fibrosis has only recently been recognized (21,110). At first glance, the GTPase itself appears to be the most logical target, however, developing potent and selective inhibitors of small GTPases offers multiple challenges. The most successful attempts have used virtual screening against the structural interface between RhoA and its GEFs. This approach has identified Rhosin and Y16, small molecule inhibitors which display high binding affinity and cellular activity in cancer models (111,112). These compounds have not yet been tested in fibrosis.

Instead of targeting the GTPase itself, most pharmaceutical development on this pathway has targeted the effector kinase, ROCK. ROCK is a ~160 kDa serine/threonine kinase which is, itself regulated by phosphorylation as well as by interaction with Rho GTPase. The two best studied inhibitors, fasudil and Y-27632 both bind the ATP site on the kinase enzymatic domain effectively inhibiting ROCK activity and both have shown actions in in vitro cardiovascular models and in cancer (113). Related to fibrosis, Y-27632 treatment of SSc patient-derived fibroblasts inhibits myofibroblast differentiation as well as collagen deposition (110). *In vivo* treatment with fasudil protected mice against experimental lung fibrosis (114). Interestingly, fasudil has been used in Japan to treat cerebral vasospasm for nearly twenty years and has a safe clinical profile (115). Currently, fasudil is being tested in clinical trials for pulmonary

hypertension (116) and Raynaud's phenomenon (NCT00498615) associated with SSc. While ROCK inhibitors may have greater efficacy than blocking individual receptors, the critical gene-transcription signals downstream of Rho are only partially blocked by Y-27632 (117), perhaps because mDia or other mechanisms can bypass ROCK to induce actin stress fibers and nuclear translocation of MRTF.

In our laboratory we identified CCG-1423, the first small molecule inhibitor of Rho/MRTF/SRF-regulated gene transcription by use of a SRE-luciferase reporter-based high-throughput screen. CCG-1423 was shown to inhibit LPA receptor-stimulated DNA synthesis, cell growth, cell survival, and Matrigel invasion in multiple cancer cell lines (117). CCG-1423, as well as other structurally related analogs, inhibits Rho/MRTF signaling downstream of Rho/ROCK and blocks MRTF nuclear accumulation, possibly through modulation of an intranuclear actin-binding protein MICAL-2 (124-127). However, it was recently reported that CCG-1423 may directly inhibit MRTF binding to importins (128). In pulmonary fibroblasts, CCG-1423 blocked TGF-β induced SRF and α-SMA expression independent of SMAD mediated signaling (129). In an *in vivo* chlorhexidine model of peritoneal fibrosis, CCG-1423 reduced collagen synthesis and CTGF expression (50). A new analog from this compound series, CCG-203971, blocked TGFβ and stiff-matrix-induced expression of profibrotic genes in human colonic fibroblasts (130). Taken together these data suggest that further exploration of targeting the Rho/MRTF/SRF transcriptional pathway is warranted as a potential new therapy for diseases of fibrosis.

My Work

Based on previous evidence supporting a major role for Rho GTPase mediated MRTF/SRF-regulated gene transcription in tissue fibrosis and cancer metastasis, the goal of my thesis work was twofold: 1.) Identify mechanisms in scleroderma and metastatic melanoma which drive this pathway in these diseases, and 2.) determine efficacy of our current lead small-molecule inhibitor of this pathway, CCG-203971, in preclinical models on these diseases. This work not only assessed the importance of Rho signaling in these diseases but it also identifies potential steps in the pathway that could be utilized for novel therapeutic approaches. The efficacy studies with CCG-203971, especially the *in vivo* models, support the continued development of these small-molecules.

In Chapter II, I focused on answering an imporant biological question identified earlier in this section, how does TGFβ activate Rho signaling, actin stress fiber formation, and MRTF/SRF-regulated gene transcription? The bulk of this work focused on two very robust and simple experimental readouts: F-actin staining assessed through fluorescence microscopy and MRTF/SRF luciferase reporter assays. Using NIH-3T3 fibroblasts we observed F-actin stress fibers (a hallmark of Rho GTPase activation) and MRTF activation with the luciferase reporter within three hours after TGFβ ligand treatment. The F-actin formation was dependent on ROCK activity and *de novo* protein synthesis. With this information, we next analyzed gene expression in primary human dermal fibroblasts following TGFβ treatment. Based on the delayed kinetics, and sensitivity to ROCK inhibition we identified COL1A1 (Collagen 1α1) and EDN1 (Endothelin 1) to be TGFβ/SMAD dependent and COL1A2 (Collagen 1α2) and ACTA2 (α-SMA) to be Rho/MRTF dependent. We also show that endothelin and CTGF both have the capacity to stimulate F-actin stress fibers and MRTF activity. Most interestingly, a neutralizing

antibody for CTGF and an endothelin receptor type A antagonist can together block TGFβ induced stress fibers and MRTF/SRF gene transcription.

In Chapter III, we began studies of CCG-203971 in models of scleroderma. Scleroderma patient-derived fibroblasts displayed increased expression of MRTF target genes (CTGF, ACTA2, and COL1A2) relative to normal healthy donor samples. CCG-203971 was able to reduce expression of these genes and selectively blocked proliferation of scleroderma patient fibroblasts without effecting fibroblasts from normal donors. CCG-203971 also inhibited TGFβ induced protein expression of α-SMA as well as constitutive α-SMA expression observed in the scleroderma patient derived fibroblasts. For an in vivo prevention model of scleroderma, we injected mice intradermally with bleomycin while treating mice intraperitoneally with CCG-203971. The compound-treated mice showed decreased dermal layer thickening compared to the control group and had reduced total collagen in the treated area. CCG-203971 produced positive efficacy in both measured parameters of the model.

In Chapter IV, recent evidence for the role of MRTF/SRF in melanoma metastasis, and similarities between cancer progression and pathological fibrosis lead us to analyze Rho signaling and MRTF/SRF transcription in a panel of five human metastatic melanoma cell lines. Using in vitro assays designed to mimic steps in cancer metastasis (colonization, migration, and invasion) we identified a clear dichotomy between the cells lines. Three of the lines formed colonies, and were highly migratory and invasive in these assays, while the other two were less effective. In the aggressive melanomas. RhoC protein expression was dramatically increased and MRTF-A was predominantly localized to the nucleus, even in serum-starved cells. These melanoma lines also expressed high levels of MRTF target genes; CTGF, MYL9, and CYR61. Treatment with CCG-203971 blocked MRTF activity and constitutive nuclear localization in the

aggressive melanomas. CCG-203971 also inhibited cellular invasion and migration of the aggressive melanomas. To move into an in vivo model of cancer metastasis, we injected melanoma cells into the tail-vein of immunocompromised mice and treated with CCG-203971. At the end of the study, lung sections were analyzed for the presence of the melanoma cells. The compound-treated group displayed a reduction in the total number of metastatic lung colonies, as well as decreased size of the colonies. Similar to the efficacy observed in the fibrosis model, CCG-203971 dramatically reduced the ability of melanoma cells to colonize the lungs after entering systemic circulation.

Collaboration was essential for the success of the work presented here. In Chapter III, Eliza Tsou, Phillip Campbell, Jeffrey Ruth, and Asif Amin from the University of Michigan, Department of Rheumatology, performed the in vivo study shown in Fig. 3-6. In Chapter IV, the label-free invasion and migration assays shown in Figs. 4-1 and 4-2 were performed in Dr. Beth Lawlor's lab by Melanie Krook and Merlin Airik from the University of Michigan, Department of Pediatrics. Also in Chapter IV, the cell proliferation and effect of CCG-203971 on SRE-Luciferase shown in Fig. 4-2 and Fig. 4-6, were performed by Sue Wade from our laboratory. I performed the remaining experiments at both The University of Michigan Department of Pharmacology and Michigan State University Department of Pharmacology and Toxicology.

References

1. Wynn, T. A. (2008) *J Pathol* **214**, 199-210

2. Alhamad, E. H., Cal, J. G., AlBoukai, A. A., Shaik, S. A., and Omair, M. A. (2014) *Clin Respir J*

3. Coward, W. R., Saini, G., and Jenkins, G. (2010) *Ther Adv Respir Dis* **4**, 367-388

4. Jelaska, A., and Korn, J. H. (2000) *Arthritis Rheum* **43**, 2230-2239

5. Sit, S. T., and Manser, E. (2011) *J Cell Sci* **124**, 679-683

6. Vega, F. M., Fruhwirth, G., Ng, T., and Ridley, A. J. (2011) *J Cell Biol* **193**, 655-665

7. Schwartz, M. (2004) *J Cell Sci* **117**, 5457-5458

8. Leung, T., Manser, E., Tan, L., and Lim, L. (1995) *J Biol Chem* **270**, 29051-29054

9. Ishizaki, T., Maekawa, M., Fujisawa, K., Okawa, K., Iwamatsu, A., Fujita, A., Watanabe, N., Saito, Y., Kakizuka, A., Morii, N., and Narumiya, S. (1996) *Embo J* **15**, 1885-1893

10. Tominaga, T., Sahai, E., Chardin, P., McCormick, F., Courtneidge, S. A., and Alberts, A. S. (2000) *Mol Cell* **5**, 13-25

11. Miralles, F., Posern, G., Zaromytidou, A. I., and Treisman, R. (2003) *Cell* **113**, 329-342

12. Mouilleron, S., Langer, C. A., Guettler, S., McDonald, N. Q., and Treisman, R. (2011) *Sci Signal* **4**, ra40

13. Pawlowski, R., Rajakyla, E. K., Vartiainen, M. K., and Treisman, R. (2010) *EMBO J* **29**, 3448-3458

14. Mack, C. P., Somlyo, A. V., Hautmann, M., Somlyo, A. P., and Owens, G. K. (2001) *J Biol Chem* **276**, 341-347

15. Cen, B., Selvaraj, A., Burgess, R. C., Hitzler, J. K., Ma, Z., Morris, S. W., and Prywes, R. (2003) *Mol Cell Biol* **23**, 6597-6608

16. Luchsinger, L. L., Patenaude, C. A., Smith, B. D., and Layne, M. D. (2011) *J Biol Chem* **286**, 44116-44125

17. Selvaraj, A., and Prywes, R. (2004) *BMC Mol Biol* **5**, 13

18. Hanna, M., Liu, H., Amir, J., Sun, Y., Morris, S. W., Siddiqui, M. A., Lau, L. F., and Chaqour, B. (2009) *J Biol Chem* **284**, 23125-23136

19. Yang, Y., Zhe, X., Phan, S. H., Ullenbruch, M., and Schuger, L. (2003) *Am J Respir Cell Mol Biol* **29**, 583-590

20. Chai, J., Norng, M., Tarnawski, A. S., and Chow, J. (2007) *Gut* **56**, 621-630

21. Sandbo, N., Kregel, S., Taurin, S., Bhorade, S., and Dulin, N. O. (2009) *Am J Respir Cell Mol Biol* **41**, 332-338

22. Tsou, P. S., Haak, A. J., Khanna, D., and Neubig, R. R. (2014) *Am J Physiol Cell Physiol* **307**, C2-13

23. Sterclova, M., and Vasakova, M. (2014) *World J Clin Cases* **2**, 668-675

24. Yan, Z., Kui, Z., and Ping, Z. (2014) *Autoimmun Rev* **13**, 1020-1025

25. Castelino, F. V., and Varga, J. (2014) *Curr Opin Rheumatol* **26**, 607-614

26. Duscher, D., Maan, Z. N., Wong, V. W., Rennert, R. C., Januszyk, M., Rodrigues, M., Hu, M., Whitmore, A. J., Whittam, A. J., Longaker, M. T., and Gurtner, G. C. (2014) *J Biomech* **47**, 1997-2005

27. Fett, N. (2013) *Clin Dermatol* **31**, 432-437

28. Xu, X., Dai, H., and Wang, C. (2014) *Clin Respir J*

29. Lafyatis, R. (2014) *Nat Rev Rheumatol* **10**, 706-719

30. Zeisberg, M., and Kalluri, R. (2013) *American journal of physiology. Cell physiology* **304**, C216-225

31. Schultz Jel, J., Witt, S. A., Glascock, B. J., Nieman, M. L., Reiser, P. J., Nix, S. L., Kimball, T. R., and Doetschman, T. (2002) *J Clin Invest* **109**, 787-796

32. Zhao, J., Shi, W., Wang, Y. L., Chen, H., Bringas, P., Jr., Datto, M. B., Frederick, J. P., Wang, X. F., and Warburton, D. (2002) *Am J Physiol Lung Cell Mol Physiol* **282**, L585-593

33. Lakos, G., Takagawa, S., Chen, S. J., Ferreira, A. M., Han, G., Masuda, K., Wang, X. J., DiPietro, L. A., and Varga, J. (2004) *Am J Pathol* **165**, 203-217

34. Latella, G., Vetuschi, A., Sferra, R., Catitti, V., D'Angelo, A., Zanninelli, G., Flanders, K. C., and Gaudio, E. (2009) *Liver international : official journal of the International Association for the Study of the Liver* **29**, 997-1009

35. Meng, X. M., Huang, X. R., Xiao, J., Chung, A. C., Qin, W., Chen, H. Y., and Lan, H. Y. (2012) *Kidney Int* **81**, 266-279

36. Denton, C. P., Merkel, P. A., Furst, D. E., Khanna, D., Emery, P., Hsu, V. M., Silliman, N., Streisand, J., Powell, J., Akesson, A., Coppock, J., Hoogen, F., Herrick, A., Mayes, M. D., Veale, D., Haas, J., Ledbetter, S., Korn, J. H., Black, C. M., Seibold, J. R., Cat-192 Study, G., and Scleroderma Clinical Trials, C. (2007) *Arthritis Rheum* **56**, 323-333

37. Sandbo, N., Lau, A., Kach, J., Ngam, C., Yau, D., and Dulin, N. O. (2011) *Am J Physiol Lung Cell Mol Physiol* **301**, L656-666

38. Parada, C., Li, J., Iwata, J., Suzuki, A., and Chai, Y. (2013) *Mol Cell Biol* **33**, 3482-3493

39. Rodriguez-Pascual, F., Redondo-Horcajo, M., and Lamas, S. (2003) *Circ Res* **92**, 1288-1295

40. Yamanaka, M., Shegogue, D., Pei, H. P., Bu, S. Z., Bielawska, A., Bielawski, J., Pettus, B., Hannun, Y. A., Obeid, L., and Trojanowska, M. (2004) *J Biol Chem* **279**, 53994-54001

41. Lee, J., Moon, H. J., Lee, J. M., and Joo, C. K. (2010) *J Biol Chem* **285**, 26618-26627

42. Shen, X., Li, J. M., Hu, P. P. C., Waddell, D., Zhang, J., and Wang, X. F. (2001) *J Biol Chem* **276**, 15362-15368

43. Tsapara, A., Luthert, P., Greenwood, J., Hill, C. S., Matter, K., and Balda, M. S. (2010) *Mol Biol Cell* **21**, 860-870

44. Budd, D. C., and Qian, Y. (2013) *Future Med Chem* **5**, 1935-1952

45. Fukushima, N., Kimura, Y., and Chun, J. (1998) *Proc Natl Acad Sci U S A* **95**, 6151-6156

46. Contos, J. J., Ishii, I., and Chun, J. (2000) *Molecular pharmacology* **58**, 1188-1196

47. Castelino, F. V., Seiders, J., Bain, G., Brooks, S. F., King, C. D., Swaney, J. S., Lorrain, D. S., Chun, J., Luster, A. D., and Tager, A. M. (2011) *Arthritis Rheum* **63**, 1405-1415

48. Tager, A. M., LaCamera, P., Shea, B. S., Campanella, G. S., Selman, M., Zhao, Z., Polosukhin, V., Wain, J., Karimi-Shah, B. A., Kim, N. D., Hart, W. K., Pardo, A., Blackwell, T. S., Xu, Y., Chun, J., and Luster, A. D. (2008) *Nature medicine* **14**, 45-54

49. Pradere, J. P., Klein, J., Gres, S., Guigne, C., Neau, E., Valet, P., Calise, D., Chun, J., Bascands, J. L., Saulnier-Blache, J. S., and Schanstra, J. P. (2007) *J Am Soc Nephrol* **18**, 3110-3118

50. Sakai, N., Chun, J., Duffield, J. S., Wada, T., Luster, A. D., and Tager, A. M. (2013) *FASEB J* **27**, 1830-1846

51. Watanabe, N., Ikeda, H., Nakamura, K., Ohkawa, R., Kume, Y., Tomiya, T., Tejima, K., Nishikawa, T., Arai, M., Yanase, M., Aoki, J., Arai, H., Omata, M., Fujiwara, K., and Yatomi, Y. (2007) *Life Sci* **81**, 1009-1015

52. Swaney, J. S., Chapman, C., Correa, L. D., Stebbins, K. J., Bundey, R. A., Prodanovich, P. C., Fagan, P., Baccei, C. S., Santini, A. M., Hutchinson, J. H., Seiders, T. J., Parr, T. A., Prasit, P., Evans, J. F., and Lorrain, D. S. (2010) *Br J Pharmacol* **160**, 1699-1713

53. PRNewswire. (2011) http://www.prnewswire.com/news-releases/amira-pharmaceuticals-announces-completion-of-phase-1-clinical-study-for-am152-a-novel-lpa1-receptor-antagonist-121087874.html.

54. Levin, E. R. (1995) *N Engl J Med* **333**, 356-363

55. Meyers, K. E., and Sethna, C. (2013) *Pediatr Nephrol* **28**, 711-720

56. Mallat, A., Fouassier, L., Preaux, A. M., Gal, C. S., Raufaste, D., Rosenbaum, J., Dhumeaux, D., Jouneaux, C., Mavier, P., and Lotersztajn, S. (1995) *J Clin Invest* **96**, 42-49

57. Hafizi, S., Wharton, J., Chester, A. H., and Yacoub, M. H. (2004) *Cell Physiol Biochem* **14**, 285-292

58. Mallat, A., Fouassier, L., Preaux, A. M., Mavier, P., and Lotersztajn, S. (1995) *J Cardiovasc Pharmacol* **26 Suppl 3**, S132-134

59. Xu, S. W., Howat, S. L., Renzoni, E. A., Holmes, A., Pearson, J. D., Dashwood, M. R., Bou-Gharios, G., Denton, C. P., du Bois, R. M., Black, C. M., Leask, A., and Abraham, D. J. (2004) *J Biol Chem* **279**, 23098-23103

60. Shi-Wen, X., Chen, Y., Denton, C. P., Eastwood, M., Renzoni, E. A., Bou-Gharios, G., Pearson, J. D., Dashwood, M., du Bois, R. M., Black, C. M., Leask, A., and Abraham, D. J. (2004) *Mol Biol Cell* **15**, 2707-2719

61. Hocher, B., Schwarz, A., Fagan, K. A., Thone-Reineke, C., El-Hag, K., Kusserow, H., Elitok, S., Bauer, C., Neumayer, H. H., Rodman, D. M., and Theuring, F. (2000) *Am J Respir Cell Mol Biol* **23**, 19-26

62. Lagares, D., Garcia-Fernandez, R. A., Jimenez, C. L., Magan-Marchal, N., Busnadiego, O., Lamas, S., and Rodriguez-Pascual, F. (2010) *Arthritis Rheum* **62**, 878-889

63. Kawaguchi, Y., Suzuki, K., Hara, M., Hidaka, T., Ishizuka, T., Kawagoe, M., and Nakamura, H. (1994) *Ann Rheum Dis* **53**, 506-510

64. Yamane, K., Miyauchi, T., Suzuki, N., Yuhara, T., Akama, T., Suzuki, H., and Kashiwagi, H. (1992) *J Rheumatol* **19**, 1566-1571

65. Siehler, S. (2009) *Brit J Pharmacol* **158**, 41-49

66. Shraga-Levine, Z., and Sokolovsky, M. (2000) *Cell Mol Neurobiol* **20**, 305-317

67. Yung, Y. C., Stoddard, N. C., and Chun, J. (2014) *J Lipid Res* **55**, 1192-1214

68. Kawanabe, Y., Okamoto, Y., Nozaki, K., Hashimoto, N., Miwa, S., and Masaki, T. (2002) *Mol Pharmacol* **61**, 277-284

69. Lutz, S., Freichel-Blomquist, A., Yang, Y., Rumenapp, U., Jakobs, K. H., Schmidt, M., and Wieland, T. (2005) *J Biol Chem* **280**, 11134-11139

70. Campanholle, G., Ligresti, G., Gharib, S. A., and Duffield, J. S. (2013) *American journal of physiology. Cell physiology* **304**, C591-603

71. Babic, A. M., Chen, C. C., and Lau, L. F. (1999) *Mol Cell Biol* **19**, 2958-2966

72. Gao, R., and Brigstock, D. R. (2004) *J Biol Chem* **279**, 8848-8855

73. Segarini, P. R., Nesbitt, J. E., Li, D., Hays, L. G., Yates, J. R., 3rd, and Carmichael, D. F. (2001) *J Biol Chem* **276**, 40659-40667

74. Wahab, N. A., Weston, B. S., and Mason, R. M. (2005) *J Am Soc Nephrol* **16**, 340-351

75. Hashimoto, G., Inoki, I., Fujii, Y., Aoki, T., Ikeda, E., and Okada, Y. (2002) *J Biol Chem* **277**, 36288-36295

76. Abreu, J. G., Ketpura, N. I., Reversade, B., and De Robertis, E. M. (2002) *Nature cell biology* **4**, 599-604

77. Hoshijima, M., Hattori, T., Inoue, M., Araki, D., Hanagata, H., Miyauchi, A., and Takigawa, M. (2006) *FEBS letters* **580**, 1376-1382

78. Jun, J. I., and Lau, L. F. (2011) *Nat Rev Drug Discov* **10**, 945-963

79. Mori, T., Kawara, S., Shinozaki, M., Hayashi, N., Kakinuma, T., Igarashi, A., Takigawa, M., Nakanishi, T., and Takehara, K. (1999) *Journal of cellular physiology* **181**, 153-159

80. Sonnylal, S., Shi-Wen, X., Leoni, P., Naff, K., Van Pelt, C. S., Nakamura, H., Leask, A., Abraham, D., Bou-Gharios, G., and de Crombrugghe, B. (2010) *Arthritis Rheum* **62**, 1523-1532

81. Liu, S., Shi-wen, X., Abraham, D. J., and Leask, A. (2011) *Arthritis Rheum* **63**, 239-246

82. Lang, C., Sauter, M., Szalay, G., Racchi, G., Grassi, G., Rainaldi, G., Mercatanti, A., Lang, F., Kandolf, R., and Klingel, K. (2008) *Journal of molecular medicine* **86**, 49-60

83. Uchio, K., Graham, M., Dean, N. M., Rosenbaum, J., and Desmouliere, A. (2004) *Wound repair and regeneration : official publication of the Wound Healing Society [and] the European Tissue Repair Society* **12**, 60-66

84. Okada, H., Kikuta, T., Kobayashi, T., Inoue, T., Kanno, Y., Takigawa, M., Sugaya, T., Kopp, J. B., and Suzuki, H. (2005) *J Am Soc Nephrol* **16**, 133-143

85. Chen, P. S., Wang, M. Y., Wu, S. N., Su, J. L., Hong, C. C., Chuang, S. E., Chen, M. W., Hua, K. T., Wu, Y. L., Cha, S. T., Babu, M. S., Chen, C. N., Lee, P. H., Chang, K. J., and Kuo, M. L. (2007) *J Cell Sci* **120**, 2053-2065

86. Hinz, B., Phan, S. H., Thannickal, V. J., Prunotto, M., Desmouliere, A., Varga, J., De Wever, O., Mareel, M., and Gabbiani, G. (2012) *Am J Pathol* **180**, 1340-1355

87. Liu, F., Mih, J. D., Shea, B. S., Kho, A. T., Sharif, A. S., Tager, A. M., and Tschumperlin, D. J. (2010) *J Cell Biol* **190**, 693-706

88. Wells, R. G. (2008) *Hepatology* **47**, 1394-1400

89. Arora, P. D., Narani, N., and McCulloch, C. A. (1999) *Am J Pathol* **154**, 871-882

90. Wang, H. B., Dembo, M., and Wang, Y. L. (2000) *Am J Physiol Cell Physiol* **279**, C1345-1350

91. Henderson, N. C., Arnold, T. D., Katamura, Y., Giacomini, M. M., Rodriguez, J. D., McCarty, J. H., Pellicoro, A., Raschperger, E., Betsholtz, C., Ruminski, P. G., Griggs, D. W., Prinsen, M. J., Maher, J. J., Iredale, J. P., Lacy-Hulbert, A., Adams, R. H., and Sheppard, D. (2013) *Nature medicine*

92. Liu, S., Kapoor, M., Denton, C. P., Abraham, D. J., and Leask, A. (2009) *Arthritis Rheum* **60**, 2817-2821

93. Zhou, Y., Huang, X., Hecker, L., Kurundkar, D., Kurundkar, A., Liu, H., Jin, T. H., Desai, L., Bernard, K., and Thannickal, V. J. (2013) *J Clin Invest* **123**, 1096-1108

94. Schwartz, M. A., and Shattil, S. J. (2000) *Trends Biochem Sci* **25**, 388-391

95. Marinkovic, A., Liu, F., and Tschumperlin, D. J. (2013) *Am J Respir Cell Mol Biol* **48**, 422-430

96. Renshaw, M. W., Toksoz, D., and Schwartz, M. A. (1996) *J Biol Chem* **271**, 21691-21694

97. Hanna, S., and El-Sibai, M. (2013) *Cell Signal* **25**, 1955-1961

98. Murali, A., and Rajalingam, K. (2014) *Cell Mol Life Sci* **71**, 1703-1721

99. Wilson, K. F., Erickson, J. W., Antonyak, M. A., and Cerione, R. A. (2013) *Trends Mol Med* **19**, 74-82

100. Baranwal, S., and Alahari, S. K. (2011) *Curr Drug Targets* **12**, 1194-1201

101. Li, H., Peyrollier, K., Kilic, G., and Brakebusch, C. (2014) *Biofactors* **40**, 226-235

102. Ferlay, J., Shin, H. R., Bray, F., Forman, D., Mathers, C., and Parkin, D. M. (2010) *Int J Cancer* **127**, 2893-2917

103. Azoury, S. C., and Lange, J. R. (2014) *Surg Clin North Am* **94**, 945-962, vii

104. Chen, Y. Q. (2013) *Cancer Metastasis Rev* **32**, 3-4

105. Finn, L., Markovic, S. N., and Joseph, R. W. (2012) *BMC Med* **10**, 23

106. Jang, S., and Atkins, M. B. (2014) *Clin Pharmacol Ther* **95**, 24-31

107. Clark, E. A., Golub, T. R., Lander, E. S., and Hynes, R. O. (2000) *Nature* **406**, 532-535

108. van Golen, K. L., Wu, Z. F., Qiao, X. T., Bao, L. W., and Merajver, S. D. (2000) *Cancer Res* **60**, 5832-5838

109. van Golen, K. L., Wu, Z. F., Qiao, X. T., Bao, L., and Merajver, S. D. (2000) *Neoplasia* **2**, 418-425

110. Akhmetshina, A., Dees, C., Pileckyte, M., Szucs, G., Spriewald, B. M., Zwerina, J., Distler, O., Schett, G., and Distler, J. H. (2008) *Arthritis Rheum* **58**, 2553-2564

111. Shang, X., Marchioni, F., Sipes, N., Evelyn, C. R., Jerabek-Willemsen, M., Duhr, S., Seibel, W., Wortman, M., and Zheng, Y. (2012) *Chem Biol* **19**, 699-710

112. Shang, X., Marchioni, F., Evelyn, C. R., Sipes, N., Zhou, X., Seibel, W., Wortman, M., and Zheng, Y. (2013) *Proc Natl Acad Sci U S A* **110**, 3155-3160

113. Liao, J. K., Seto, M., and Noma, K. (2007) *J Cardiovasc Pharmacol* **50**, 17-24

114. Zhou, Y., Huang, X. W., Hecker, L., Kurundkar, D., Kurundkar, A., Liu, H., Jin, T. H., Desai, L., Bernard, K., and Thannickal, V. J. (2013) *J Clin Invest* **123**, 1096-1108

115. Ying, H., Biroc, S. L., Li, W. W., Alicke, B., Xuan, J. A., Pagila, R., Ohashi, Y., Okada, T., Kamata, Y., and Dinter, H. (2006) *Mol Cancer Ther* **5**, 2158-2164

116. Raja, S. G. (2012) *Recent Pat Cardiovasc Drug Discov* **7**, 100-104

117. Evelyn, C. R., Wade, S. M., Wang, Q., Wu, M., Iniguez-Lluhi, J. A., Merajver, S. D., and Neubig, R. R. (2007) *Molecular Cancer Therapeutics* **6**, 2249-2260

118. Etienne-Manneville, S., and Hall, A. (2002) *Nature* **420**, 629-635

119. Turner, S. J., Zhuang, S., Zhang, T., Boss, G. R., and Pilz, R. B. (2008) *Biochem Pharmacol* **75**, 405-413

120. Brandes, R. P. (2005) *Circ Res* **96**, 927-929

121. Watts, K. L., Sampson, E. M., Schultz, G. S., and Spiteri, M. A. (2005) *Am J Resp Cell Mol* **32**, 290-300

122. Xu, J. F., Washko, G. R., Nakahira, K., Hatabu, H., Patel, A. S., Fernandez, I. E., Nishino, M., Okajima, Y., Yamashiro, T., Ross, J. C., Estepar, R. S., Diaz, A. A., Li, H. P., Qu, J. M., Himes, B. E., Come, C. E., D'Aco, K., Martinez, F. J., Han, M. K., Lynch, D. A., Crapo, J. D., Morse, D., Ryter, S. W., Silverman, E. K., Rosas, I. O., Choi, A. M., and Hunninghake, G. M. (2012) *Am J Respir Crit Care Med* **185**, 547-556

123. Nadrous, H. F., Ryu, J. H., Douglas, W. W., Decker, P. A., and Olson, E. J. (2004) *Chest* **126**, 438-446

124. Evelyn, C. R., Bell, J. L., Ryu, J. G., Wade, S. M., Kocab, A., Harzdorf, N. L., Showalter, H. D. H., Neubig, R. R., and Larsen, S. D. (2010) *Bioorg Med Chem Lett* **20**, 665-672

125. Bell, J. L., Haak, A. J., Wade, S. M., Kirchhoff, P. D., Neubig, R. R., and Larsen, S. D. (2013) *Bioorg Med Chem Lett* **23**, 3826-3832

126. Jin, W. Z., Goldfine, A. B., Boes, T., Henry, R. R., Ciaraldi, T. P., Kim, E. Y., Emecan, M., Fitzpatrick, C., Sen, A., Shah, A., Mun, E., Vokes, M., Schroeder, J., Tatro, E., Jimenez-Chillaron, J., and Patti, M. E. (2011) *Journal of Clinical Investigation* **121**, 918-929

127. Lundquist, M. R., Storaska, A. J., Liu, T. C., Larsen, S. D., Evans, T., Neubig, R. R., and Jaffrey, S. R. (2014) *Cell* **156**, 563-576

128. Hayashi, K., Watanabe, B., Nakagawa, Y., Minami, S., and Morita, T. (2014) *Plos One* **9**, e89016

129. Sandbo, N., Kregel, S., and Dulin, N. O. (2009) *Am J Resp Crit Care* **179**

130. Johnson, L. A., Rodansky, E. S., Haak, A. J., Larsen, S. D., Neubig, R. R., and Higgins, P. D. (2014) *Inflamm Bowel Dis* **20**, 154-165

CHAPTER II

THE ROLE OF CTGF AND ET-1 IN TGF-BETA STIMULATED ACTIN STRESS FIBERS AND RHO-KINASE DEPENDENT TRANSCRIPTION OF PROFIBROTIC GENES ACTA2 AND COL1A2

Abstract

Fibrotic disorders like systemic sclerosis and idiopathic pulmonary fibrosis remain debilitating diseases that have only recently been the target for approved therapeutics. Although tissue fibrosis is driven by a variety of mediators, the best established is transforming growth factor beta (TGFβ). Canonical TGFβ signaling modulates gene expression through activation of the SMAD family transcription factors. TGFβ also induces a delayed stimulation of Rho GTPase and myocardin-related transcription factor (MRTF) however; the mechanism for this activation and the dependence of specific profibrotic genes being expressed by MRTF vs. SMAD has not been examined. Here we report an analysis of stress fiber formation, MRTF activation, and gene expression following TGFβ stimulation in NIH-3T3 fibroblasts and primary human dermal fibroblasts. Specifically, TGFβ stimulates stress fiber formations peaking at 3 hours and maintains them out to 24 hours post treatment. Known SMAD target genes COL1A1, and EDN1 (ET-1) were expressed rapidly following TGFβ, while MRTF target genes COL1A2 and ACTA2, were not expressed until 12-18 hours after treatment and were dependent on Rho-kinase (ROCK) activity. CTGF, which is a known target for both SMAD and MRTF regulated

transcription, was rapidly expressed, and later enhanced at 12-18 hours after TGFβ. To assess intermediary signaling on TGFβ activation of the Rho pathway we used a neutralizing antibody for CTGF and an ET-1 receptor antagonist, which were able to block TGFβ stimulated stress fiber formation and MRTF activity. These data point towards a mechanism were canonical TGFβ/SMAD signaling leads to transcription of CTGF and ET-1 that additively stimulate F-actin stress fibers, and MRTF to promote fibrosis through expression of COLA1A2, ACTA, and CTGF.

Introduction

Pathological tissue fibrosis which occurs in systemic sclerosis (SSc) and idiopathic pulmonary fibrosis (IPF) develops into progressive and poorly managed diseases. These disorders are characterized by aberrant wound healing, rigid structural irregularities of the affective tissue leading to deteriorating organ function, and potential fatality (1-3). At the cellular level, fibrosis is driven in part, by local fibroblasts differentiated into active myofibroblasts which display enhanced proliferation and extra-cellular matrix deposition (4,5). The myofibroblasts also induce contraction of the matrix substrate that further promotes stiff, fibrotic tissue (6,7). Multiple micro-environment factors can influence signaling cascades to promote myofibroblast differentiation; however the best established is transforming growth factor-beta (TGFβ) (8,9). TGFβ superfamily ligands bind to a type II receptor, (TGFβRII) which then phosphorylates and activates a type I receptor (TGFβRI). Once active, TGFβRI phosphorylates receptor-regulated SMADs (R-SMADs), (SMAD2/3). To activate gene transcription, SMAD2/3 complexes with SMAD4 and accumulates in the nucleus where it induces transcription of a variety genes involved in extracellular matrix neogenesis (10). Known profibrotic, TGFβ/SMAD target genes include: COL1A1 (collagen type 1 α1), CTGF (connective tissue growth factor/CCN2), and EDN1 (endothelin-1) (11-13). Clinically, TGFβ expression is elevated in the dermis of patients with SSc (14,15), and in the plasma of IPF patients (16). TGFβ also participates in non-canonical signaling through a variety of mechanisms (17).

Rho family GTPases regulate cytoskeletal organization, cell motility, and gene expression through multiple effector proteins (18). As a means to regulate gene expression, Rho-

GTPase stimulates the formation of F-actin filaments through the Rho kinase (ROCK), thereby depleting cellular stores of G-actin. Myocardin-related transcription factors (MRTF) are normally sequestered in the cytosol by G-actin but following Rho activation accumulate in the nucleus to cooperatively activate gene transcription with the serum response factor (SRF) (19,20). Known profibrotic, MRTF/SRF target genes include: COL1A2 (collagen type 1 α2), ACTA2 (alpha- smooth muscle actin), and CTGF (21-24). One well-established mechanism for Rho GTPase activation and F-actin stress fiber formation is through G protein-coupled receptors (GPCRs) which bind to $G_{12/13}$ subunits to activate one of the RhoGEFs (p115-RhoGEF, PDZ-RhoGEF, leukemia-associated RhoGEF) which directly binds to and activates RhoA and RhoC (25). The kinetics of this pathway are also well established and relatively rapid; following LPA ligand addition, fibroblasts form actin stress fibers within 10 minutes (26). TGFβ activation of Rho and Rho effector mechanisms has been observed in multiple cell types. In fibroblasts, F-actin stress fibers are observed following TGFβ treatment, however their formation is delayed relative to that seen with GPCR signaling, developing on the scale of hours after TGFβ rather than minutes after LPA (27,28). Rapid activation of RhoA by TGFβ (10 minutes) has been observed in epithelial cells, but was found to be independent of canonical SMAD signaling (29). The delayed activation occurring in fibroblasts however, is dependent on SMAD transcriptional activity and *de novo* protein synthesis, (28) suggesting that TGFβ/SMAD signaling promotes expression of some Rho activating mediator. Also, TGFβ stimulation activates Rho kinase-dependent MRTF/SRF-regulated gene expression as well as pulmonary myofibroblast differentiation (28).

Recent evidence suggests that SRF-regulated gene transcription through MRTF is essential for the differentiation and stabilization of activated myofibroblasts (30-32), a critical

step in tissue fibrosis. Taken together, these results suggest that MRTF/SRF regulated gene transcription driven by Rho GTPase induced F-actin dynamics is potentially a key component for TGFβ induced fibrosis. There are, however, major gaps in the understanding of TGFβ activation of Rho GTPase and MRTF transcription; this includes the kinetics of actin reorganization and MRTF-regulated gene transcription following TGFβ treatment of fibroblasts, and potential intermediate mediators by which this activation occurs. Enhanced understanding of these factors could identify novel therapeutic targets in tissue fibrosis, or promote a combination therapy with currently approved therapeutics to target these complex diseases.

Materials and Methods

Patient sample and Animal Use

Primary human dermal fibroblasts were obtained by two punch biopsies (4 mm) taken from the forearm of mixed sex, healthy volunteers. The tissue was digested using enzyme digestion solution containing 2.4 units/ml dispase, 650 units/ml type II collagenase, and 10,000 Dornase units/ml DNase. Dermal fibroblasts were maintained in DMEM with 10% fetal bovine serum (FBS), penicillin, and streptomycin. Cells of passages between 4 and 6 were used. Written informed consent was obtained for all subjects and the study was approved by the University of Michigan Institutional Review Board. NIH-3T3 cells obtained from ATCC were also maintained in 10% FBS containing DMEM, penicillin, and streptomycin.

F-actin Fluorescence Microscopy

NIH-3T3 cells ($6.0X10^3$) were plated into each well of an 8-well tissue culture treated chamber slide (Falcon) and allowed to attach overnight. Medium was changed to DMEM containing 0.5% FBS for 24 hours +/- the indicated concentrations and times of TGFβ1 (R&D Systems), 1-Palmitoyl Lysophosphatidic Acid (Cayman Chemical), recombinant human CTGF (Life Technologies), recombinant human endothelin-1 (Sigma-Aldrich), Y-27632 (Sigma-Aldrich), CI 1020 (Tocris Chemical), and/or CTGF neutralizing antibody (Abcam ab109606). Cells were then fixed in 3.7% formaldehyde for 10' at room temperature (RT) and permeabilized with 0.25% Triton X-100 for 10' at RT. For F-actin staining one unit of Acti-Stain® 488 phalloidin (Cytoskeleton Inc.) was added to each cover slip for 30' at RT. Cells were mounted with Prolong Gold® antifade reagent with DAPI (Invitrogen) and imaged on an inverted fluorescence microscope (EVOS FL, Life Technologies).

qPCR

Primary human dermal fibroblasts ($1.0X10^5$) were plated into 6-well plates (Falcon #353046) and starved for 24 hours in DMEM containing 0.5% FBS with the indicated concentrations and times of TGFβ1, LPA, and/or Y-27632. Cells were lysed and RNA was isolated using the RNeasy® kit (Qiagen) following the manufacturer's directions. DNAse-treated RNA was quantified using a NanoDrop® spectrophotometer and 1 µg was used as a template for synthesizing cDNA utilizing the Taqman® Reverse-Transcription Reagents kit (Invitrogen). SYBR green qPCR (SABiosciences) was performed using a Stratagene Mx3000P (Agilent Technologies). Ct values were determined and mRNA expression calculated relative to that of GAPDH. Fold changes were calculated using ΔΔCt calculation. Primer sequences were: GAPDH; 5' GGAAGGGCTCATGACCACAG. 3' ACAGTCTTCTGGGTGGCAGTG. CTGF; 5' CAGAGTGGAGCGCCTGTT. 3' CTGCAGGAGGCGTTGTCA. ACTA2; 5' AATGCAGAAGGAGATCACGC. 3' TCCTGTTTGCTGATCCACATC. COL1A2-hn; 5' CTTGCAGTAACCTTATGCCTAGCA. 3' CCCATCTAACCTCTCTACCCAGTCT. EDN1; 5' CTTCGTTTTCCTTTGGGTTCAG. 3' GCTCAGCGCCTAAGACTG. COL1A1-hn; 5' CTTGCAGTAACCTTATGCCTAGCA. 3' CCAACTCCTTTTCCATCATACTGA. All mRNA values were normalized to a control (either normal fibroblasts or a vehicle control) run the same day.

Statistics

Statistical analysis was performed by ANOVA comparison between groups followed by Bonferonni posttest where * p> 0.05, ** P>0.01, and *** P>0.001.

Results

TGFβ stimulates delayed but stabilized F-actin stress fibers.

TGFβ has been shown to produce F-actin stress fibers very rapidly (10 minutes) (29), as well as in a delayed manner up to and beyond 24 hours (28). To directly assess TGFβ stimulated stress fiber formation kinetics, we treated NIH-3T3 fibroblasts with 10ng/mL TGFβ for various times up to 24 hours. As a positive control, we treated cells with 10μM LPA for 30 minutes, as previously reported LPA induced stress fibers within the first 5-10 minutes, (data not shown). TGFβ stimulates actin stress fibers peaking around 3 hours, and interestingly maintains around 40% positive cells throughout the time course (Fig. 2-1A). To determine if the F-actin stimulation at the peak (3 hours) is dependent on the Rho-GTPase pathway, cells were treated with 10μM Y-27632 (Rho-kinase inhibitor). Similarly to previous findings, (28) Y-27632 blocked TGFβ induced stress fibers (Fig. 2-1B). Using cycloheximide (CHX), we assessed the requirement of *de novo* protein synthesis following TGFβ signaling in F-actin stimulation (Fig. 2-1B). CHX also blocked the presence of TGFβ-stimulated stress fibers at 3 hours. To verify that the CHX treatment is not just non-specifically blocking F-actin formation, we stimulated cells with LPA in the presence of CHX and found no inhibition of stress fiber formation (Fig. 2-2). Together these data further suggest some newly synthesized protein mediator drives Rho activation of the actin cytoskeleton following TGFβ signaling.

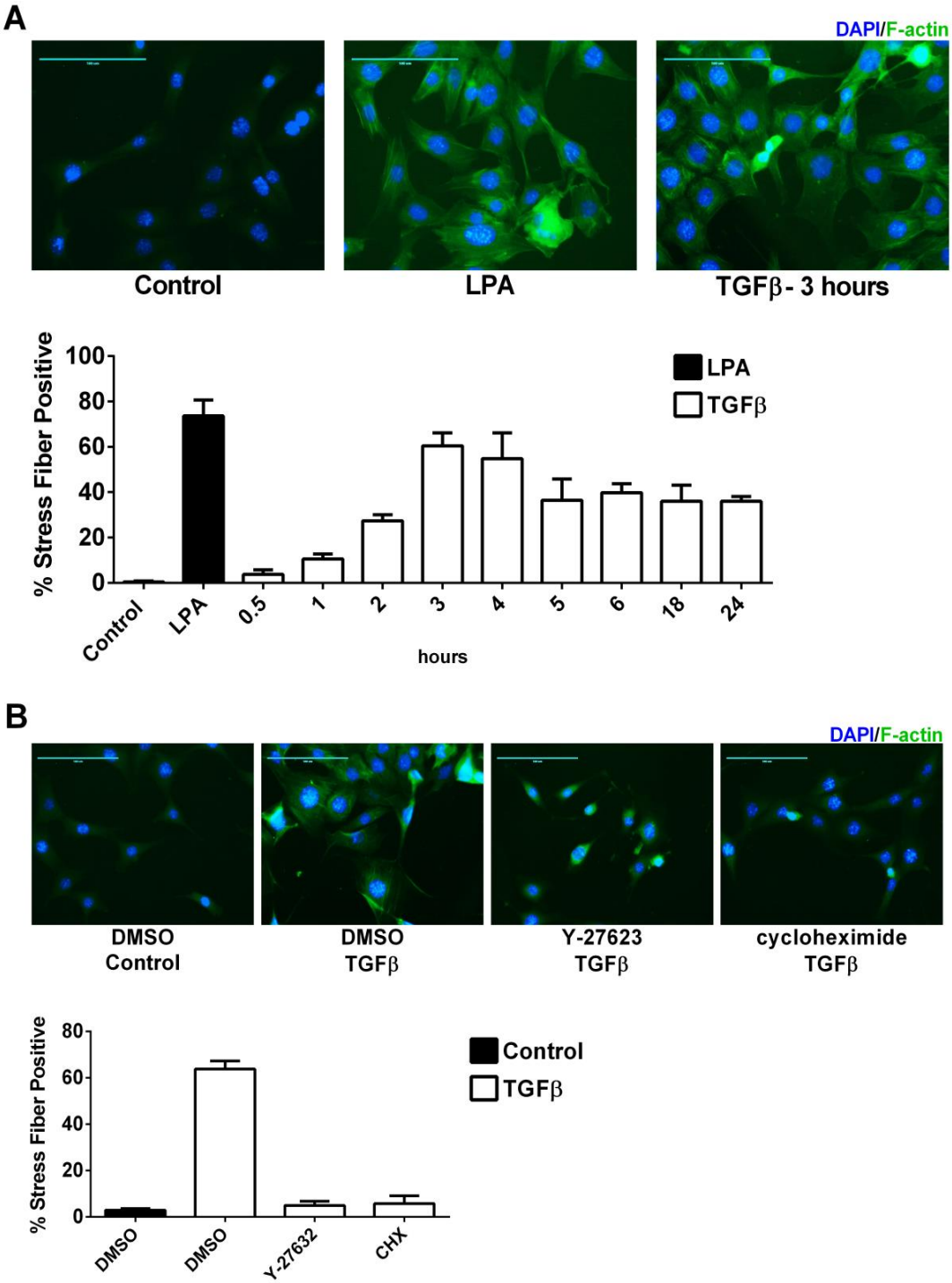

Figure 2-1. TGFβ stimulated F-actin stress fibers are dependent on Rho-kinase and de novo protein synthesis.

A.) Kinetic profile of TGFβ stimulated F-actin stress fibers. NIH-3T3 fibroblasts were starved in 0.5% FBS medium +/- 10ng/mL TGFβ for the indicated amount of time (hours). 10μM LPA treated for 30 minutes was used for comparison and positive control for stress fibers stimulated through established mechanism and kinetics.

Figure. 2-1. (continued) Representative images are shown for non-treated control, LPA, and TGFβ at 3 hours. F-actin was stained along with DAPI nuclear staining and four images from each experiment were examined for cells which displayed F-actin stress fiber formations. Data represents the mean (+/- SEM) from three independent experiments. Shown are representative images from each condition. Scale bar represents 100μm. B.) TGFβ stimulated stress fibers are blocked through Rho-kinase inhibition and cycloheximide (CHX) inhibition of protein synthesis. Starved NIH-3T3 cells were treated with 10μM ROCK inhibitor, Y-27632 (24 hours) or 10μg/mL CHX (3 hours) and stimulated with TGFβ for 3 hours and quantified as above. Data represents the mean (+/- SEM) from three independent experiments. Scale bar represents 100μm.

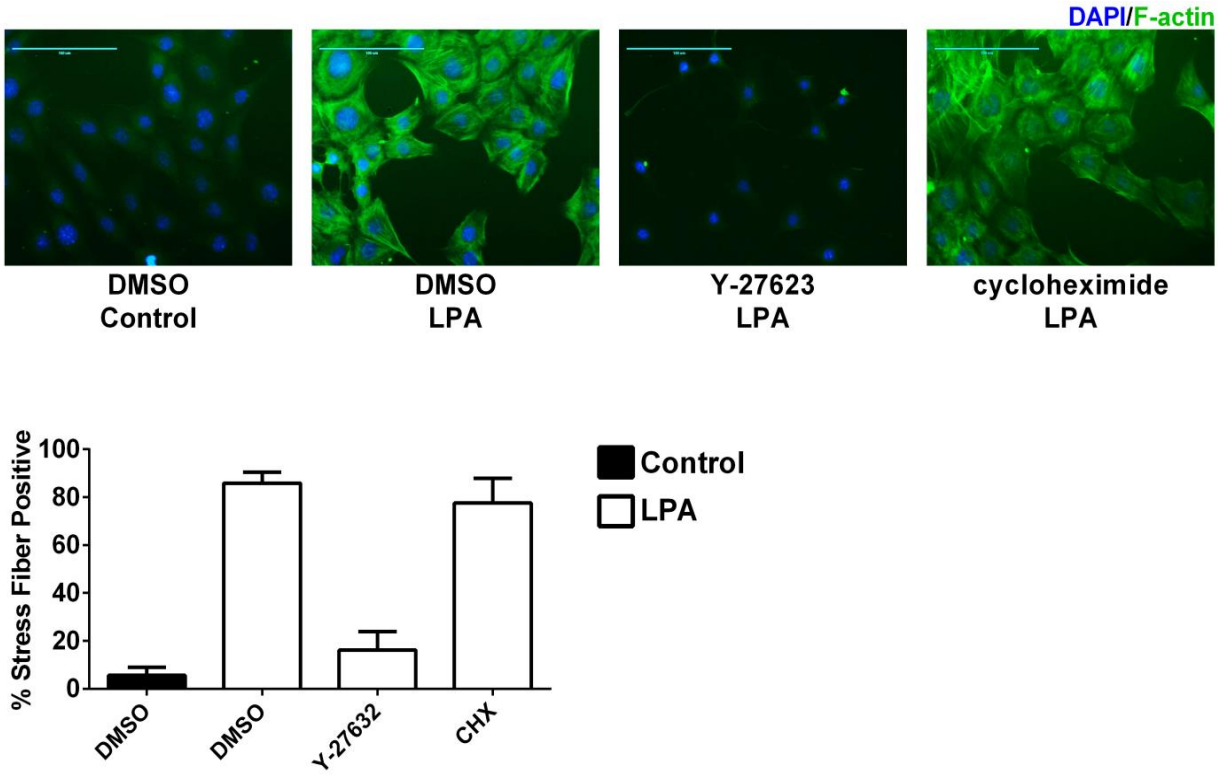

Figure 2-2. LPA stimulated stress fibers are independent of *de novo* protein synthesis.

LPA stimulated stress fibers are blocked through Rho-kinase inhibition but not cycloheximide (CHX) inhibition of protein synthesis. Starved NIH-3T3 cells were treated with 10µM ROCK inhibitor, Y-27632 (24 hours) or 10µg/mL CHX (3 hours), stimulated with 10µM LPA for 30 minutes, and quantified as above. Data represents the mean (+/- SEM) from three independent experiments. Scale bar represents 100µm.

TGFβ initiates delayed but prolonged activation of MRTF/SRF transcription.

To investigate the downstream transcriptional outputs following TGFβ signaling, we used a luciferase transcription reporter of SRF that is specific for MRTF/SRF activity (33). Evaluating concentration response curves with TGFβ and LPA we focused at 6 and 18 hours after ligand addition (Fig. 2-3A). This revealed that at 6 hours TGFβ was unable to produce an appreciable signal. In comparison, LPA produced a robust response, peaking at ~8 fold induction relative to control (EC50 ~3μM). The opposite was seen at 18 hours after treatment. The LPA signal was lost and TGFβ produced a peak response of ~5 fold over control (EC50 ~0.6ng/mL) (Fig. 2-3A). This suggests the MRTF/SRF luciferase reporter is relatively dynamic and can be used to produce a kinetic profile of TGFβ signaling. Using this reporter, we investigated a time course out to 30 hours for MRTF activity following LPA and TGFβ treatment (Fig. 2-3B). LPA produces a rapid, but transient activation of MRTF while TGFβ activates a delayed, but stable MRTF activation. To show that activation through either ligand is dependent on the Rho signaling pathway we pre-treated the cells with the Rho-kinase inhibitor Y-27632 for 24 hours then stimulated with 10ng/mL TGFβ (18 hours) or 10μM LPA (6 hours) (Fig. 2-3C). Through either regulated transcription mechanism, Y-27632 displayed equal potency and efficacy for inhibition of MRTF-activated luciferase expression (IC50~ 3μM).

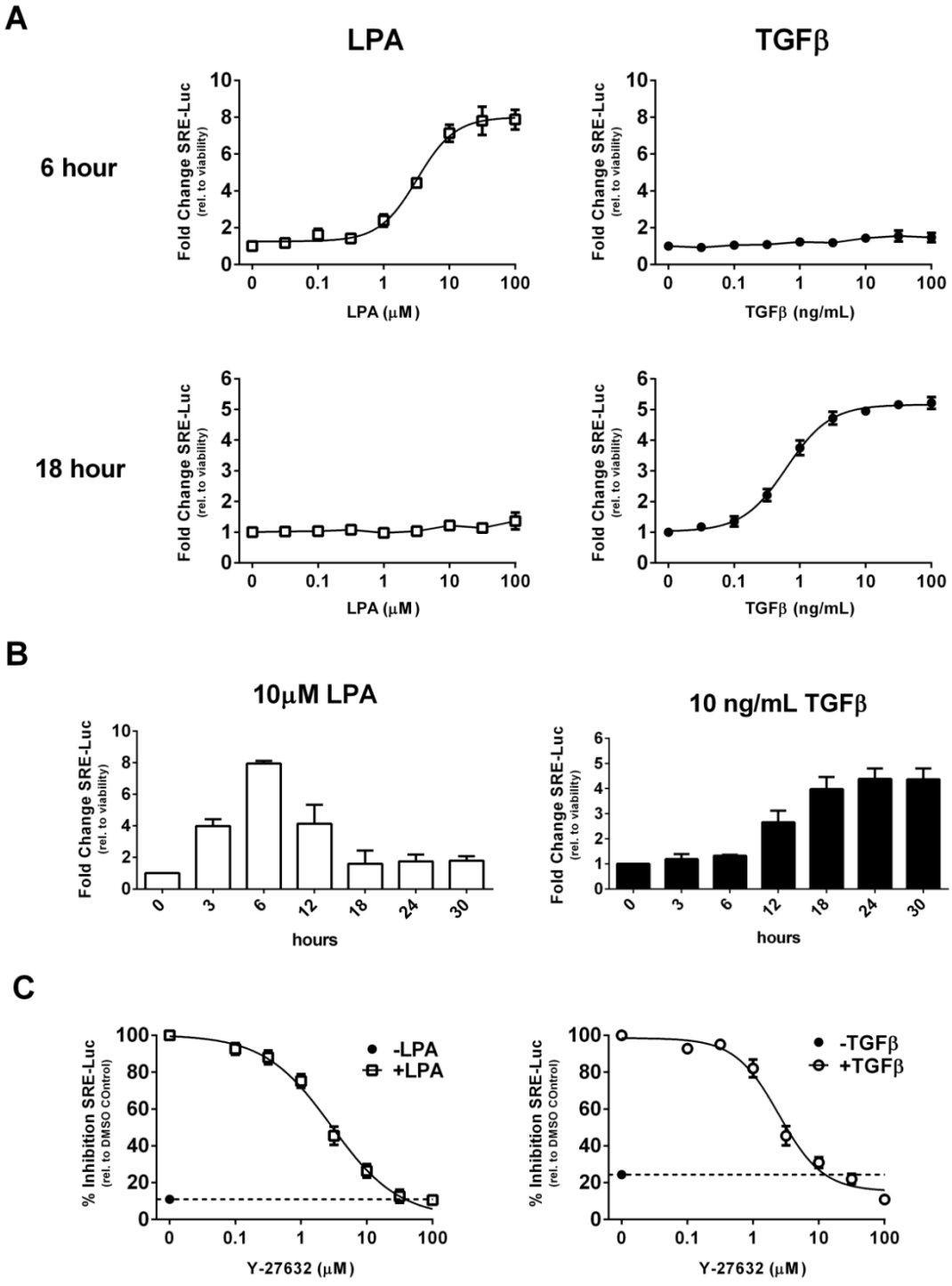

Figure 2-3. TGFβ activates delayed MRTF/SRF regulated transcription.

A.) Dose-response curves of acute (6 hour) and delated (18 hour) MRTF/SRF regulated luciferase reporter assays with LPA and TGFβ. NIH-3T3 fibroblasts were transfected with MRTF dependent SRE-Luciferase reporter plasmids then stimulated at either 18 or 6 hours with the indicated concentrations of LPA and TGFβ.

Figure 2-3. (continued) B.) Kinetic profile of LPA and TGFβ activated MRTF/SRF luciferase reporter. As above, NIH-3T3 cells were transfected with SRE-Luc reporter plasmid and treated for the indicated number of hours with 10μM LPA or 10ng/mL TGFβ (near maximum response concentrations). C.) LPA and TGFβ stimulated MRTF/SRF luciferase are dependent on Rho-kinase activity. NIH-3T3 cells transfected with the MRTF/SRF luciferase reporter were treated for 24 hours with the indicated concentrations of the Rho-kinase inhibitor Y-27632 then stimulated with 10μM LPA (6 hours) or 10ng/mL TGFβ (18 hours). Luciferase experiments were multiplexed with WST-1 to monitor cellular proliferation/toxicity and data represents the mean (+/- SEM) of luciferase luminescence relative to WST-1 absorbance and normalized to the untreated control of three (A,C) or two (B) independent experiments.

TGFβ initiates rapid SMAD target gene transcription and delayed expression of MRTF target genes.

To assess the significance of the postponed stress fibers and MRTF activation observed in NIH-3T3 cells following TGFβ treatment we assessed transcriptional levels of known SMAD and MRTF profibrotic target genes in human primary dermal fibroblasts through a 30-hour time course after TGFβ addition (Fig. 2-4). To identify MRTF target genes, we also performed the 30-hour time course following LPA addition (Fig. 2-4). Previously identified SMAD target genes COL1A1 (11), and EDN1 (13), displayed robust (~3 fold) stimulation within the first hour of TGFβ treatment and no stimulation following LPA treatment. However, previously identified MRTF target genes COL1A2 (21), and ACT2 (23), show enhanced mRNA levels within the first hour of LPA stimulation. Consistent with the kinetics that we observed for stress fiber formation and MRTF luciferase reporter activation, TGFβ begins stimulating expression of MRTF target genes at some point after 6 hours and they continue to rise up to the 30 hour mark (Fig. 2-4). CTGF (the gene encoding CCN2 protein), has been shown to be a target for TGFβ/SMAD signaling as well as for Rho/MRTF signaling (10, 27). Consistent with these findings we observe rapid stimulation of CTGF within the first few hours of TGFβ treatment and further enhancment at the later time points, suggesting based on the COL1A2 and ACTA2 TGFβ stimulated profiles, that around the 12 hour mark MRTF transcription is activated and driving peak CTGF expression (>10 fold at 30 hours). This is further supported by the LPA stimulated CTGF profile which promotes 5 fold expression within the first few hours after treatment (Fig. 2-4).

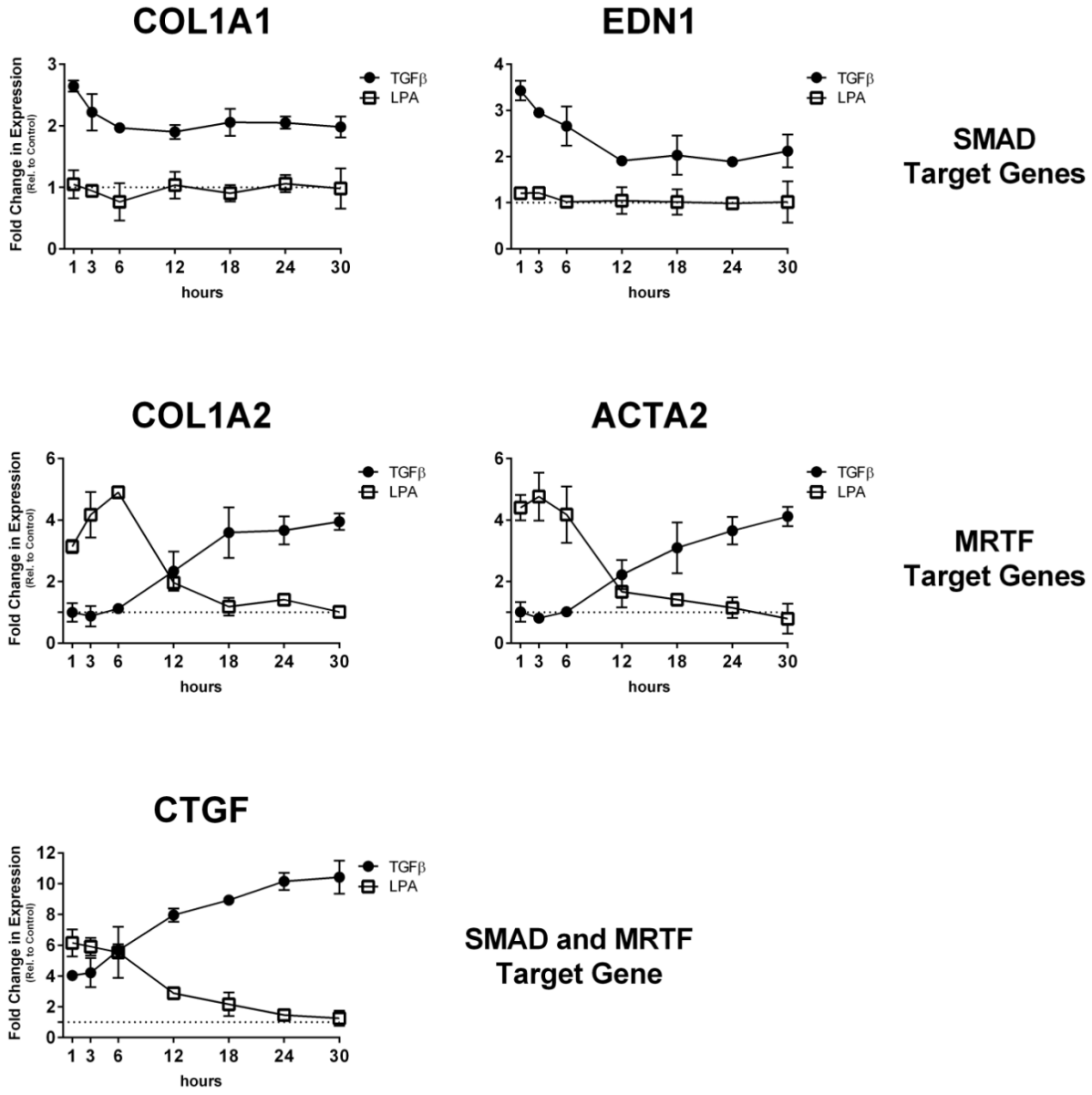

Figure 2-4. Kinetic profile of profibrotic gene transcription following TGFβ and LPA treatment.

Primary human dermal fibroblasts obtained from healthy donors (≤ passage 6) were stimulated for the indicated amount of time with 10ng/mL TGFβ or 10μM LPA in 0.5% serum starved medium. RNA was analyzed by qPCR to determine relative expression levels of profibrotic genes COL1A1, EDN1, COL1A2, ACTA2, and CTGF. Based on previous literature and the results obtained here these genes categorize into SMAD target genes, MRTF target genes, or combined SMAD/MRTF target genes. Data represents the mean (+/- STD) of two independent experiments; expression levels were quantified relative to GAPDH and normalized to the untreated control.

TGFβ stimulation of MRTF target genes is dependent on Rho-kinase activity.

To further support our discrimination of the role of MRTF and SMADs in controlling genes stimulated by TGFβ, we measured gene expression following 6 and 24 hours of TGFβ and 6 hours of LPA, with and without 10 μM Y-27632 (Fig. 2-5). As predicted, the expression of SMAD target genes COL1A1 and EDN1 is not blocked by ROCK inhibition, however, transcription of the MRTF target genes COL1A2 and ACTA2, which are transcribed late (24 hours) after TGFβ and early (6 hours) with LPA are blocked by ROCK inhibition. Also consistent with this model, the early TGFβ stimulation of CTGF with is not affected by Y-27632 but the later enhancement at 24 hours, as well LPA stimulated transcription, is blocked with the Rho-kinase inhibitor Y-27632.

CTGF and ET-1 stimulate stress fiber formation and activate MRTF/SRF regulated transcription.

Previous findings, as well as the effect of cycloheximide on stress fibers following TGFβ treatment, (Fig. 2-1B), suggest that a target gene product(s) of TGFβ mediates the delayed activation of Rho GTPase and stress fiber formations. As shown throughout the experiments performed here, LPA potently induces Rho activation and MRTF regulated gene transcription. To assess the potential role of LPA in TGFβ stimulated stress fibers, we measured RNA levels of ENPP2 (autotaxin or ATX), the gene encoding the enzyme that regulates LPA production (34). Following TGFβ treatment, ATX levels decreased in a time depenent maner (Fig. 2-6A). Contrary to the expectation if LPA was the mediator of TGFβ induced Rho activation. We also found that the LPA receptor1/3 antagonist, Ki16425 reduced the background level of MRTF-

regulated luciferase reporter in starved fibroblasts even in the absense of ligand. However it did not suppress TGFβ induced MRTF activity (Fig. 2-6B). Alternative mediators could be endothelin and CTGF. Along with being identified as TGFβ/SMAD target genes, both ET-1 and CTGF have been shown to activate the Rho GTPase pathway and stimulate actin stress fibers (35-37). Here we show that both CTGF and ET-1 stimulate stress fibers in starved NIH-3T3 fibroblasts as early as 1 hour after adding ligand, similar to LPA (Fig.2-7A). We also measured MRTF activity following addition of CTGF and ET-1 using the SRE-Lucifferase reporter and found both treatsments activated MRTF activity (Fig. 2-8B). The individual ligands, however, were only able to activate the reporter ~2.5-3 fold compared to the ~6-8 fold induction found with TGFβ and LPA (Fig. 2-3A). This suggests that neither ET-1 or CTGF alone could account for the TGFβ mediated SRE-Luc activation.

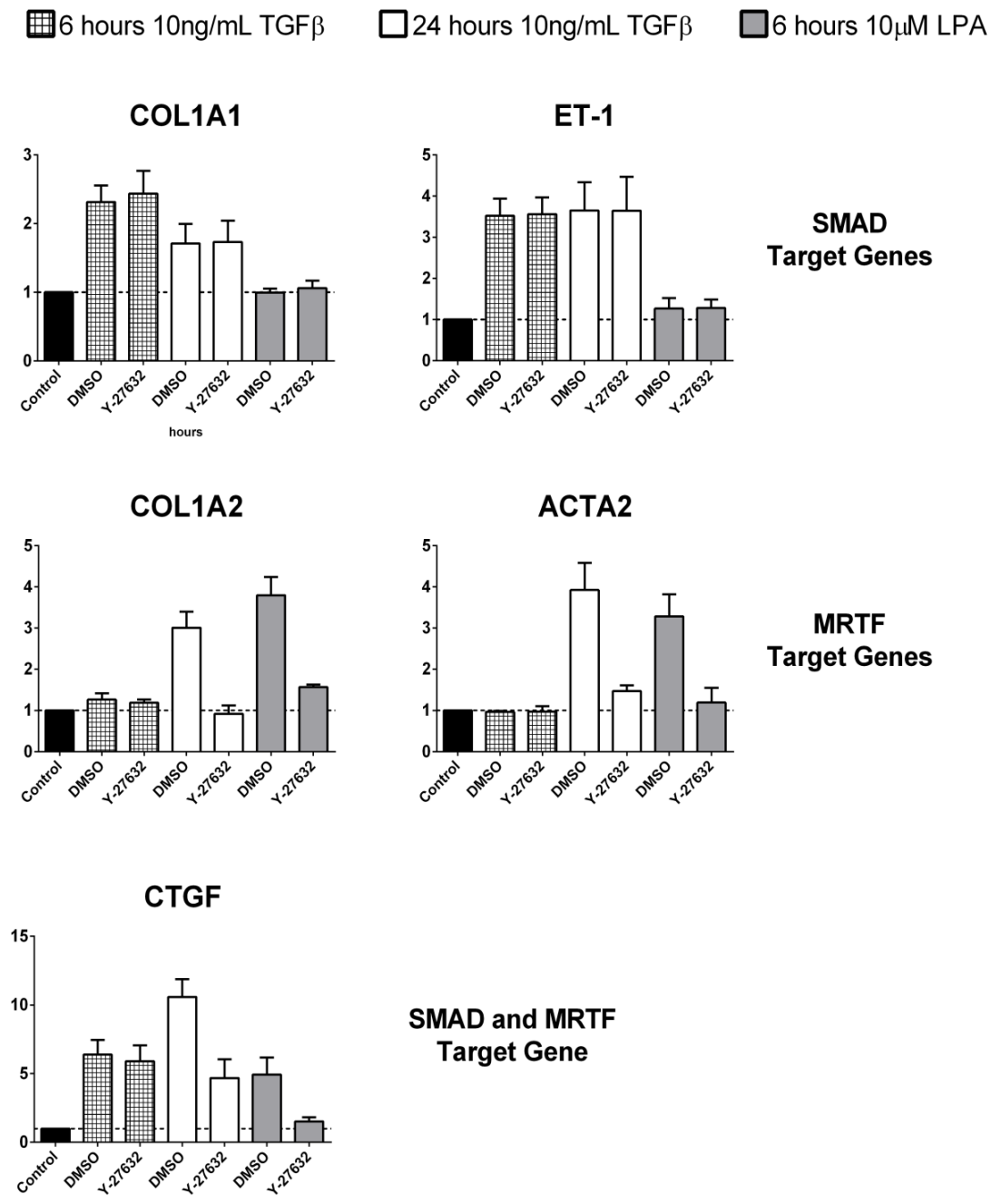

Figure. 2-5. Rho kinase inhibitor blocks TGFβ-induced delayed expression of MRTF target genes COL1A2 and ACT2.

Primary human dermal fibroblasts obtained from healthy donors (≤ passage 6) were stimulated for 6 and 18 hours with 10ng/mL TGFβ or 6 hours with 10μM LPA in 0.5% serum starved medium. To further identify F-actin/MRTF regulated genes 10μM Y-27632 was used to inhibit Rho-kinase at each of the ligand stimulation time points. Based on these results the genes were again clustered into SMAD target genes, MRTF target genes, or combined SMAD/MRTF target genes. Data represents the mean (+/- SEM) of three independent experiments; expression levels were quantified relative to GAPDH and normalized to the untreated control.

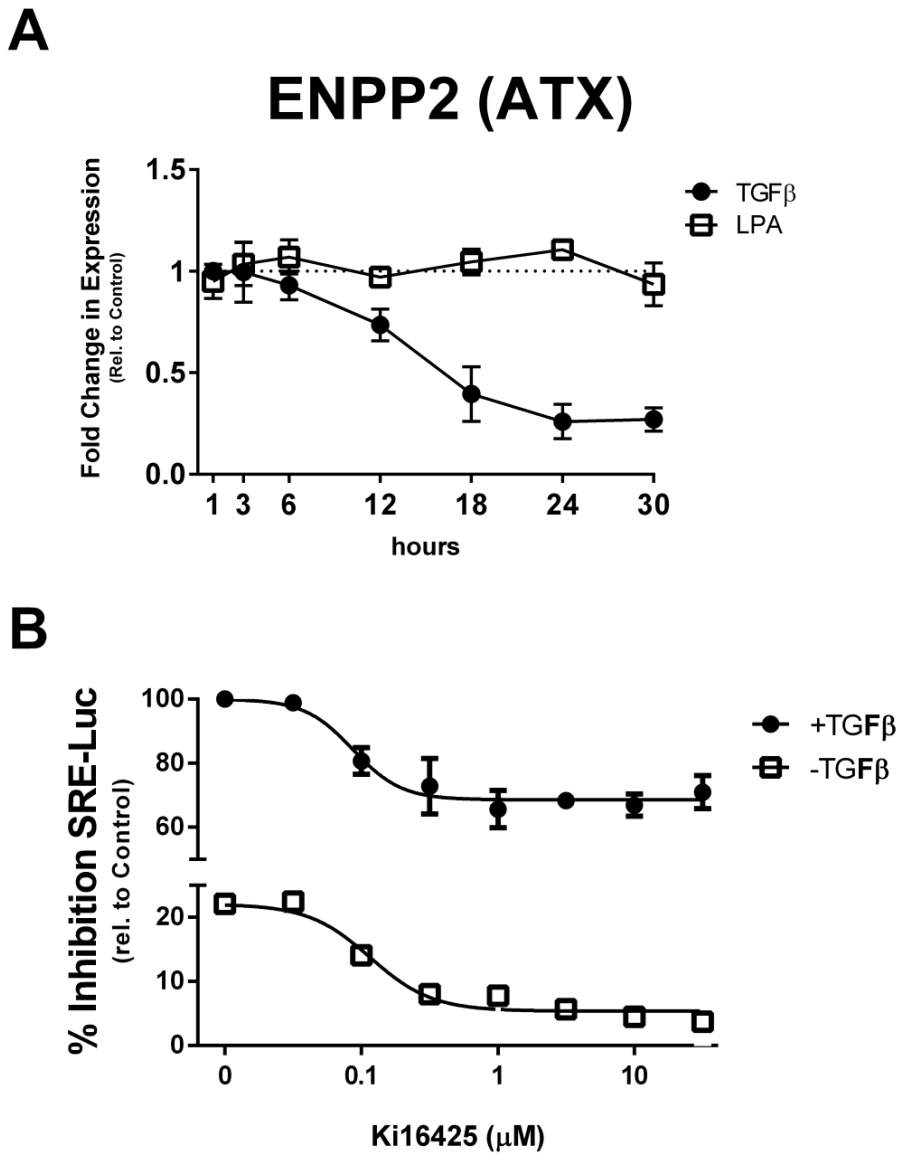

Figure. 2-6. Role of LPA in TGFβ-mediated MRTF activation.

A.) ENPP2 (Autotoxin) expression profile following TGFβ and LPA treatment. Primary human dermal fibroblasts obtained from healthy donors (≤ passage 6) were stimulated for the indicated amount of time with 10ng/mL TGFβ or 10μM LPA in 0.5% serum starved medium. RNA was analyzed by qPCR to determine relative expression levels of ENPP2. Data represents the mean (+/- STD) of two independent experiments; expression levels were quantified relative to GAPDH and normalized to the untreated control. B.) LPA Receptor 1/3 antagonist effect on TGFβ and non-stimulated MRTF activity. NIH-3T3 cells expressing SRE-luciferase were treated for 24 hours with the indicated concentrations of KI16425 +/- 10ng/mL TGFβ for 3 hours. All luciferase experiments were multiplexed with WST-1 to monitor cellular proliferation/toxicity and data represents the mean (+/- SEM) of luciferase luminescence relative to WST-1 absorbance and normalized to the untreated control of three independent experiments.

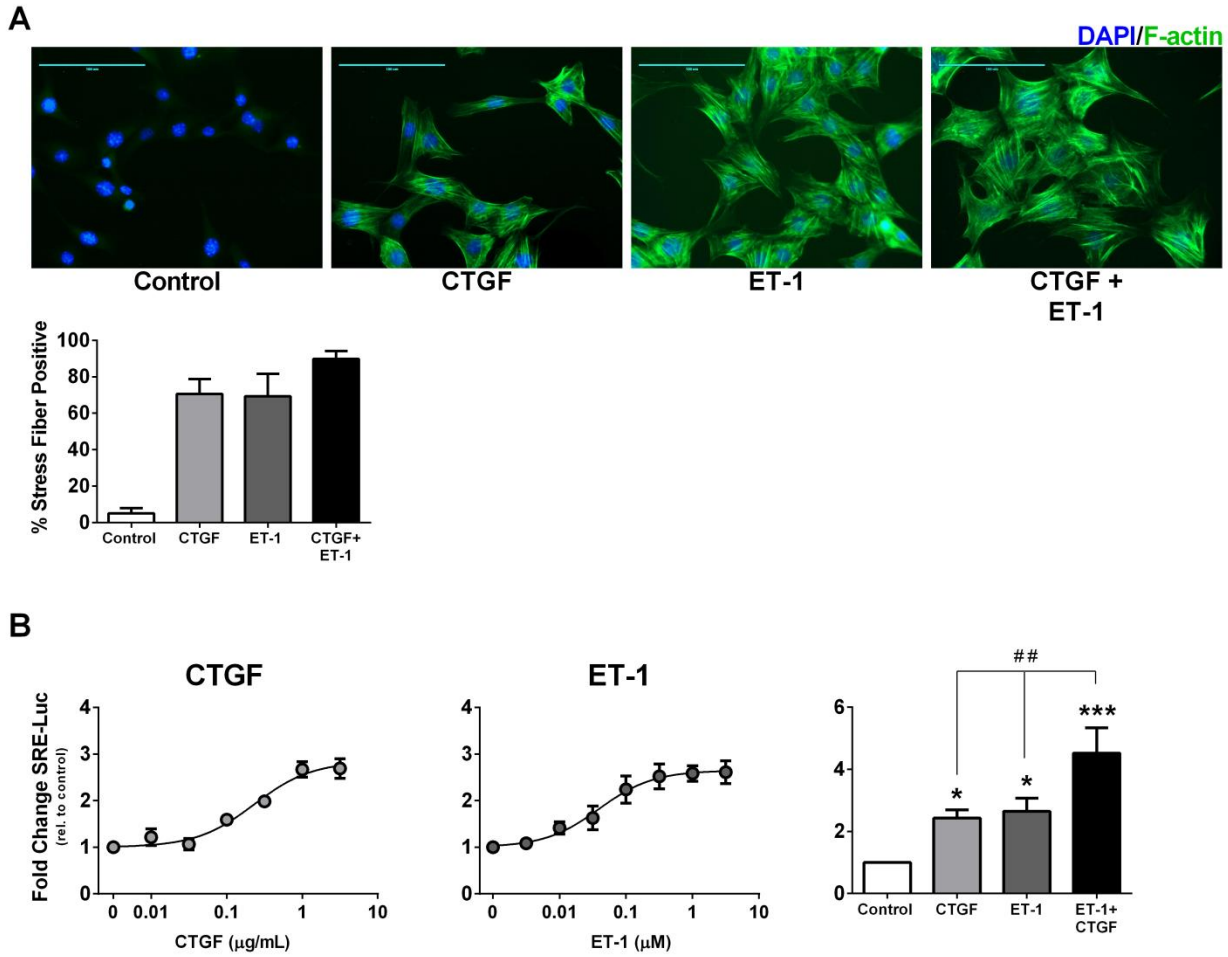

Figure. 2-7. CTGF and ET-1 stimulate actin stress fibers and MRTF/SRF activity.

A.) NIH-3T3 fibroblasts were starved for 24 hours and stimulated for 1 hour with exogenous CTGF (10µg/mL) and/or ET-1 (1µM). F-actin was stained along with DAPI nuclear staining and four images from each experiment were examined for cells which displayed F-actin stress fiber formations. Data represents the mean (+/- STD) from three independent experiments. Shown are representative images from each condition. Scale bar represents 100µm. B.) CTGF and ET-1 dose response curves for activation of MRTF/SRF luciferase. NIH-3T3 fibroblasts were transfected with MRTF specific SRE-Luciferase reporter plasmid and treated with the indicated concentrations of recombinant ET-1 and/or CTGF for 6 hours. All luciferase experiments were multiplexed with WST-1 to monitor cellular proliferation/toxicity and data represents the mean (+/- SEM) of luciferase luminescence relative to WST-1 absorbance and normalized to the untreated control of three independent experiments. (* P< 0.05, *** P< 0.001 vs. control). (## P< 0.01 vs. CTGF or ET-1 alone treatment).

CTGF and ET-1 signaling are both required for TGFβ stimulated stress fibers and MRTF activation.

To determine the role of ET-1 and CTGF in inducing stress fibers and MRTF activity following TGFβ, we tested the endothelin receptor type A (ET_A) antagonist, CI 1020, and a neutralizing antibody (NAb) for CTGF. Cells treated for 3 hours with TGFβ produce pronounced F-actin stress fiber formation, however treatment with the CTGF NAb or CI 1020 partially block this stimulation (Fig. 2-8A). Importantly, combined treatment with the neutralizing antibody and ET_A receptor antagonist further blocks TGFβ stimulated stress fibers. Similarly, CTGF NAb and CI 1020 were able to partially block MRTF acvity (Fig. 2-8B). Unlike the LPA receptor antagonist Ki16425, both the CTGF NAb and CI 1020 have no effect on baseline MRTF activity in the absense of TGFβ (Fig. 2-9). Combined treatment with the CTGF neutralizing antibody and ETA receptor antagonist produced a significantly greater inhibition of TGFβ stimulated MRTF activity than either inhibitor alone. These two mediators together apprear to account for atleast ~80% of the TGF-β stimulated Rho/MRTF activity.

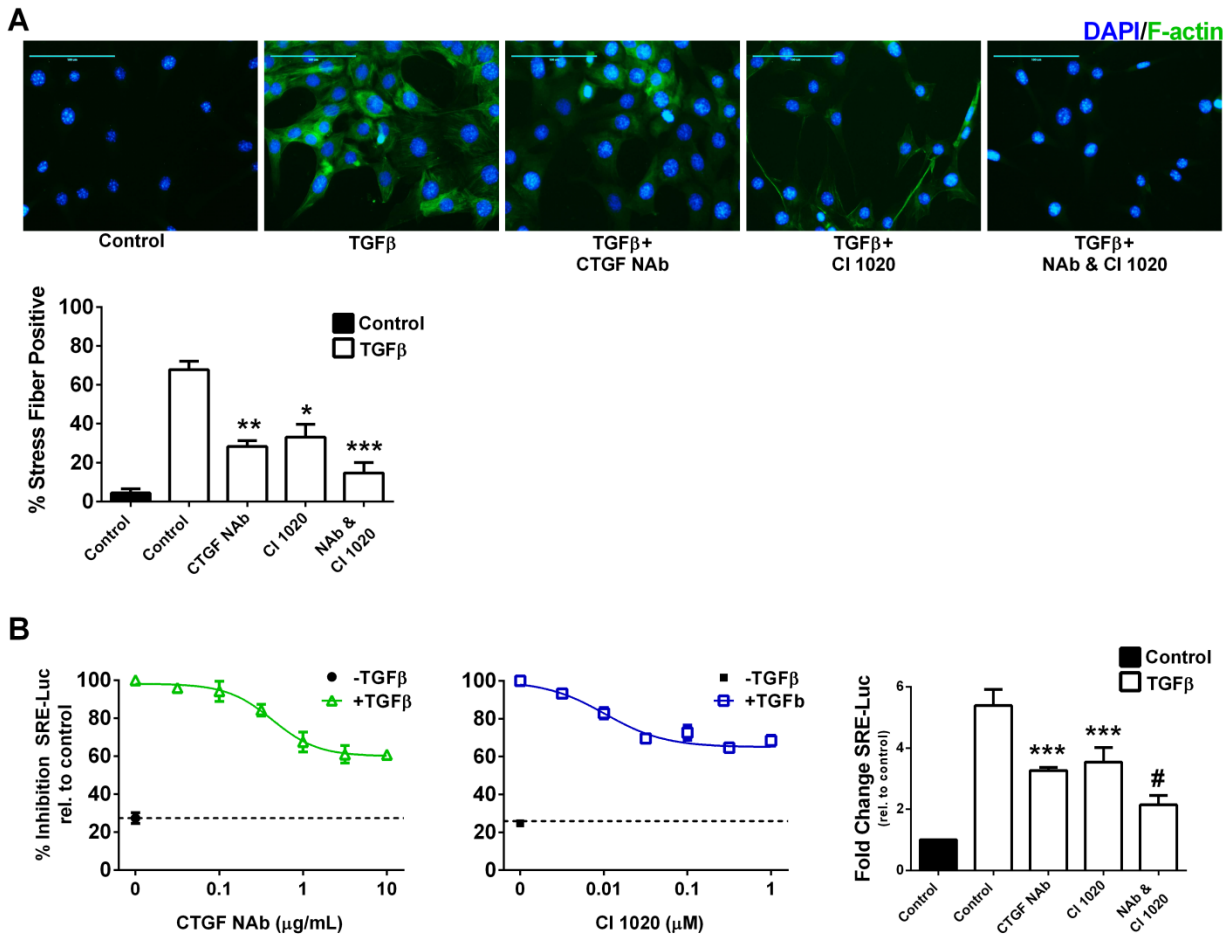

Figure. 2-8. CTGF and ET-1 signaling is essential for TGFβ induced F-actin stress fibers and MRTF/SRF gene transcription.

A.) NIH-3T3 fibroblasts were starved for 24 hours in 0.5% serum medium +/- 10μg/mL CTGF neutralizing antibody (CTGF NAb) and/or 100nM ET_A antagonist, CI 1020, and stimulated with 10ng/mL TGFβ for three hours. F-actin was stained along with DAPI nuclear staining and four images from each experiment were examined for cells which displayed F-actin stress fiber formations. Data represents the mean (+/- STD) from three independent experiments. (* P< 0.05, ** P< 0.01, *** P<0.001 vs. TGFβ stimulated control). Shown are representative images from each condition. Scale bar represents 100μm. B.) CTGF neutralizing antibody blocks TGFβ induced MRTF activity. NIH-3T3 cells expressing SRE-luciferase were treated for 18 hours with the indicated concentrations of a CTGF neutralizing antibody and/or 100nM CI 1020 and 10ng/mL TGFβ. All luciferase experiments were multiplexed with WST-1 to monitor cellular proliferation/toxicity and data represents the mean (+/- SEM) of luciferase luminescence relative to WST-1 absorbance and normalized to the untreated control of three independent experiments. (*** P< 0.001 vs. TGFβ stimulated control). (# P<0.05 vs. CTGF NAb or CI 1020).

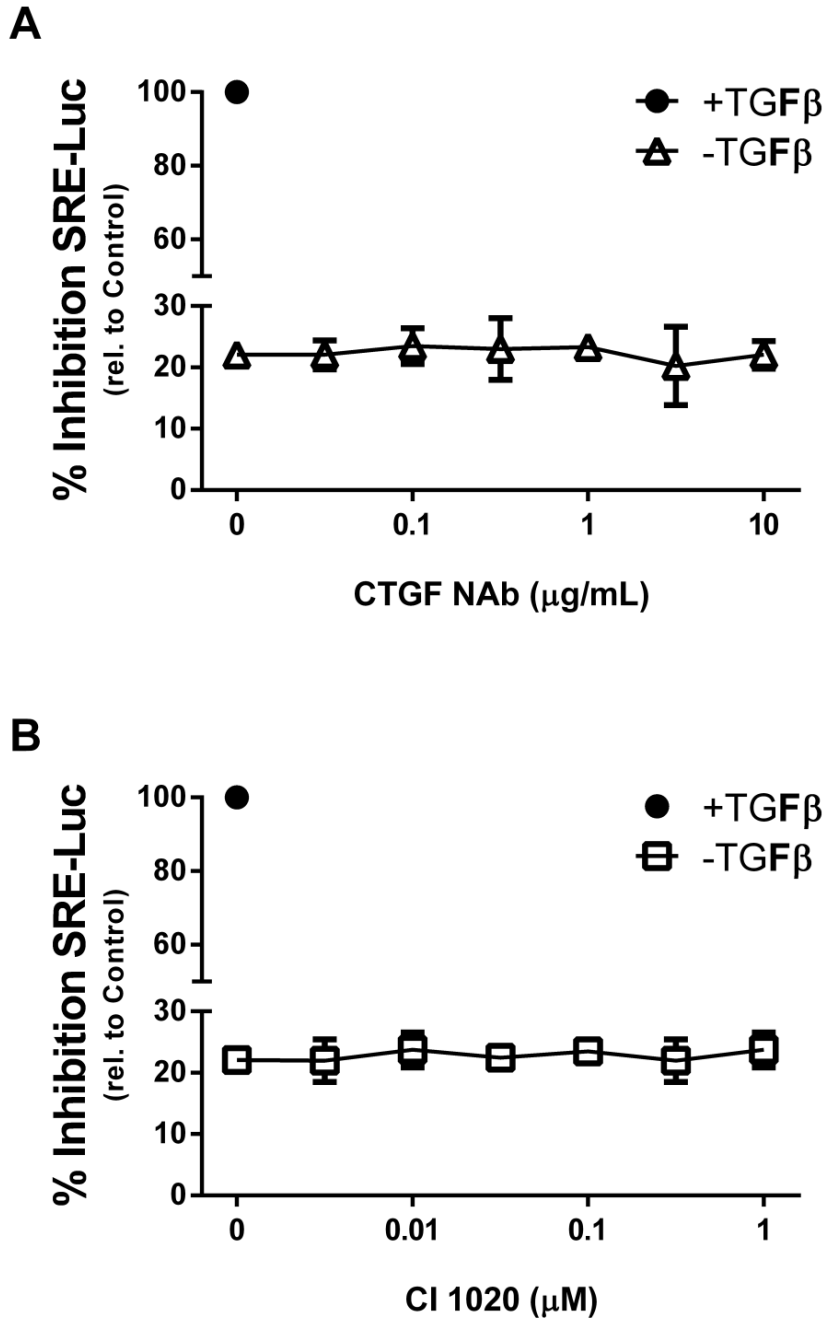

Figure. 2-9. CTGF neutralizing antibody and endothelin antagonist CI 1020 do not inhibit MRTF/SRF activity in the absence of TGFβ.

NIH-3T3 cells expressing SRE-luciferase were treated for 24 hours with the indicated concentrations of A.) CTGF NAb or B.) CI 1020 +/- 10ng/mL TGFβ for 3 hours. All luciferase experiments were multiplexed with WST-1 to monitor cellular proliferation/toxicity and data represents the mean (+/- SEM) of luciferase luminescence relative to WST-1 absorbance and normalized to the untreated control of three independent experiments.

Discussion

TGFβ continues to garner status as the master cytokine involved in tissue fibrosis associated with IPF and systemic sclerosis. Understanding the mechanisms that mediate TGFβ driven fibrosis is therefore extremely crucial. Transcriptional programs that mediate the transformation of myofibroblasts have potential to be prime targets to treat these diseases; here we set out to characterize the activation of MRTF/SRF regulated gene expression downstream of TGFβ. The pathways following TGFβ receptor activation involve a complex crosstalk between canonical and non-canonical signaling (38). These networks are separated not only by the mediators which traffic the signals but also temporally, as we show here. One important non-canonical mediator downstream of TGFβ signaling is Rho GTPase. Previous work has shown that TGFβ activates hallmarks of Rho signaling; actin stress fiber formations, ROCK phosphorylation, and MRTF/SRF gene transcription (27-29). As shown here, TGFβ mediated activation of Rho-kinase dependent stress fibers peaked around three hours, but it was also relatively stable out to 24 hours. In contrast, LPA induces a rapid but transient activation of Rho-GTPase peaking within two minutes but turned off within ten (39). GPCR deactivation is carried out through a variety of mechanisms involving receptor phosphorylation, internalization, leading to either recycling or degradation (40). Endothelin (ET-1), which was shown to play a role as one mediator of TGFβ induced stress fibers also signals through a GPCR, ET_A. One major difference between LPA and ET-1 in this system however is the magnitude to which they can activate MRTF/SRF-mediated gene transcription (8 vs. 3 fold respectively).

The F-actin stress fibers and MRTF/SRF activation following TGFβ stimulation were completely blocked by Rho-kinase (ROCK) inhibitor Y-27632. This efficacy is also evident in previous work in vitro (41), as well as in vivo, in models of IPF (42), and hepatic fibrosis (43). One potential problem for selective ROCK inhibitors as they move towards clinical trials however is they have previously been found to only partially inhibit MRTF/SRF gene transcription depending on what level the pathway is stimulated (44,45).

The effects of the ROCK inhibitor also helped differentiate between SMAD or MRTF mechanisms for the profibrotic genes upregulated following TGFβ treatment. Here we saw COL1A2 and ACTA2 expression to be dependent on Rho-kinase while COL1A1 and EDN1 to be ROCK independent. This was also in agreement with the time course of their expression profiles. COL1A2 and ACTA2 were relatively delayed, consistent with the need to produce a secondary mediator to activate Rho and MRTF. CTGF however was identified as being regulated by both SMAD and MRTF. Within the promoter sequence for CTGF, there are binding elements for a variety of transcription factors have been predicted including: SMAD, SRF, AP-1, SP-1, and TATA box binding sites (46). Experimentally however, only the SMAD and MRTF/SRF binding elements have been functionally shown to induce CTGF expression (47-49). Interestingly while the initial expression of CTGF following TGFβ is SMAD-dependent, the constitutive expression observed in scleroderma patient derived fibroblasts is independent of SMAD (12,49). This is in good agreement with what we find here regarding a shift from SMAD-regulated expression to MRTF occurring around 12 hours following TGFβ stimulation of primary dermal fibroblasts. This also supports the possibility that therapeutic targeting of scleroderma patients using TGFβ inhibiting agents may lack efficacy because the genetic program has shifted over to a Rho/MRTF mechanisms.

We have highlighted two known TGFβ/SMAD target gene products that are capable of stimulating stress fibers and MRTF/SRF-regulated gene transcription, ET-1 and CTGF. Similar to LPA, ET-1 signals through GPCRs that can couple to both $G_{12/13}$ and $G_{q/11}$ family G-proteins, (50), and in the context of stress fibers and ROCK phosphorylation, both mechanisms maybe be important (51). CTGF signaling mechanisms, however, are much less well established, especially concerning downstream activation of Rho GTPase. CTGF has been shown to directly bind to or signal though fibroblast growth factor receptor 2, tyrosine kinase receptor TrkA, and integrins αvβ3, α5β1, α4β1 (37,52-55). Here we find that CTGF is able to stimulate prominent stress fiber formation and MRTF/SRF gene transcription very rapidly, similar to GPCR systems. It should be acknowledged that CTGF is also functioning as a positive feedback mediator where CTGF autocrine signaling stimulates stress fiber formation leading to MRTF/SRF activation that, as previously discussed stimulates expression of CTGF.

Relevant to therapeutic approaches, we have shown that with combined treatment with an endothelin receptor type A antagonist and a CTGF neutralizing antibody almost completely blocks the TGFβ mediated stress fiber formation and MRTF activation. Endothelin antagonists have been well studied for the treatment of tissue fibrosis (56). Intriguingly, endothelin antagonists are clinically approved and have been used with minimal side effects for several years. Several clinical trials on the use of non-selective and selective endothelin antagonists against IPF and related diseases have been attempted but terminated early due to lack of efficacy (57-59). CTGF signaling inhibitors or antagonists have been difficult to develop because of the multitude of receptors to which CTGF binds. Preliminary studies determining the efficacy of blocking CTGF have used genetic knockdowns and have shown efficacy in models of cardiac, renal, and liver fibrosis (60-62). Based on these findings, a humanized anti-CTGF antibody has

been developed. Results are currently pending in phase II clinical trials of FG-3029 in IPF (ClinicalTrails.gov NCT01890265) and liver fibrosis (ClinicalTrails.gov NCT01217632). Based on our findings here, a combined approach of treating patients with a selective ET_A receptor antagonist and a CTGF neutralizing antibody would provide the greatest efficacy against TGFβ-mediated fibrosis. An alternative approach would be targeting signaling downstream of Rho, where these pathways converge. MRTF/SRF mediated gene transcription has been shown to be the essential step activating fibroblasts (30-32). Small-molecule inhibitors for the MRTF pathway previously developed in our lab block myofibroblast transformation, expression of pro-fibrotic genes including CTGF, COL1A2, and ACTA2 *in vitro*, and show efficacy in experimental models of peritoneal, and dermal fibrosis *in vivo* (63-65).

Taken together, these data suggest pro-fibrotic disorders like IPF and scleroderma are driven by complex signaling mechanisms which feedback and cross-talk each other through spatial and temporal ranges. This essentially offers a multitude of receptors and pathways which can be used for targeted therapies but also advocates against blocking a specific upstream receptor system as a single therapy. Continued investigations into non-canical and downstream mediators of TGFβ and other stimulatory cytokines will lead to well-designed therapeutic approaches for these debilitating diseases.

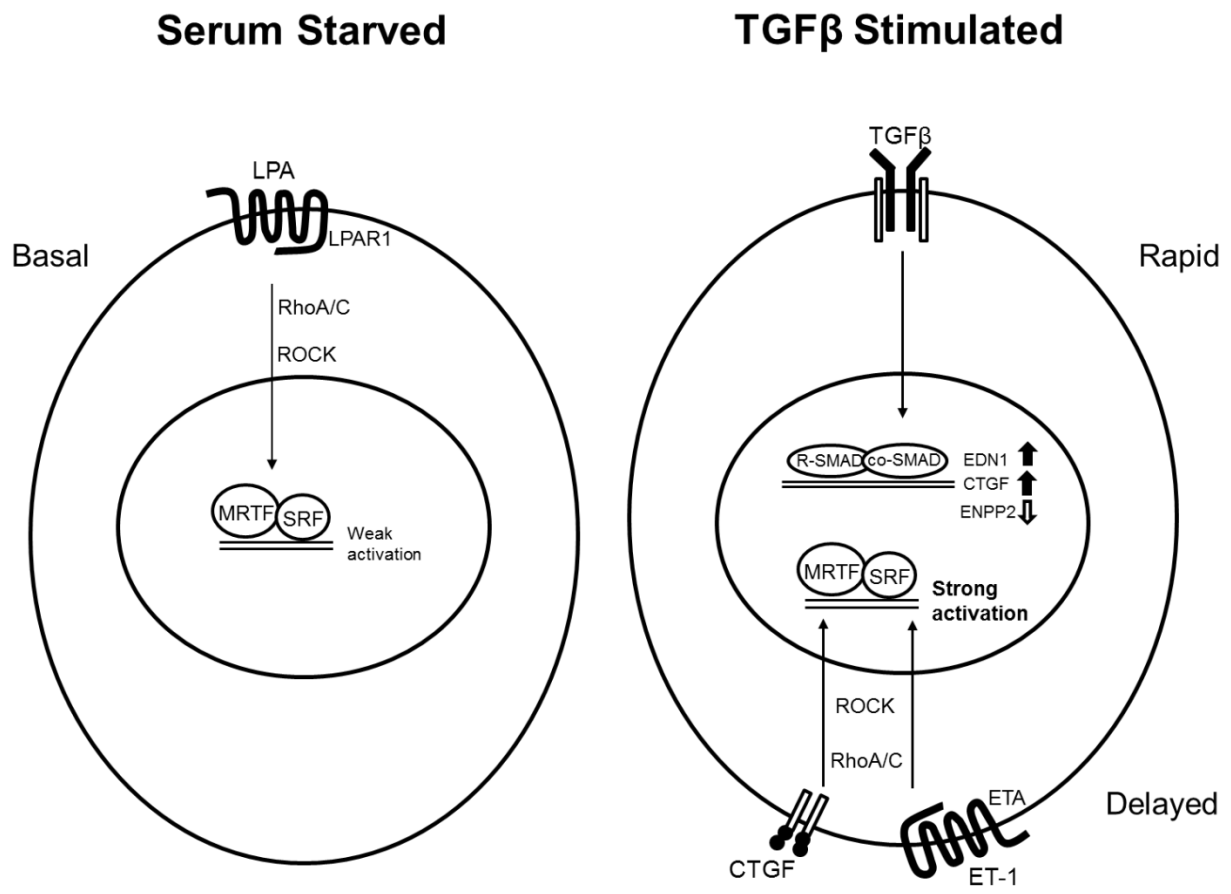

Figure. 2-10. Current model of TGFβ stimulation of the Rho/MRTF pathway.

In the absence of TGFβ, serum starved fibroblasts display very modest activation of the Rho/MRTF pathway, mediated by basal levels of LPA. TGFβ treatment produces a rapid transcription of SMAD family target genes including EDN1 (ET-1) and CTGF. TGFβ treatment reduces expression of ENPP2 (autotaxin) which is responsible for LPA synthesis. Newly synthesized ET-1 and CTGF stimulate strong, but delayed activation of the Rho/MRTF pathway.

References

1. Fan, M. H., Feghali-Bostwick, C. A., and Silver, R. M. (2014) *Curr Opin Rheumatol* **26**, 630-636

2. Renzoni, E., Srihari, V., and Sestini, P. (2014) *F1000Prime Rep* **6**, 69

3. Ryu, J. H., Moua, T., Daniels, C. E., Hartman, T. E., Yi, E. S., Utz, J. P., and Limper, A. H. (2014) *Mayo Clin Proc* **89**, 1130-1142

4. Lawrance, I. C., Rogler, G., Bamias, G., Breynaert, C., Florholmen, J., Pellino, G., Reif, S., Speca, S., and Latella, G. (2014) *J Crohns Colitis*

5. Kendall, R. T., and Feghali-Bostwick, C. A. (2014) *Front Pharmacol* **5**, 123

6. Huang, C., and Ogawa, R. (2012) *Connect Tissue Res* **53**, 187-196

7. Darby, I. A., and Hewitson, T. D. (2007) *Int Rev Cytol* **257**, 143-179

8. Fernandez, I. E., and Eickelberg, O. (2012) *Proc Am Thorac Soc* **9**, 111-116

9. Ueha, S., Shand, F. H., and Matsushima, K. (2012) *Front Immunol* **3**, 71

10. Gonzalez, D. M., and Medici, D. (2014) *Sci Signal* **7**, re8

11. Verrecchia, F., and Mauviel, A. (2004) *Cell Signal* **16**, 873-880

12. Holmes, A., Abraham, D. J., Sa, S., Shiwen, X., Black, C. M., and Leask, A. (2001) *J Biol Chem* **276**, 10594-10601

13. Rodriguez-Pascual, F., Redondo-Horcajo, M., and Lamas, S. (2003) *Circ Res* **92**, 1288-1295

14. Rudnicka, L., Varga, J., Christiano, A. M., Iozzo, R. V., Jimenez, S. A., and Uitto, J. (1994) *J Clin Invest* **93**, 1709-1715

15. Higley, H., Persichitte, K., Chu, S., Waegell, W., Vancheeswaran, R., and Black, C. (1994) *Arthritis Rheum* **37**, 278-288

16. Molina-Molina, M., Lario, S., Luburich, P., Ramirez, J., Carrion, M. T., and Xaubet, A. (2006) *Arch Bronconeumol* **42**, 380-383

17. Zhang, Y. E. (2009) *Cell Res* **19**, 128-139

18. Etienne-Manneville, S., and Hall, A. (2002) *Nature* **420**, 629-635

19. Miralles, F., Posern, G., Zaromytidou, A. I., and Treisman, R. (2003) *Cell* **113**, 329-342

20. Wang, D. Z., Li, S., Hockemeyer, D., Sutherland, L., Wang, Z., Schratt, G., Richardson, J. A., Nordheim, A., and Olson, E. N. (2002) *Proc Natl Acad Sci U S A* **99**, 14855-14860

21. Luchsinger, L. L., Patenaude, C. A., Smith, B. D., and Layne, M. D. (2011) *J Biol Chem* **286**, 44116-44125

22. Sun, Q., Chen, G., Streb, J. W., Long, X., Yang, Y., Stoeckert, C. J., Jr., and Miano, J. M. (2006) *Genome Res* **16**, 197-207

23. Esnault, C., Stewart, A., Gualdrini, F., East, P., Horswell, S., Matthews, N., and Treisman, R. (2014) *Genes Dev* **28**, 943-958

24. Hinkel, R., Trenkwalder, T., Petersen, B., Husada, W., Gesenhues, F., Lee, S., Hannappel, E., Bock-Marquette, I., Theisen, D., Leitner, L., Boekstegers, P., Cierniewski, C., Muller, O. J., le Noble, F., Adams, R. H., Weinl, C., Nordheim, A., Reichart, B., Weber, C., Olson, E., Posern, G., Deindl, E., Niemann, H., and Kupatt, C. (2014) *Nat Commun* **5**, 3970

25. Siehler, S. (2009) *Br J Pharmacol* **158**, 41-49

26. Ridley, A. J., and Hall, A. (1992) *Cell* **70**, 389-399

27. Vaughan, M. B., Howard, E. W., and Tomasek, J. J. (2000) *Exp Cell Res* **257**, 180-189

28. Sandbo, N., Lau, A., Kach, J., Ngam, C., Yau, D., and Dulin, N. O. (2011) *Am J Physiol Lung Cell Mol Physiol* **301**, L656-666

29. Bhowmick, N. A., Ghiassi, M., Bakin, A., Aakre, M., Lundquist, C. A., Engel, M. E., Arteaga, C. L., and Moses, H. L. (2001) *Mol Biol Cell* **12**, 27-36

30. Small, E. M. (2012) *J Cardiovasc Transl Res* **5**, 794-804

31. Small, E. M., Thatcher, J. E., Sutherland, L. B., Kinoshita, H., Gerard, R. D., Richardson, J. A., Dimaio, J. M., Sadek, H., Kuwahara, K., and Olson, E. N. (2010) *Circ Res* **107**, 294-304

32. Sandbo, N., Kregel, S., Taurin, S., Bhorade, S., and Dulin, N. O. (2009) *Am J Respir Cell Mol Biol* **41**, 332-338

33. Suzuki, N., Nakamura, S., Mano, H., and Kozasa, T. (2003) *Proc Natl Acad Sci U S A* **100**, 733-738

34. Nagai, J., Uchida, H., Matsushita, Y., Yano, R., Ueda, M., Niwa, M., Aoki, J., Chun, J., and Ueda, H. (2010) *Mol Pain* **6**, 78

35. Miao, L., Dai, Y., and Zhang, J. (2002) *Am J Physiol Heart Circ Physiol* **283**, H983-989

36. Kawanabe, Y., Okamoto, Y., Nozaki, K., Hashimoto, N., Miwa, S., and Masaki, T. (2002) *Mol Pharmacol* **61**, 277-284

37. Chen, P. S., Wang, M. Y., Wu, S. N., Su, J. L., Hong, C. C., Chuang, S. E., Chen, M. W., Hua, K. T., Wu, Y. L., Cha, S. T., Babu, M. S., Chen, C. N., Lee, P. H., Chang, K. J., and Kuo, M. L. (2007) *J Cell Sci* **120**, 2053-2065

38. Munger, J. S., and Sheppard, D. (2011) *Cold Spring Harb Perspect Biol* **3**, a005017

39. Van Leeuwen, F. N., Olivo, C., Grivell, S., Giepmans, B. N., Collard, J. G., and Moolenaar, W. H. (2003) *J Biol Chem* **278**, 400-406

40. Ritter, S. L., and Hall, R. A. (2009) *Nat Rev Mol Cell Biol* **10**, 819-830

41. Akhmetshina, A., Dees, C., Pileckyte, M., Szucs, G., Spriewald, B. M., Zwerina, J., Distler, O., Schett, G., and Distler, J. H. (2008) *Arthritis Rheum* **58**, 2553-2564

42. Bei, Y., Hua-Huy, T., Duong-Quy, S., Nguyen, V. H., Chen, W., Nicco, C., Batteux, F., and Dinh-Xuan, A. T. (2013) *Pulm Pharmacol Ther* **26**, 635-643

43. Tada, S., Iwamoto, H., Nakamuta, M., Sugimoto, R., Enjoji, M., Nakashima, Y., and Nawata, H. (2001) *J Hepatol* **34**, 529-536

44. Bell, J. L., Haak, A. J., Wade, S. M., Kirchhoff, P. D., Neubig, R. R., and Larsen, S. D. (2013) *Bioorg Med Chem Lett* **23**, 3826-3832

45. Evelyn, C. R., Wade, S. M., Wang, Q., Wu, M., Iniguez-Lluhi, J. A., Merajver, S. D., and Neubig, R. R. (2007) *Mol Cancer Ther* **6**, 2249-2260

46. Blom, I. E., van Dijk, A. J., de Weger, R. A., Tilanus, M. G., and Goldschmeding, R. (2001) *Mol Pathol* **54**, 192-196

47. Grotendorst, G. R., Okochi, H., and Hayashi, N. (1996) *Cell Growth Differ* **7**, 469-480

48. Holmes, A., Abraham, D. J., Sa, S., Shiwen, X., Black, C. M., and Leask, A. (2001) *J Biol Chem* **276**, 10594-10601

49. Leask, A., Sa, S., Holmes, A., Shiwen, X., Black, C. M., and Abraham, D. J. (2001) *Mol Pathol* **54**, 180-183

50. Shraga-Levine, Z., and Sokolovsky, M. (2000) *Cell Mol Neurobiol* **20**, 305-317

51. Suzuki, E., Nagata, D., Kakoki, M., Hayakawa, H., Goto, A., Omata, M., and Hirata, Y. (1999) *Circ Res* **84**, 611-619

52. Aoyama, E., Kubota, S., and Takigawa, M. (2012) *FEBS Lett* **586**, 4270-4275

53. Wahab, N. A., Weston, B. S., and Mason, R. M. (2005) *J Am Soc Nephrol* **16**, 340-351

54. Gao, R., and Brigstock, D. R. (2006) *Gut* **55**, 856-862

55. Chen, Y., Abraham, D. J., Shi-Wen, X., Pearson, J. D., Black, C. M., Lyons, K. M., and Leask, A. (2004) *Mol Biol Cell* **15**, 5635-5646

56. Clozel, M., and Salloukh, H. (2005) *Ann Med* **37**, 2-12

57. King, T. E., Jr., Behr, J., Brown, K. K., du Bois, R. M., Lancaster, L., de Andrade, J. A., Stahler, G., Leconte, I., Roux, S., and Raghu, G. (2008) *Am J Respir Crit Care Med* **177**, 75-81

58. King, T. E., Jr., Brown, K. K., Raghu, G., du Bois, R. M., Lynch, D. A., Martinez, F., Valeyre, D., Leconte, I., Morganti, A., Roux, S., and Behr, J. (2011) *Am J Respir Crit Care Med* **184**, 92-99

59. Raghu, G., Behr, J., Brown, K. K., Egan, J. J., Kawut, S. M., Flaherty, K. R., Martinez, F. J., Nathan, S. D., Wells, A. U., Collard, H. R., Costabel, U., Richeldi, L., de Andrade, J., Khalil, N., Morrison, L. D., Lederer, D. J., Shao, L., Li, X., Pedersen, P. S., Montgomery, A. B., Chien, J. W., and O'Riordan, T. G. (2013) *Ann Intern Med* **158**, 641-649

60. Lang, C., Sauter, M., Szalay, G., Racchi, G., Grassi, G., Rainaldi, G., Mercatanti, A., Lang, F., Kandolf, R., and Klingel, K. (2008) *J Mol Med (Berl)* **86**, 49-60

61. Okada, H., Kikuta, T., Kobayashi, T., Inoue, T., Kanno, Y., Takigawa, M., Sugaya, T., Kopp, J. B., and Suzuki, H. (2005) *J Am Soc Nephrol* **16**, 133-143

62. Uchio, K., Graham, M., Dean, N. M., Rosenbaum, J., and Desmouliere, A. (2004) *Wound Repair Regen* **12**, 60-66

63. Haak, A. J., Tsou, P. S., Amin, M. A., Ruth, J. H., Campbell, P., Fox, D. A., Khanna, D., Larsen, S. D., and Neubig, R. R. (2014) *J Pharmacol Exp Ther* **349**, 480-486

64. Johnson, L. A., Rodansky, E. S., Haak, A. J., Larsen, S. D., Neubig, R. R., and Higgins, P. D. (2014) *Inflamm Bowel Dis* **20**, 154-165

65. Sakai, N., Chun, J., Duffield, J. S., Wada, T., Luster, A. D., and Tager, A. M. (2013) *FASEB J* **27**, 1830-1846

CHAPTER III

TARGETING THE MYOFIBROBLAST GENETIC SWITCH: INHIBITORS OF MRTF/SRF-REGULATED GENE TRANSCRIPTION PREVENT FIBROSIS IN A MURINE MODEL OF SKIN INJURY

Abstract

Systemic sclerosis (SSc) or scleroderma, like many fibrotic disorders, lacks effective therapies. Current trials focus on anti-inflammatory drugs or targeted approaches aimed at one of the many receptor mechanisms initiating fibrosis. In light of evidence that a myocardin-related transcription factor (MRTF) and serum response factor (SRF)-regulated gene transcriptional program induced by Rho GTPases is essential for myofibroblast activation, we explore the hypothesis that inhibitors of this pathway may represent novel antifibrotics. MRTF-SRF-regulated genes show spontaneously increased expression in primary dermal fibroblasts from patients with diffuse cutaneous SSc. A novel small-molecule inhibitor of MRTF/SRF-regulated transcription (CCG-203971) inhibits expression of connective tissue growth factor (CTGF), alpha-smooth muscle actin (α-SMA), and collagen 1 (COL1A2) in both SSc fibroblasts and in LPA- and transforming growth factor β (TGFβ)-stimulated fibroblasts. *In vivo* treatment with CCG-203971 also prevented bleomycin-induced skin thickening and collagen deposition. Thus targeting the MRTF/SRF gene transcription pathway could provide an efficacious new approach to therapy for SSc and other fibrotic disorders.

Introduction

Systemic sclerosis (scleroderma, SSc) is a multisystem autoimmune disorder that can cause fibrosis of the skin and internal organ systems (lungs, heart, kidneys, and gastrointestinal system). It has the highest case fatality of any rheumatic disease. SSc predominately affects women (4-8:1) and increases with age. The precise pathogenesis of SSc is yet to be defined but the major clinical features of SSc— collagen production, vascular damage and inflammation/autoimmunity—require environmental triggers and genetic effects which interact with the three cardinal features of the disease at several points (1). Generally, there is initial inflammation but fibrosis persists even after the inflammation has resolved or has been suppressed by medications (2,3). This has led to the concept that understanding and targeting the fibrosis mechanism *per se* will be critical to successful therapies (2-4).

A central feature of virtually all diseases of fibrosis is the activation of fibroblasts and transition into myofibroblasts (2,4-10). The expression of alpha-smooth muscle actin (α-SMA) is a widely recognized marker for this transition but it also contributes to the maintenance of fibrosis (4-7,9,11). There are multiple signaling pathways that induce myofibroblast transition. TGFβ is a critical mediator but lysophosphatidic acid (LPA), endothelin, thombin, angiotensin, and connective tissue growth factor (CTGF) have all been implicated (2-4). Additionally, tissue stiffness has been identified as a positive feedback mechanism that leads to further myofibroblast activation – probably through integrins and focal adhesion kinase (FAK) mechanisms (2,11,12).

Emerging evidence implicates gene transcription induced by serum response factor (SRF) as a critical driver of myofibroblast activation by nearly all of these mechanisms (13-15). Indeed, key genes involved in fibrosis are direct SRF targets including CTGF, COL1A2, and even

ACTA2, the gene for α-SMA itself. This concept of a central role for SRF helps rationalize the complex signaling mechanisms that have been implicated in fibrosis. SRF-regulated gene expression is dependent on Rho-GTPase stimulated nuclear localization of its transcriptional coactivator MRTF. RhoA appears to be a convergent downstream mediator activated by virtually all of the signal pathways controlling the of myofibroblast transition (12,13,15,16). G protein-coupled receptors for LPA, endothelin, thrombin, angiotensin and even chemokines activate RhoA (17,18). Other factors important in fibrosis including TGFβ and FAK also modulate MRTF/SRF activity through activation of Rho signaling and actin dynamics (19-21) which in turn drives expression of connective tissue growth factor (CTGF or CCN2) which synergizes with TGFβ in its pro-fibrotic actions (22-24). Indeed, recent evidence suggests that CTGF release from SSc endothelial cells can enhance fibrosis, providing a connection between the vascular and mesenchymal attributes of SSc (24).

Disruption of the Rho pathway with ROCK inhibitors has reversed myofibroblast differentiation *in vitro* and fibrosis in several animal models (13,14,25-29). We recently identified, in high throughput screens, a compound, CCG-1423, which blocks MRTF nuclear localization by interfering with the microtubule associated monooxygenase, calponin and LIM domain containing 2 (MICAL-2), mediated regulation of intranuclear actin polymerization (30,31). CCG-1423 is more effective than ROCK inhibitors in reducing SRF-mediated transcription (30). Several groups have used this compound to interdict myofibroblast formation (16,29) and it was recently shown to have *in vivo* activity in a chlorhexidine gluconate model of peritoneal fibrosis (20). We have now optimized this chemical series to reduce off-target toxicity (32,33).

In the present study, we demonstrate in human SSc dermal fibroblasts that there is spontaneous activation of an MRTF-regulated gene transcription program. CCG-203971, a new MRTF/SRF-gene transcription inhibitor, reverses the myofibroblast phenotype of both TGFβ-stimulated normal dermal fibroblasts as well as the spontaneous activation of SSc-derived fibroblasts *in vitro*. Furthermore, it prevents the development of fibrosis in a mouse bleomycin skin injury model. These results suggest that targeting the MRTF/SRF gene transcription mechanism may provide a novel and particularly effective approach to antifibrotic therapy.

Materials and Methods

Patient sample and Animal Use

All SSc patients fulfilled the American College of Rheumatology criteria for classification of SSc (34). Two punch biopsies (4 mm) were taken from the forearm of mixed sex, SSc patients with the diffuse cutaneous variant. Normal skin tissue was obtained similarly from mixed sex, healthy volunteers. Written informed consent was obtained for all subjects and the study was approved by the University of Michigan Institutional Review Board. All experiments performed with animals were done with approval from the University of Michigan Committee on Use and Care of Animals. C57BL/6 mice were used for the bleomycin prevention model.

Primary Cell Culture

Both normal and SSc dermal fibroblasts were isolated from human skin (ages 53.4±13.1 years for SSc; 47.5±18.4 years for normal). The tissue was digested using enzyme digestion solution containing 2.4 units/ml dispase, 650 units/ml type II collagenase, and 10,000 Dornase units/ml DNase. Dermal fibroblasts were maintained in DMEM with 10% fetal bovine serum (FBS), penicillin, and streptomycin. Cells of passages between 4 and 6 were used.

qPCR

Dermal fibroblasts ($1.0X10^5$) were plated into 6-well plates (Falcon #353046) and starved for 24 hours in DMEM containing 0.5% FBS with the indicated concentrations of CCG-203971, 0.1% DMSO, and stimulated with 10ng/mL TGFβ1 (R&D Systems). Cells were lysed and RNA was isolated using the RNeasy® kit (Qiagen) following the manufacturer's directions. DNAse-treated RNA was quantified using a NanoDrop® spectrophotometer and 1µg was used as a template for

synthesizing cDNA utilizing the Taqman® Reverse-Transcription Reagents kit (Invitrogen). SYBR green qPCR (SABiosciences) was performed using a Stratagene Mx3000P (Agilent Technologies). Ct values were determined and mRNA expression calculated relative to that of GAPDH. Primer sequences were: GAPDH; 5' GGAAGGGCTCATGACCACAG. 3' ACAGTCTTCTGGGTGGCAGTG. CTGF; 5' CAGAGTGGAGCGCCTGTT. 3' CTGCAGGAGGCGTTGTCA. ACTA2; 5' AATGCAGAAGGAGATCACGC. 3' TCCTGTTTGCTGATCCACATC. COL1A2-hn; 5' CTTGCAGTAACCTTATGCCTAGCA. 3' CCCATCTAACCTCTCTACCCAGTCT. EDN1; 5' CTTCGTTTTCCTTTGGGTTCAG. 3' GCTCAGCGCCTAAGACTG. COL1A1-hn; 5' CTTGCAGTAACCTTATGCCTAGCA. 3' CCAACTCCTTTTCCATCATACTGA. All mRNA values were normalized to a control (either normal fibroblasts or a vehicle control) run the same day.

Proliferation

Human dermal fibroblasts ($2.0X10^4$) were plated into a 96-well plate and grown overnight in DMEM containing 10% FBS. Media was removed and replaced with DMEM containing 2% FBS and 30μM CCG-203971 or 0.1% DMSO control. After 72 hours WST-1 dye was added to each well according to the manufacturer and after 60 minutes absorbance at 490nm was read using a Wallac Victor II plate reader.

Immunocytochemistry

Dermal fibroblasts ($3.0X10^4$) from normal individuals or from patients with diffuse SSc were plated on 20mm glass cover slips in DMEM containing 10% FBS and allowed to attach overnight. Medium was changed to low-serum medium (DMEM with 0.5% FBS) for 72 hours with the indicated concentration of CCG-203971 (and 0.1% DMSO control) with or without

stimulation by 10 ng/mL TGFβ1 (R&D Systems, Minneapolis, MN). The 3-day time point was chosen because in initial experiments TGFβ did not induce significant myofibroblast transition at 24 hours (data not shown). Cells were then fixed in 3.7% formaldehyde for 10' at room temperature and permeabilized with 0.25% Triton X-100 for 10' at room temperature (RT). Primary antibody for α-SMA (ab5694, Abcam, Cambridge, MA) was diluted 1:300 and incubated for 2 hours at RT. Fluorophore-conjugated secondary antibody (Alexa Fluor® 594 goat anti-rabbit IgG, Invitrogen, Carlsbad, CA) was diluted 1:1,000 and added for 1 hour at RT. Cover slips were mounted (Prolong Gold ® antifadereagent with DAPI, Invitrogen) and imaged on an upright fluorescence microscope (Nikon E-800) at 40X magnification. For quantification; cells from three, random non-overlapping fields of view were scored as α-SMA positive or negative by an observer blinded to the treatment.

Bleomycin-induced skin fibrosis model

Skin fibrosis was induced in C57BL/6 mice (female, 8 weeks old) by local intracutaneous injection of 100 μL of bleomycin (1 mg/ml) in phosphate-buffered saline (PBS), every day for 2 weeks in a defined area (~ 1 cm^2) on the upper back. Intracutaneous injection of 100 μL PBS was used as a control. Three groups of mice with a total of 21 mice were used. One group received injections of PBS, and the other two were challenged with bleomycin. Twice-a-day intraperitoneal administration of CCG-203971 (100 mg/kg in 50 μL DMSO) was initiated together with the first challenge of bleomycin and continued for 2 weeks. DMSO was used as the vehicle control. The three groups of animals were: (1) PBS/DMSO; (2) bleomycin/DMSO; (3) bleomycin/CCG-203971. After treatment, animals were sacrificed by cervical dislocation and tissue was collected.

Histology analysis

Skin obtained from the upper back at the site of the Bleomycin or PBS injections was fixed and embedded in paraffin at the University of Michigan Comprehensive Cancer Center Histology Core. Skin sections were stained with Masson's trichrome. Dermal thickness was determined by measuring the maximal distance between the epidermal-dermal junction and the dermal-subcutaneous fat junction. Three measurements were averaged from each skin section. The measurement was performed using the analysis tool in Photoshop.

Hydroxyproline assay

The collagen content from lesional skin samples was quantified using a hydroxyproline assay kit from Sigma (St. Louis, MO), and normalized with tissue weight.

Statistics

Statistical analysis for two-group comparisons used a two-tailed, unpaired t-test. For three or more groups analysis was performed by one-way ANOVA in GraphPad Prism (La Jolla, CA) followed by a Bonferroni posttest comparing all pairs in the dataset. Statistical significance was defined as $p<0.05$.

Results

LPA and TGFβ activate the Rho/MRTF/SRF transcriptional pathway and stimulate expression of pro-fibrotic genes in NIH-3T3 fibroblasts.

LPA (10μM, 6 hours), and TGFβ (10ng/mL, 18 hours) treatment of NIH-3T3 fibroblasts activates MRTF specific SRF gene expression and the previously described MRTF/SRF pathway inhibitor CCG-203971 (32) blocked this activation (Fig. 3-1A). The magnitude for TGFβ vs. LPA activation of MRTF was 4 and 5 fold respectively, and the IC_{50} for the inhibition by CCG-203971 was ~2.5μM. LPA treatment of NIH-3T3 fibroblasts also stimulates expression of several Rho-regulated, pro-fibrotic genes (Fig. 3-1B). Levels of mRNA for CTGF and ACTA2, both known MRTF/SRF targets, were induced 1.5- and 17.5-fold, respectively. Similarly, the heterogeneous nuclear precursor RNA for COL1A2 (COL1A2-hn), another MRTF/SRF target gene was also increased by LPA (4.6-fold). Induction of all three genes was blocked by CCG-203971 in a concentration-dependent manner. The IC_{50} for these effects is ~1-3 μM. As a follow-up to Fig. 2-5 found in Chapter II, we also tested the ability of CCG-203971 to block expression of LPA and TGFβ stimulated gene expression in primary human dermal fibroblasts obtained from healthy donors (Fig. 3-2). Unlike the results with the ROCK inhibitor Y-27632, we found CCG-203971 blocked the induction of profibrotic genes under all conditions, 6 hour stimulation with LPA and 24 hour stimulation with TGFβ.

SSc dermal fibroblasts overexpress MRTF/SRF target genes.

Multiple MRTF/SRF target genes are both markers and drivers of dermal fibrosis. CTGF, ACTA2 and COL1A2 are overexpressed in the SSc dermal fibroblasts when compared to the normal donor samples (Fig. 3-3A). To further assess the involvement of the MRTF/SRF pathway in pro-fibrotic gene expression we treated the SSc cells with increasing concentrations of our MRTF/SRF pathway inhibitor, CCG-203971, which reduced expression of CTGF, ACTA2, and COL1A2 (Fig. 3-3B). In light of the long half-life of mRNA for COL1A2, the primers were designed to amplify the 1st exon/intron border of the gene (COL1A2-hn). About 50% inhibition of these MRTF/SRF target genes was seen with 10 μM CCG-203971. Pirfenidone, which is the only approved therapy directly targeting fibrosis, significantly inhibited ACTA2 gene expression but only showed a trend toward inhibition of CTGF and COL1A2-hn. The pirfenidone effect, however, required a concentration of 300 μM which is 30-100 times greater than the effective concentrations of CCG-203971.

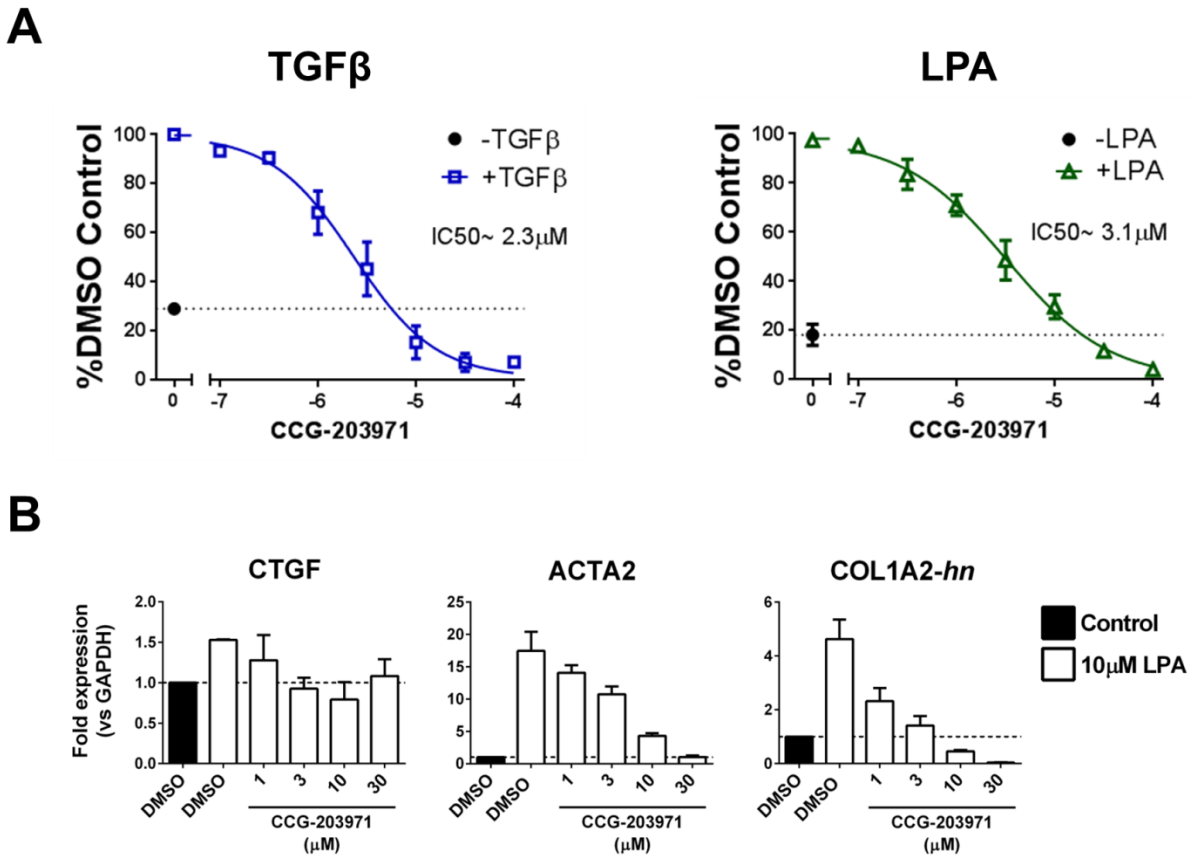

Figure 3-1. TGFβ and LPA activate MRTF/SRF and pro-fibrotic gene expression in 3T3 fibroblasts in a Rho/MRTF-dependent manner.

A.) NIH-3T3 cells were transiently transfected with a MRTF specific, SRF reporter (SRE-Luc.) then treated with the indicated concentrations of CCG-203971 overnight, then stimulated with TGFβ (10ng/mL, 18 hours) or LPA (10μM, 6 hours). Prior to cell lysis and luminescence reading, WST-1 viability reagent was added to each well to control for cellular proliferation and compound toxicity. Data shown are the mean, ±SEM relative to viability, expressed as a percentage of the change compared to the DMSO control of three independent experiments. B.) NIH-3T3 cells were treated with the indicated concentration of CCG-203971 or DMSO for 23 hours. One hour prior to RNA isolation, cells were stimulated with 10μM LPA. Expression of MRTF target genes CTGF, ACTA2, and COL1A2 was assessed by qPCR. For COL1A2, primers were designed to amplify newly synthesized heterogeneous nuclear RNA (hnRNA). Expression levels were quantified relative to GAPDH. Data are mean, ±SD of two independent experiments. (Reproduced with permission from The Journal of Pharmacology and Experimental Therapeutics)

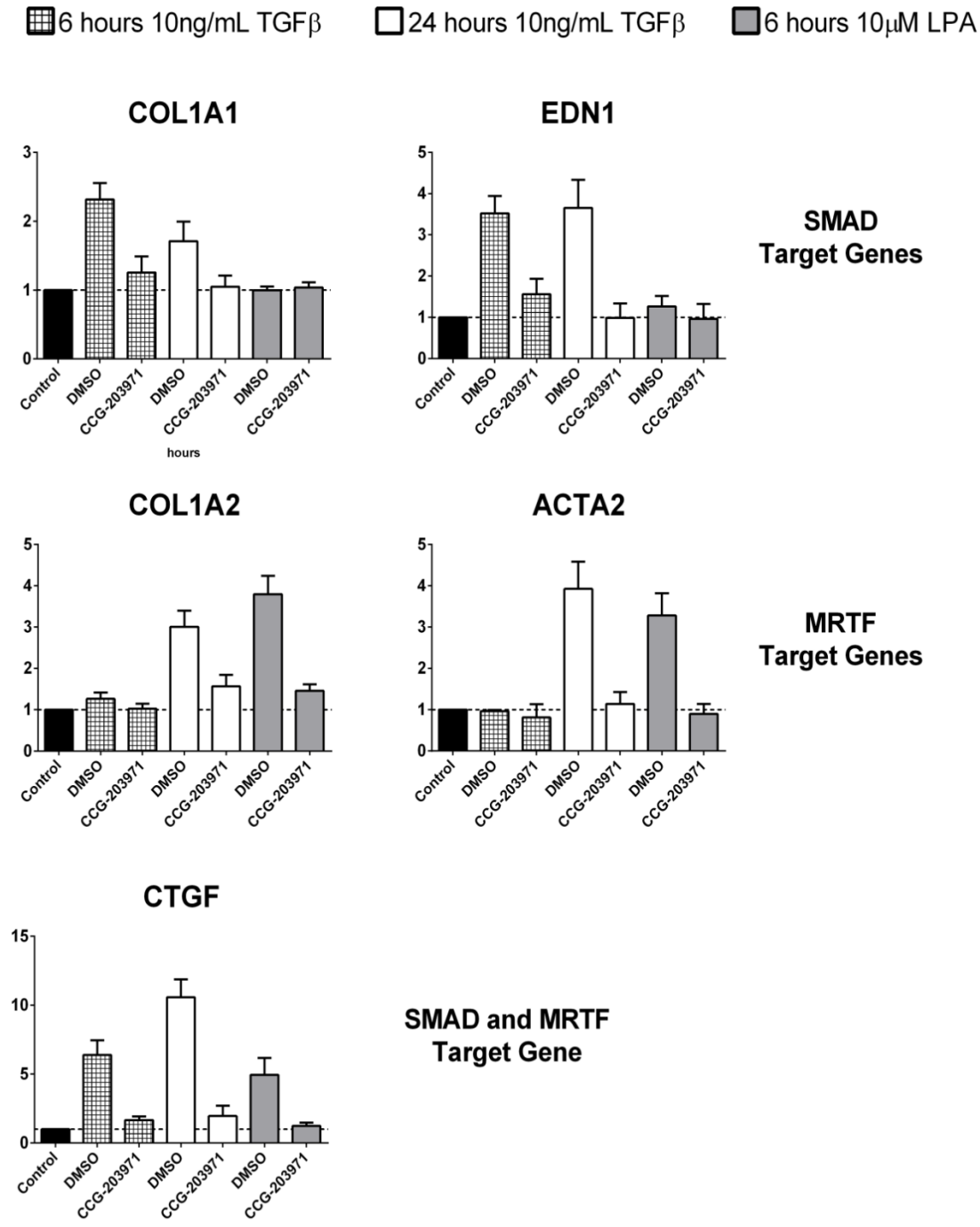

Figure. 3-2. The Rho/MRTF pathway inhibitor CCG-203971 prevents pro-fibrotic gene expression.

Primary human dermal fibroblasts obtained from healthy donors (≤ passage 6) were stimulated for 6 and 24 hours with 10ng/mL TGFβ or 6 hours with 10μM LPA in 0.5% serum starved medium +/- 10μM CCG-203971. Based on previous findings the genes were clustered into SMAD target genes, MRTF target genes, or combined SMAD/MRTF target genes. Data represents the mean (+/- SEM) of three independent experiments; expression levels were quantified relative to GAPDH and normalized to the untreated control.

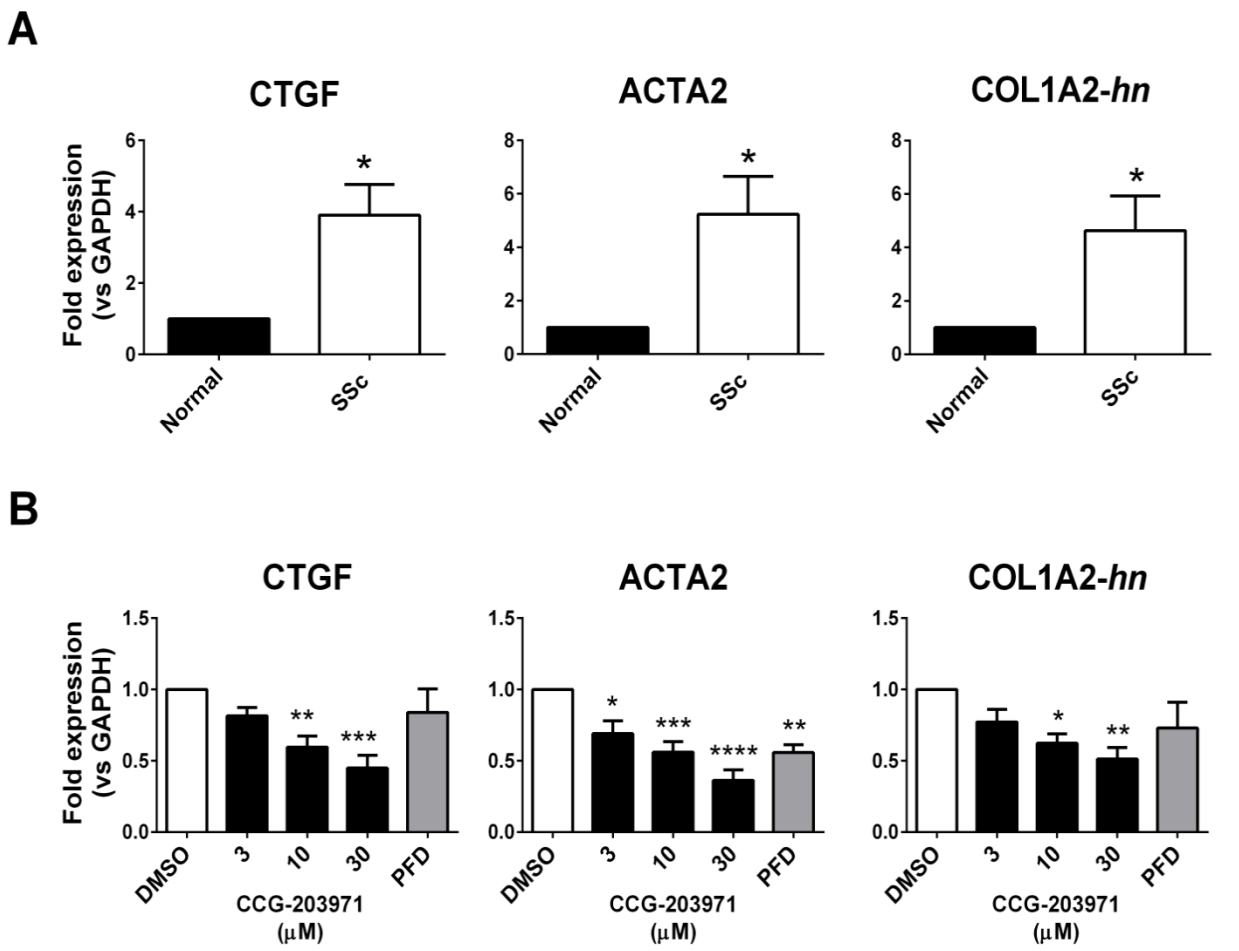

Figure. 3-3. SSc patient dermal fibroblasts show increased expression of fibrosis markers/MRTF target genes which are inhibited by CCG-203971.

A.) mRNA expression for fibrotic markers: connective tissue growth factor (CTGF), alpha smooth muscle actin (ACTA2), and collagen (COL1A2) were quantified by qPCR. Primary human dermal fibroblasts isolated from normal donors or patients with SSc were grown in culture for no more than 5 passages prior to mRNA isolation. Data are mean ±SEM of samples from three individuals. B.) CCG-203971 treatment reduces expression of CTGF, ACTA2, and COL1A2. Prior to mRNA isolation, SSc dermal fibroblasts were treated for 24 hours in the presence of the indicated concentration (μM) of CCG-203971 or 300 μM pirfenidone (PFD). Data are mean ±SEM of samples from at least four individuals. (* P< 0.05, ** P< 0.01, *** P<0.001, **** P<0.0001 vs. DMSO control.) (Reproduced with permission from The Journal of Pharmacology and Experimental Therapeutics)

Scleroderma fibroblasts proliferate faster than normal cells and CCG-203971 selectively blocks their growth.

Autocrine secretion of LPA and overexpression of mitogenic cytokines like CTGF contributes to cell proliferation in fibrotic tissues (35,36). SSc cells proliferated faster than normal dermal fibroblasts and this increase in growth was selectively blocked by CCG-203971 (Fig. 3-4). Combined with the effect on gene expression, these data suggest that the MRTF/SRF pathway is important for the transition of normal dermal fibroblasts into the faster proliferating myofibroblast-like SSc cells.

Inhibition of the MRTF/SRF pathway modulates myofibroblast transition of dermal fibroblasts.

α-SMA is involved in cellular motility and the contractile apparatus. It is also a well-recognized protein marker for myofibroblasts (11,12,27). Dermal fibroblasts from normal donors exhibit TGFβ-stimulated α-SMA expression which is blocked by CCG-203971 (Fig. 3-5A,C). In these experiments at 72 hours, 10 μM completely blocks the myofibroblast transition of normal fibroblasts. Consistent with the mRNA expression data above, SSc patient-derived fibroblasts display spontaneously high levels of α-SMA protein which can be reversed by treatment with CCG-203971 (Fig. 3-5B,C). Here also, pirfenidone reversed the α-SMA expression but with a 50% reduction occurring at 300 μM pirfenidone; it is 100X less potent than CCG-203971 which shows an IC_{50} of ~3 μM in this assay (Fig. 3-5C).

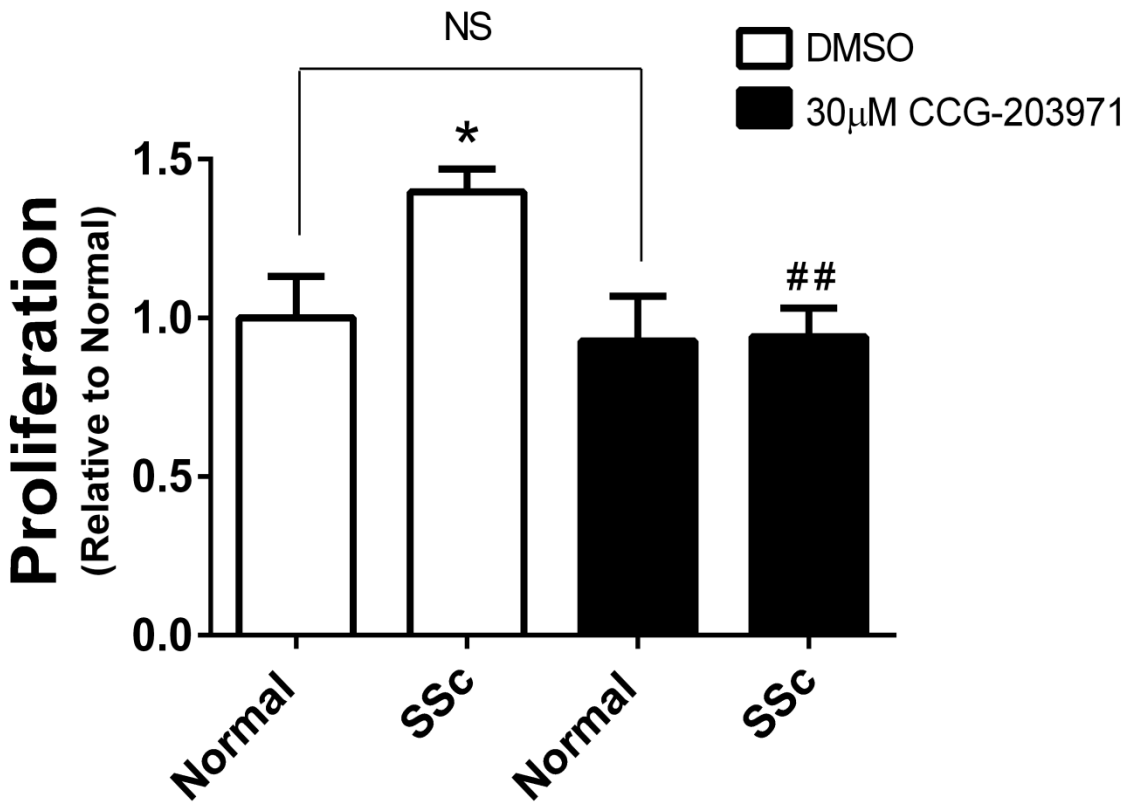

Figure. 3-4. Scleroderma dermal fibroblasts proliferate faster than normal cells and this is inhibited by CCG-203971.

Cells were plated onto 96-well plates and allowed to grow for 3 days in the presence of 30 μM CCG-203971 or DMSO vehicle. Viable cell density was assessed through enzymatic reduction of the water-soluble tetrazolium dye WST-1. Data are mean ±SEM of samples from three individuals. (* P< 0.05 vs. DMSO treated nomal, # # P< 0.01 vs. DMSO treated SSc.) (Reproduced with permission from The Journal of Pharmacology and Experimental Therapeutics)

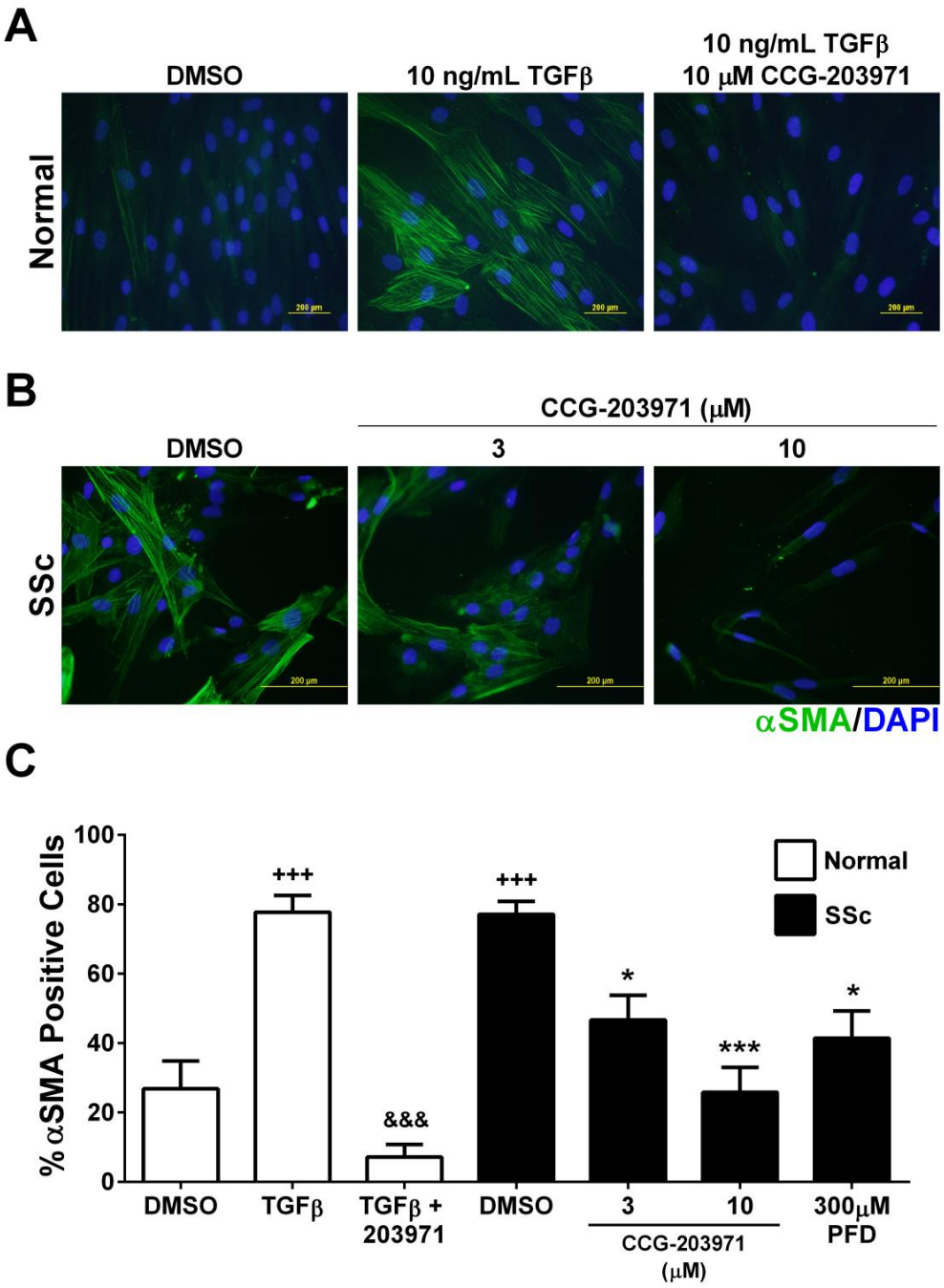

Figure. 3-5. CCG-203971 modulates myofibroblast transition of dermal fibroblasts.

A.) Primary human dermal fibroblasts from normal donors were plated onto coverslips and treated with or without 10ng/mL TGFβ for three days to induce a myofibroblast transition; during stimulation cells were also treated with 10 μM CCG-203971 or DMSO. Cells were then fixed and α-SMA was visualized using immunocytochemistry along with nuclear DAPI staining. Shown are two representative individual samples.

Figure. 3-5. (continued) B.) Human dermal fibroblasts from diffuse SSc patients were plated onto coverslips and treated with the indicated concentration of CCG-203971. Cells were then fixed and visualized using immunocytochemistry along with nuclear DAPI staining. Shown are two representative individual samples. C.) The fraction of cells positive for α-SMA was scored by an observer blinded to the sample identification. Data are mean ±SEM of samples from at least four individuals. (* $P< 0.05$, *** $P<0.001$, vs. DMSO Scleroderma, +++ $P< 0.001$ vs. Normal DMSO, &&& $P< 0.001$ vs. Normal TGFβ) (Reproduced with permission from The Journal of Pharmacology and Experimental Therapeutics)

CCG-203971 blocks dermal fibrosis in bleomycin induced injury model

To determine whether these effects would translate *in vivo*, we tested CCG-203971 in a bleomycin skin injury model. Due to its modest solubility, it was administered in 50 μL DMSO intraperitoneally. Preliminary studies showed that the compound administered in this manner was well-tolerated at 100 mg/kg twice a day. Intradermal bleomycin for two weeks along with the DMSO control (50 μL i.p.) resulted in marked dermal thickening ($p<0.0001$) compared to the PBS+DMSO group which did not receive bleomycin (Fig.3-6A-B). CCG-203971 treatment strongly and significantly ($p<0.001$) suppressed the bleomycin-induced skin thickening in this model (Fig. 3-6A-B). Skin collagen amounts, assessed by measurement of hydroxyproline content, showed similar results. Bleomycin injections promoted collagen deposition ($p<0.01$) and CCG-203971 was able to block this effect ($p<0.05$, Fig. 3-6C).

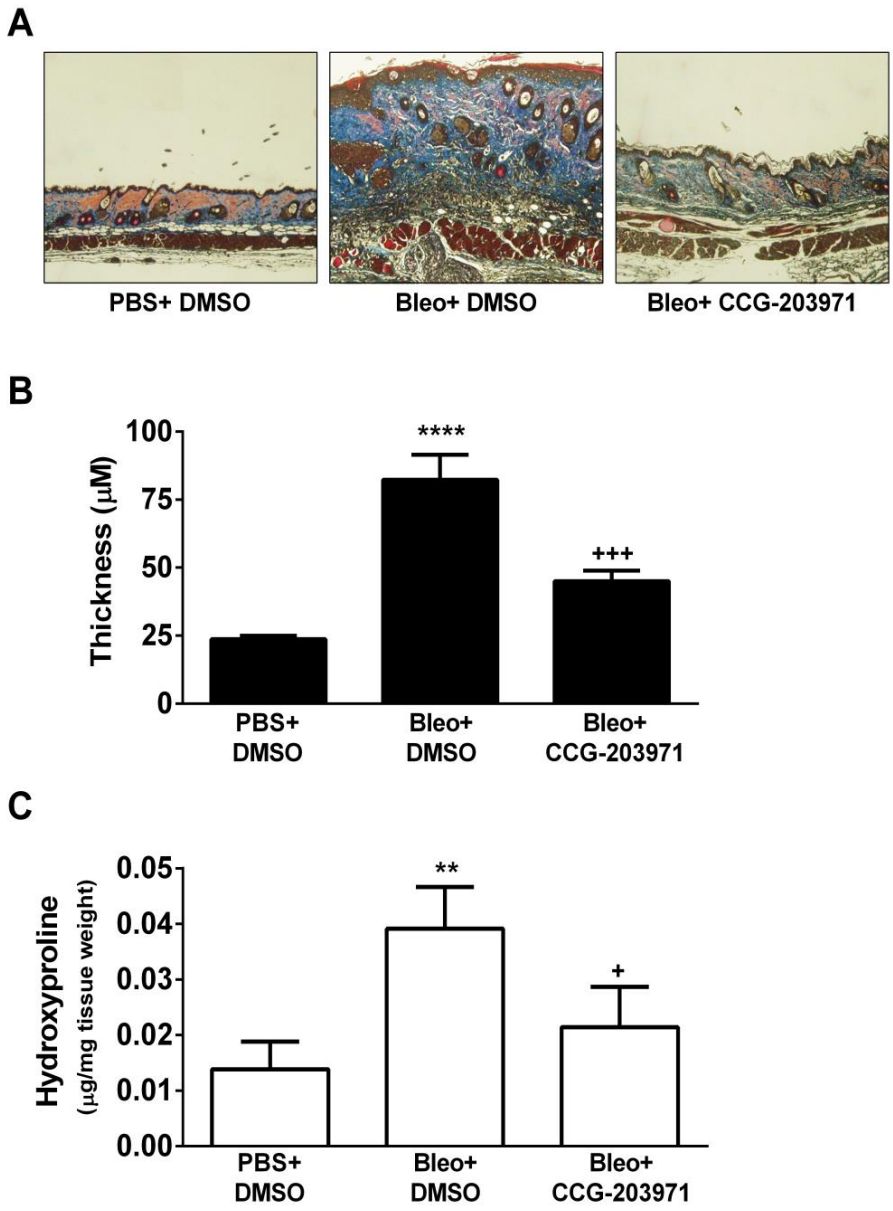

Figure. 3-6. CCG-203971 prevents bleomycin-induced fibrosis *in vivo*.

Bleomycin (0.1 mg) or vehicle (PBS) were injected intradermally in three groups of seven C57BL/6J mice for two weeks. Mice were also treated with twice daily i.p. injections of either CCG-203971 (100 mg/kg) or vehicle control (DMSO 50 μL). At the end of the treatment period, skin samples were collected and either stained with Masson's trichrome (panels A and B) or analyzed for hydroxyl-proline content (panel C) as described in Materials and Methods. Differences in skin thickness (triplicate measures from each mouse) and hydroxyproline content were assessed by one-way ANOVA with the Bonferroni post-test to correct for multiple comparisons. (** P< 0.01, **** P<0.0001, Bleomycin vs. PBS control, + P<0.05, +++ P< 0.001 Bleo & CCG-203971 vs. Bleo & DMSO) (Reproduced with permission from The Journal of Pharmacology and Experimental Therapeutics)

Discussion

There are no effective therapeutics for SSc and only very recently have therapeutics been approved for the treatment of other diseases with fibrosis as a primary feature. Most current approaches target the inflammation that initiates fibrosis but don't directly address the process of fibrosis *per se*. In light of recent evidence for a central role of gene transcription regulated by the MRTF/SRF complex, we now show that an inhibitor of this mechanism can reverse myofibroblast differentiation and reduce the fibrosis response in a bleomycin skin injury model.

In recent years, important signaling pathways of fibrosis have been elucidated (2-4). Some key receptors that drive fibrosis include those for TGFβ, lysophosphatidic acid (LPA1), endothelin, angiotensin (AT1), chemokines (CXCR4), and serotonin (5HT2). In addition, tissue stiffness itself can activate integrins and focal adhesion kinase which set up a vicious cycle to maintain fibrosis after the initial inflammatory stimulus is resolved (21,37). Many of these mechanisms are currently under consideration as antifibrotic targets (2-4,38). However, blocking each individual signal may not be effective. Indeed despite good preclinical results (39), TGFβ-1-neutralizing antibodies failed to show efficacy in SSc (40).

Targeting downstream mechanisms that are engaged by multiple fibrotic inputs may be more effective. Epigenetic mechanisms provide one promising avenue of this type with histone deacetylase and DNA methyltransfease inhibitors (3,41). Similarly kinase inhibitors such as imatinib have been considered but recent clinical trials showed conflicting results (42-44). Rho kinase (ROCK) inhibitors have also been used to reduce fibrosis (29). Our compounds, however, are more effective in reducing MRTF/SRF-regulated gene transcriptional signaling than is the ROCK inhibitor Y-27632 (30).

We propose here that the Rho/MTRF/SRF transcription mechanism may represent an important downstream target for anti-fibrotic therapy. Our results with CCG-203971 *in vitro* and *in vivo* are promising. The strong effect to inhibit CTGF expression and collagen synthesis and the reduction in myofibroblast differentiation induced by both TGFβ and LPA suggests that we are engaging a key step in the overall fibrosis gene program. Since this family of compounds blocks nuclear localization of MRTF-A and SRF-regulated gene expression regardless of the activating stimulus (30), it should have actions against many pro-fibrotic ligands. CCG-203971 was tolerated at the relatively high doses used in our study. The potency of this compound *in vitro* is only modest (IC_{50} 1-3 μM for most effects) but compared to the only approved anti-fibrotic drug, pirfenidone, it is nearly 100x more potent (see Fig.3-5C). Unlike pirfenidone, the direct molecular target of CCG-1423 to which CCG-203971 is related, was recently identified (31). This should facilitate the development of new, more potent analogs.

RNAi-mediated MRTF knock-down produces strong antifibrotic effects in several models (13,15,16,29), which provides important target validation for this pathway. Perhaps the greatest limitation currently is the very short *in vivo* half-life of CCG-203971 ($T_{1/2}$ ~25 minutes after i.p. administration, data not shown). Improvements to its pharmacokinetic properties will clearly facilitate clinical translation.

The Rho/MRTF/SRF-regulated transcription pathway plays a critical role in fibrosis by switching on the myofibroblast state. Many different fibrosis signals that are targets of current therapeutic development feed into this pathway. This mechanism is spontaneously active in human dermal fibroblasts from diffuse SSc patients. We show that a novel small molecule inhibitor of MRTF/SRF-regulated gene transcription, CCG-203971, reverses myofibroblast activation and collagen synthesis by human SSc dermal fibroblasts and by LPA- and TGFβ-

stimulated fibroblasts. It also prevents skin thickening and collagen deposition in a bleomycin skin injury model. Consequently, MRTF/SRF transcription pathway inhibitors may represent an efficacious new approach to SSc and other diseases of fibrosis.

References

1. Charles, C., Clements, P., and Furst, D. E. (2006) *Lancet* 367, 1683-1691

2. Wynn, T. A., and Ramalingam, T. R. (2012) *Nat Med* 18, 1028-1040

3. Beyer, C., Distler, O., and Distler, J. H. (2012) *Curr Opin Rheumatol* 24, 274-280

4. Gilbane, A. J., Denton, C. P., and Holmes, A. M. (2013) *Arthritis Res Ther* 15, 215

5. Boukhalfa, G., Desmouliere, A., Rondeau, E., Gabbiani, G., and Sraer, J. D. (1996) *Exp Nephrol* 4, 241-247

6. Sappino, A. P., Masouye, I., Saurat, J. H., and Gabbiani, G. (1990) *Am J Pathol* 137, 585-591

7. Zhang, H. Y., Gharaee-Kermani, M., Zhang, K., Karmiol, S., and Phan, S. H. (1996) *Am J Pathol* 148, 527-537

8. Hinz, B., Phan, S. H., Thannickal, V. J., Prunotto, M., Desmouliere, A., Varga, J., De Wever, O., Mareel, M., and Gabbiani, G. (2012) *Am J Pathol* 180, 1340-1355

9. Hu, B., and Phan, S. H. (2013) *Curr Opin Rheumatol* 25, 71-77

10. Beyer, C., Schett, G., Distler, O., and Distler, J. H. (2010) *Arthritis Rheum* 62, 2831-2844

11. Tomasek, J. J., Gabbiani, G., Hinz, B., Chaponnier, C., and Brown, R. A. (2002) *Nat Rev Mol Cell Biol* 3, 349-363

12. Tomasek, J. J., Haaksma, C. J., McRae, J. K., Risinger, G. M., and Howard, E. W. (2008) *Faseb Journal* 22

13. Small, E. M. (2012) *J Cardiovasc Transl Res* 5, 794-804

14. Sandbo, N., Lau, A., Kach, J., Ngam, C., Yau, D., and Dulin, N. O. (2011) *Am J Physiol Lung Cell Mol Physiol* 301, L656-666

15. Small, E. M., Thatcher, J. E., Sutherland, L. B., Kinoshita, H., Gerard, R. D., Richardson, J. A., Dimaio, J. M., Sadek, H., Kuwahara, K., and Olson, E. N. (2010) *Circ Res* 107, 294-304

16. Sandbo, N., Kregel, S., Taurin, S., Bhorade, S., and Dulin, N. O. (2009) *Am J Respir Cell Mol Biol* 41, 332-338

17. Seasholtz, T. M., Majumdar, M., and Brown, J. H. (1999) *Mol Pharmacol* 55, 949-956

18. Kranenburg, O., Poland, M., van Horck, F. P., Drechsel, D., Hall, A., and Moolenaar, W. H. (1999) *Mol Biol Cell* 10, 1851-1857

19. Crider, B. J., Risinger, G. M., Jr., Haaksma, C. J., Howard, E. W., and Tomasek, J. J. (2011) *J Invest Dermatol* 131, 2378-2385

20. Sakai, N., Chun, J., Duffield, J. S., Wada, T., Luster, A. D., and Tager, A. M. (2013) *FASEB J* 27, 1830-1846

21. Huang, X., Yang, N., Fiore, V. F., Barker, T. H., Sun, Y., Morris, S. W., Ding, Q., Thannickal, V. J., and Zhou, Y. (2012) *Am J Respir Cell Mol Biol* 47, 340-348

22. Chaqour, B., and Goppelt-Struebe, M. (2006) *FEBS J* 273, 3639-3649

23. Liu, S., Parapuram, S. K., and Leask, A. (2013) *Arthritis Rheum*

24. Serrati, S., Chilla, A., Laurenzana, A., Margheri, F., Giannoni, E., Magnelli, L., Chiarugi, P., Dotor, J., Feijoo, E., Bazzichi, L., Bombardieri, S., Kahaleh, B., Fibbi, G., and Del Rosso, M. (2013) *Arthritis Rheum* 65, 258-269

25. Akhmetshina, A., Dees, C., Pileckyte, M., Szucs, G., Spriewald, B. M., Zwerina, J., Distler, O., Schett, G., and Distler, J. H. (2008) *Arthritis Rheum* 58, 2553-2564

26. Buhl, A. M., Johnson, N. L., Dhanasekaran, N., and Johnson, G. L. (1995) *J Biol Chem* 270, 24631-24634

27. Masszi, A., Di Ciano, C., Sirokmany, G., Arthur, W. T., Rotstein, O. D., Wang, J., McCulloch, C. A., Rosivall, L., Mucsi, I., and Kapus, A. (2003) *Am J Physiol Renal Physiol* 284, F911-924

28. Zhao, X. H., Laschinger, C., Arora, P., Szaszi, K., Kapus, A., and McCulloch, C. A. (2007) *J Cell Sci* 120, 1801-1809

29. Zhou, Y., Huang, X., Hecker, L., Kurundkar, D., Kurundkar, A., Liu, H., Jin, T. H., Desai, L., Bernard, K., and Thannickal, V. J. (2013) *J Clin Invest* 123, 1096-1108

30. Evelyn, C. R., Wade, S. M., Wang, Q., Wu, M., Iniguez-Lluhi, J. A., Merajver, S. D., and Neubig, R. R. (2007) *Mol Cancer Ther* 6, 2249-2260

31. Lundquist, M. R., Storaska, A. J., Liu, T. C., Larsen, S. D., Evans, T., Neubig, R. R., and Jaffrey, S. R. (2014) *Cell*

32. Bell, J. L., Haak, A. J., Wade, S. M., Kirchhoff, P. D., Neubig, R. R., and Larsen, S. D. (2013) *Bioorg Med Chem Lett* 23, 3826-3832

33. Evelyn, C. R., Bell, J. L., Ryu, J. G., Wade, S. M., Kocab, A., Harzdorf, N. L., Hollis Showalter, H. D., Neubig, R. R., and Larsen, S. D. (2010) *Bioorg Med Chem Lett* 20, 665-672

34. LeRoy, E. C., Black, C., Fleischmajer, R., Jablonska, S., Krieg, T., Medsger, T. A., Jr., Rowell, N., and Wollheim, F. (1988) *J Rheumatol* 15, 202-205

35. Badri, L., and Lama, V. N. (2012) *Stem Cells* 30, 2010-2019

36. Sakai, N., Chun, J., Duffield, J. S., Wada, T., Luster, A. D., and Tager, A. M. (2013) *FASEB J*

37. Guiducci, S., Distler, J. H., Milia, A. F., Miniati, I., Rogai, V., Manetti, M., Falcini, F., Ibba-Manneschi, L., Gay, S., Distler, O., and Matucci-Cerinic, M. (2009) *Rheumatology (Oxford)* 48, 849-852

38. Leask, A. (2012) *Expert Opin Emerg Drugs* 17, 173-179

39. Varga, J., and Abraham, D. (2007) *Journal of Clinical Investigation* 117, 557-567

40. Denton, C. P., Merkel, P. A., Furst, D. E., Khanna, D., Emery, P., Hsu, V. M., Silliman, N., Streisand, J., Powell, J., Akesson, A., Coppock, J., van den Hoogen, F., Herrick, A., Mayes, M. D., Veale, D., Haas, J., Ledbetter, S., Korn, J. H., Black, C. M., Seibold, J. R., Grp, C.-S., and Consor, S. C. T. (2007) *Arthritis and Rheumatism* 56, 323-333

41. Huber, L. C., Distler, J. H., Moritz, F., Hemmatazad, H., Hauser, T., Michel, B. A., Gay, R. E., Matucci-Cerinic, M., Gay, S., Distler, O., and Jungel, A. (2007) *Arthritis Rheum* 56, 2755-2764

42. Khanna, D., Saggar, R., Mayes, M. D., Abtin, F., Clements, P. J., Maranian, P., Assassi, S., Singh, R. R., and Furst, D. E. (2011) *Arthritis Rheum* 63, 3540-3546

43. Spiera, R. F., Gordon, J. K., Mersten, J. N., Magro, C. M., Mehta, M., Wildman, H. F., Kloiber, S., Kirou, K. A., Lyman, S., and Crow, M. K. (2011) *Ann Rheum Dis* 70, 1003-1009

44. Prey, S., Ezzedine, K., Doussau, A., Grandoulier, A. S., Barcat, D., Chatelus, E., Diot, E., Durant, C., Hachulla, E., de Korwin-Krokowski, J. D., Kostrzewa, E., Quemeneur, T., Paul, C., Schaeverbeke, T., Seneschal, J., Solanilla, A., Sparsa, A., Bouchet, S., Lepreux, S., Mahon, F. X., Chene, G., and Taieb, A. (2012) *Br J Dermatol* 167, 1138-1144

CHAPTER IV

PHARMACOLOGICAL INHIBITION OF MYOCARDIN-RELATED TRANSCRIPTION FACTOR PATHWAY BLOCKS LUNG METASTASIS OF RHOC OVEREXPRESSING MELANOMA

Abstract

Melanoma is the most dangerous form of skin cancer with the majority of deaths arising from metastatic disease. Evidence implicates Rho-activated gene transcription, mediated by the nuclear localization of the transcriptional coactivator, myocardin-related transcription factor (MRTF), in melanoma metastasis. Here, we compare *in vitro* and *in vivo* models of cancer metastasis (clonogenicity, migration, invasion, and murine lung colonization) to Rho expression and signaling in a panel of human metastatic melanoma cell lines. Three melanoma lines (two NRAS mutant and one BRAF mutant) show evidence of high RhoC expression and activity (stress fiber formation, spontaneous nuclear localization of MRTF-A, and increased MRTF regulated gene expression); they also show an aggressive phenotype in cellular models. Conversely, the other two BRAF mutant melanoma lines have low RhoC expression, decreased levels of MRTF-regulated genes, and display reduced migration, invasion, and clonogenicity. To probe the MRTF transcriptional mechanism, we utilized a previously developed small molecule inhibitor, CCG-203971 which at low μM concentrations blocks nuclear localization and activity of MRTF-A. CCG-203971 inhibited cellular migration and invasion, and decreased MRTF target

gene expression. In an experimental model of melanoma lung metastasis, a RhoC-overexpressing melanoma (SK-Mel-147) exhibited pronounced lung colonization compared to the low RhoC-expressing SK-Mel-19. Furthermore, pharmacological inhibition of the MRTF pathway with CCG-203971 reduced both the number and size of lung metastasis resulting in a marked reduction of total lung tumor burden. These data link RhoC signaling with aggressive phenotypes and support targeting the MRTF transcriptional pathway as a novel approach to melanoma therapeutics.

Introduction

Rho GTPases play significant roles in human cancer (1). Although RhoA and RhoC share considerable homology, they may coordinate different aspects of cancer progression. RhoC appears to be most important for cellular invasion and metastasis (2) while RhoA plays a role in transformation and tumor proliferation (3). In a screen designed to identify genes important for melanoma metastasis, RhoC was found to be up regulated and contributed to melanoma lung metastasis (4). Rho GTPases are well-known for regulating the actin cytoskeleton (5). RhoA/C activation causes the formation of myosin-rich F-actin bundles called stress fibers through their downstream effectors Rho associated kinase (ROCK) and Diaphanous-related formin-1 (mDia1) (6-8). Through their modulation of the actin cytoskeleton, Rho GTPases also regulate gene expression though myocardin-related transcription cofactors (MRTF-A/B) also known as megakaryoblastic leukemia genes (MKL1/2). In the nucleus MRTF cooperates with serum response factor (SRF) to induce transcription of genes involved in proliferation, migration, invasion, and metastasis (9,10). On the N-terminal region of MRTF are three G-actin binding (RPEL) motifs which sequester MRTF in the cytoplasm. Rho activity reduces cytosolic G-actin, allowing MRTF to translocate into the nucleus and activate gene transcription. Stable knockdown of MRTF or SRF in B16M2 melanoma cells with high RhoC expression results in a dramatic reduction of *in vivo* lung metastasis and *in vitro* cellular migration (11). This evidence suggests that gene regulation through MRTF mediates RhoC-induced cancer metastasis.

To assess the role of MRTF-regulated gene transcription in cancer metastasis, we previously identified small-molecule inhibitors of the MRTF pathway (12). Our initial compound, CCG-1423 selectively blocked Rho GTPase-regulated melanoma invasion at low micro-molar concentrations. Further SAR optimization of this compound series to reduce

toxicity (13) and to enhance potency (14) resulted in a new analog, CCG-203971 that blocks MRTF-induced gene expression and prostate cancer migration without cytotoxic effects. The Rho/MRTF pathway has also recently been highlighted as a major signaling crossroad in the development of pathological fibrosis in diseases including idiopathic pulmonary fibrosis, scleroderma, and Crohn's disease (15-17). We have recently shown efficacy of CCG-203971 in a murine model of skin fibrosis (18) but a close examination of MRTF pathway inhibitors in models of cancer progression has not been performed. Two potential molecular mechanisms for inhibition of the MRTF/SRF by CCG-1423 have been identified. CCG-1423 has been shown to bind MRTFA/B blocking the interaction with nuclear import mechanisms (19). Additionally, CCG-1423 binds to MICAL-2, a nuclear actin regulator (20). Either of these molecular mechanisms could account for the inhibition of nuclear accumulation of MRTF-A (12,21).

Here we investigate the Rho/MRTF pathway in a panel of five human, metastatic melanoma cell lines; SK-Mel-19, SK-Mel-29, SK-Mel-147, SK-Mel-103, and UACC-257. There is a clear dichotomy among the lines where high levels of RhoC expression, MRTF-A nuclear localization and function are closely associated with *in vivo* and *in vitro* correlates of cancer metastasis including clonogenicity, migration, and invasion. As a novel approach to anti-metastasis therapeutics, our MRTF pathway inhibitor, CCG-203971, blocks cellular migration and invasion as well as *in vivo* lung colonization in a murine tail vein injection model.

Materials and Methods

Cell Culture and Proliferation

Human cutaneous melanoma cell lines, SK-Mel-19, SK-Mel-29, SK-Mel-103, SK-Mel-147, and UACC-257, obtained from Dr. Maria Soengas, were cultured in DMEM (Life Technologies) supplemented with 10% fetal bovine serum (Life Technologies) including penicillin/streptomycin (Life Technologies). For proliferation experiments 20,000 cells were plated into 24-well plates in DMEM containing 10% FBS. Cells were allowed to attach overnight and then medium was replaced with DMEM containing 2% FBS. After 24 or 94 hours of growth, cells were suspended and stained with 0.4% trypan blue stain (Invitrogen). Cell counting was performed using the Countess® Automated Cell Counter (Invitrogen) according to manufacturer's instructions.

Immunocytochemistry and F-actin staining

Cells ($1.0X10^5$) were plated onto fibronectin-coated cover slips in 10% FBS DMEM and allowed to attach overnight. Medium was changed to 0.5% FBS DMEM for 24 hours with the indicated concentration of CCG-203971 or 0.1% DMSO. Cells were then fixed in 3.7% formaldehyde for 10' at room temperature (RT) and permeabilized with 0.25% Triton X-100 for 10' at RT. For immunocytochemistry studies, primary antibody for MRTF-A (Santa Cruz Biotechnology SC-418) was diluted 1:100 and incubated for 2 hours at RT. Fluorophore-conjugated secondary (Alexa Fluor® 594 Donkey Anti-Goat IgG, Invitrogen) was diluted 1:1,000 and added for 1 hour. For stress fiber assays, one unit of Acti-Stain® phalloidin (Cytoskeleton) was added to each cover slip for 30' at RT. Cells were mounted (Prolong Gold ® antifadereagent with DAPI,

Invitrogen) and imaged on an upright fluorescence microscope (Nikon E-800) at 60X magnification.

Real-time PCR

Cells ($1.0X10^6$) were plated into 60 mm dishes and starved overnight in DMEM containing 0.5% FBS. Cells were lysed and RNA was isolated using the RNeasy® kit (Qiagen) following the manufacturer's directions. DNAse-treated RNA (1 µg) was used as a template for synthesizing cDNA utilizing the Taqman® Reverse-Transcription Reagents kit (Invitrogen). SYBR green qPCR (SABiosciences) was performed using a Stratagene Mx3000P (Agilent Technologies) and cT values were analyzed relative to GAPDH expression. Primer sequences: GAPDH; 5' GGAAGGGCTCATGACCACAG. 3' ACAGTCTTCTGGGTGGCAGTG. CTGF; 5' CAGAGTGGAGCGCCTGTT. 3' CTGCAGGAGGCGTTGTCA. CYR61; 5' CGCGCTGCTGTAAGGTCT. 3' TTTTGCTGCAGTCCTCGTTG. MYL9; 5' CATCCATGAGGACCACCTCCG. 3' CTGGGGTGGCCTAGTCGTC.

Scratch Assay

Cells ($4.0X10^5$) were plated in DMEM containing 10% FBS and grown to confluence in a 12-well plate. After 24 hours, a scratch was made using a 200 µL pipette tip. Medium was replaced with DMEM containing 2.0% FBS and images of the wound were taken at time=0 and 24 hours using a bright field microscope (Olympus CKX41). Area quantification of the scratch was determined using ImageJ software as previously described (14,22). Briefly, the binary (white and black) threshold for each image was manually adjusted to leave only the open area of the scratch black. The area of this open area was then determined and the percent closure was calculated by comparing the difference in area of t=24 from t=0.

Transwell Migration Assay

Cells ($5.0X10^4$) were added to the top of an 8 µm pore diameter transwell chamber (Millipore) in DMEM containing 0.5% FBS with 10 µM CCG-203971 or 0.1% DMSO control. Medium containing 0.5% FBS and compound or DMSO was also added to the bottom chamber. Cells were allowed to migrate for 6 hours followed by fixation and staining in 4% formaldehyde/0.5% crystal violet. The number of migrated cells for each well was determined by examining four random non-overlapping fields of view at 20X magnification using a bright field microscope (Olympus CKX41).

Label-Free Migration and Invasion Assay

Real-Time Cell Analysis (RTCA) of cell migration and invasion was monitored using a CIM-plate 16 and xCELLigence DP System (Acea Bioscience, Inc.). Prior to cell seeding, RPMI containing 0.5% fetal bovine serum (Atlas Biologicals) was placed in the upper and lower chambers and allowed to equilibrate for 1 hour in an incubator at 37°C in 5% CO_2. For migration, cells (3×10^5/well (invasion) and 5×10^5/well (migration)) were placed in the upper chamber. After cell seeding, the CIM-plate 16 was equilibrated for 30 minutes at room temperature. The invasion assay was executed similarly, however to the upper chamber, 5% (v/v) Matrigel™ Matrix (BD BioSciences; diluted 1:20 in basal RPMI media) was added and allowed to equilibrate for 4 hours in an incubator at 37°C in 5% CO_2. For compound effects in invasion assays, cells were treated with 10 µM CCG-203971 upon placement into the upper chamber. Cell index was measured every 30 minutes.

Luciferase Assay

Cells ($3.0X10^4$) were seeded into 96-well plates in DMEM containing 10% FBS overnight. Cells were then cotransfected with 56 ng SRE- Luciferase reporter selective for Rho/MRTF described in ref. (23), and 2.3 ng RhoC plasmid diluted with Lipofectamine 2000 (Invitrogen) in Opti-MEM (Life Technologies). After 6 hours, compounds were added for overnight treatment. The next day WST-1 (10 µL/well) reagent (Promega) was added to measure viability. After 1 hour, absorbance was read (490 nm) before lysing the cells for luciferase measurement (Promega Luciferase Assay System).

Clonogenic Assay

Cells were grown for 6 days in 2.0% FBS DMEM. Two hundred live cells, determined by trypan blue exclusion assay, were seeded into a 6-well plate and allowed to form colonies in DMEM containing 2.0% FBS for 10 days. Colonies were fixed and stained in 3.7% formaldehyde/0.5% crystal violet 10 minutes at room temperature. Only cell clusters consisting of at least 50 cells were counted as colonies.

Western Blot Analysis

Cells were starved overnight in DMEM containing 0.5% FBS, protein lysates (40 µg) were resolved using 15% SDS-PAGE gels, transferred to PVDF membranes, and blocked in 5% dried milk in tween tris-buffered saline. Membranes were incubated in 1:1000 diluted primary antibodies RhoA (Santa Cruz Biotechnologies, sc-418), RhoC (Cell Signaling, D40E4) or GAPDH (Cell Signaling, 14C10) overnight at 4º C. HRP-conjugated goat anti-mouse (Santa Cruz Biotechnology, sc-2060) or HRP-conjugated goat anti-rabbit (Sigma-Aldrich, A0545)

antibodies were diluted 1:10,000. Blots were developed using SuperSignal® Pico chemiluminescent substrate (Thermo Scientific). Bands were visualized and quantified using a Li-Cor Odyssey Fc.

Mouse Metastasis Model

Ten-week old, female, NOD.CB17-Prkdc^{scid}/J (NOD SCID) mice were purchased from Jackson Laboratory Bar Harbor, ME (stock number: 001303). The mice were separated into three groups of six. One group received tail vein injection of GFP-expressing SK-Mel-19 (2X10^6 cells). The other two groups were injected with GFP-expressing SK-Mel-147 (2X10^6 cells). Following tail vein injection, the mice began twice daily I.P. injection of 100 mg/kg CCG-203971 or 50μL DMSO (vehicle control). After 18 days the mice were euthanized and lungs were collected for histological analysis. All studies were performed according to protocols approved by the University of Michigan, University Committee on the Use and Care of Animals (UCUCA).

Immunohistochemistry

For the quantification and imaging of lung tissue from the mouse metastasis model, paraffin-embedded sections were dewaxed, unmasked, and treated as previously described (24). To visualize GFP-expressing melanoma cells in the lung section, the Vector Rabbit-on-Mouse basic kit (Vector Laboratories, Burlingame, CA) was utilized according to the manufacturer's instructions. Sections were incubated with primary antibody, Rabbit anti-GFP (1:250 Invitrogen A-6455), for each experiment, two tissue sections from the same animal were developed: one with primary antibody included and one with the primary antibody left out of the reaction. Visualization of GFP was done using the Vectastain Elite ABC kit (Vector Laboratories), used according to the manufacturer's instructions. All sections were developed using 3,3′-

diaminobenzidine (Vector Laboratories) as the developing substrate and counterstained with haematoxylin. Images were taken at 20X magnification using a Nikon Eclipse Ti-S microscope with mmi Cell Tools software, Version 3.47. (MMI, Eching, Germany) For all images, treatment and control slides were sequentially imaged using the same exposure time and LUT settings. The slides were blindly quantified for the number of metastatic nodules on each section followed by the use of ImageJ software to determine the cross sectional area (μm^2) of each nodule. The area was represented as an average size for each mouse and the total tumor burden was calculated by adding together the total cross sectional areas for all tumors in each mouse then averaged for each of the three groups.

Statistics

Statistical analysis was performed by ANOVA comparison between groups followed by Bonferonni posttest where * p> 0.05, ** P>0.01, *** P>0.001, and **** P>0.0001.

Results

Three melanoma lines exhibit aggressive in vitro phenotypes, independent of Ras vs. BRAF mutation status

In our initial experiments, we analyzed the five human, metastatic melanoma cell lines using *in vitro* models of cancer aggressiveness. Using a clonogenicity assay, we find that SK-Mel-147, SK-Mel-103 and UACC-257 readily formed colonies while SK-Mel-19 and SK-Mel-29 were unable to form quantifiable colonies under these conditions (Fig. 4-1A). We next examined 2-dimensional and 3-dimensional cellular migration and invasion using the scratch-wound migration assay (Fig. 4-1B) as well as a label-free transwell migration, (Fig. 4-2B) and Matrigel® invasion assay (Fig. 4-1C). Again we saw a consistent grouping of the cells where SK-Mel-147, SK-Mel-103 and UACC-257 showed a more aggressive phenotype. These three lines included two NRAS mutants and one BRAF mutant. To assess the role of proliferation *per se* in these functions, we measured growth over 4 days and found no consistent difference among the five cell lines under the low serum conditions used for all of these studies (Fig. 4-2A). Thus the BRAF/NRAS mutational status of the melanoma cell lines was not a predictor of the outcome in any of our *in vitro* models, however there is an obvious dichotomy in aggressive phenotypes between the two groups

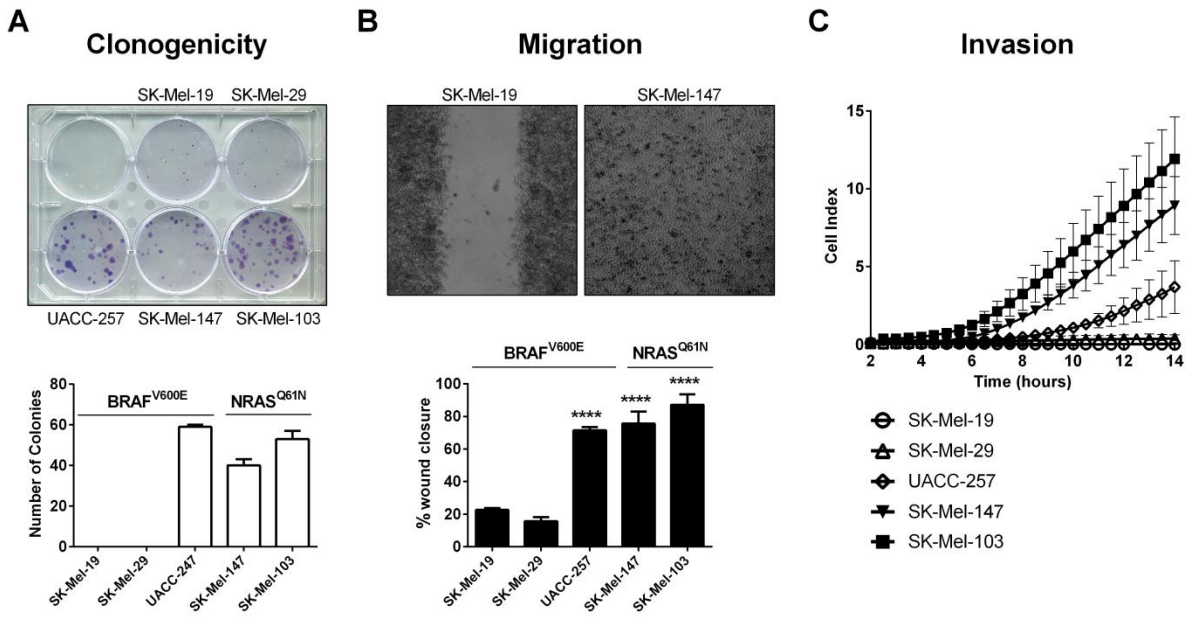

Figure 4-1. Using cell-based models of metastasis the melanoma cells separate into aggressive and nonaggressive groups.

A.) Clonogenicity was determined by seeding 200 live cells/well (determined by trypan blue exclusion) into 6-well plates. After 10 days the colonies were fixed and stained with crystal violet and the total number of colonies in each well was determined using >50 cells/colony cut off. Data are expressed as the mean (±STD) of duplicate experiments. B.) Cellular migration determined by wound assay. Cells are grown to confluence in 12-well plates then a scratch is made using a 200 µL pipette. Images are taken at 0 and 24 hours in 2.0% serum. Shown are examples of SK-Mel-19 and SK-Mel-147 after 24 hours; from experiments with similar initial wound areas. Quantification of the open area is determined computationally and the migration of each cell type relative to SK-Mel-19 after 24 hours is shown; Results are expressed as the mean (±SEM) of triplicate experiments (*** P< 0.001 vs. SK-Mel-19). C.) Real-time Analysis of Melanoma Cell Invasion. xCELLigence label-free system was used to monitor real-time Matrigel™ invasion of SK-Mel-147, UACC-257, SK-Mel-103, SK-Mel-19, and SK-Mel-29 in RPMI containing 0.5% FBS. Shown is a representative figure of the change in cell index (±SEM) from one experiment performed in triplicate. For each condition at least two independent experiments were performed.

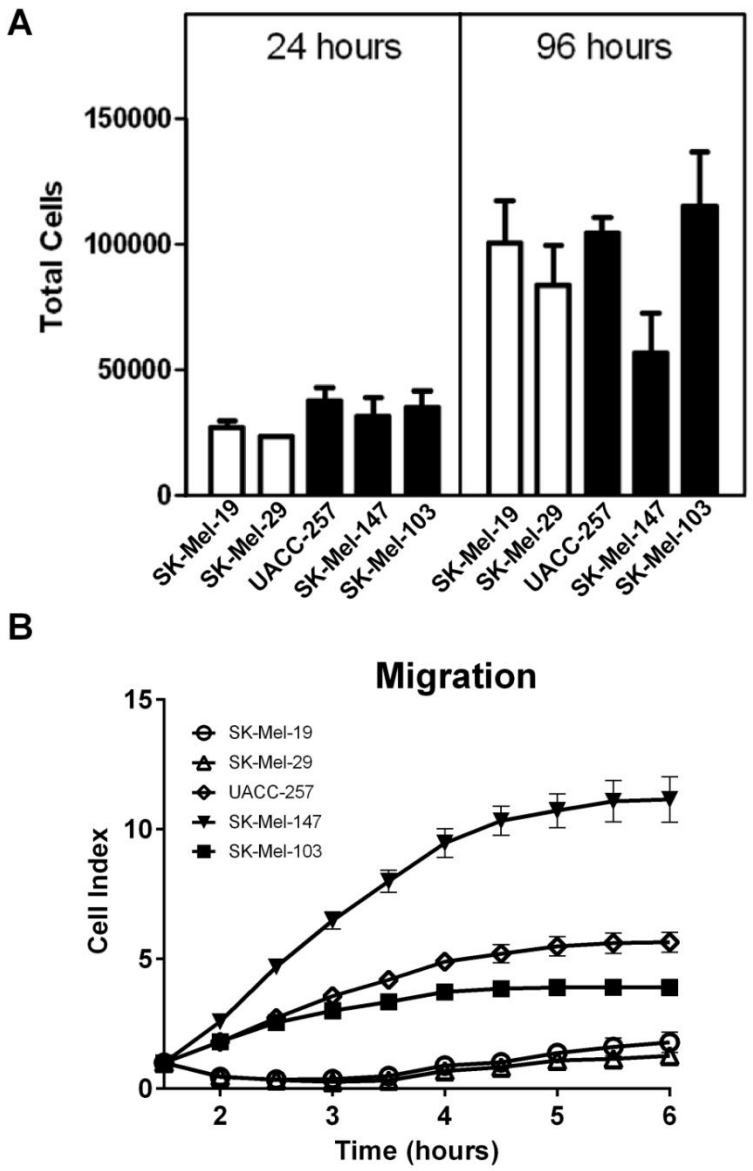

Figure. 4-2. Melanoma cell line transwell migration and proliferation.

A.) Proliferation is independent of clonogenicity, migration, and invasion in metastatic melanoma. Each cell line was grown in DMEM containing 2.0% FBS for 24 and 96 hours and proliferation was measured using the trypan blue exclusion assay. The aggressive melanomas, determined by clonogenicity, migration, and invasion assays are shown in black bars and the less aggressive melanomas are shown in white open bars. Results are expressed as the mean (±SEM) of triplicate experiments. B.) Real-time Analysis of Melanoma Cell migration. xCELLigence label-free system was used to monitor real-time transwell migration of SK-Mel-147, UACC-257, SK-Mel-103, SK-Mel-19, and SK-Mel-29 in RPMI containing 0.5% FBS. Open symbols indicate $BRAF^{V600E}$ and filled symbols $NRAS^{Q61N}$ mutants. Results are expressed as the mean (±SEM).

Aggressive melanomas selectively overexpress RhoC but not RhoA

Rho GTPase signaling has been shown to promote cellular migration and invasion (25). More specifically in melanoma, RhoC expression was increased in cell lines selected in mice for increased metastatic behavior (5). To determine the relative Rho signaling potential within our panel of melanomas we quantified RhoA and RhoC protein expression. When compared to GAPDH, RhoC protein is overexpressed in the aggressive melanomas; UACC-257, SK-Mel-147, and SK-Mel-103 (Fig. 4-3). Interestingly, RhoA levels are not significantly different within this panel of melanoma cell lines. RhoA plays an important role in proliferation and cytokinesis whereas RhoC seems to be more involved in migration, invasion, and metastasis (3,4)

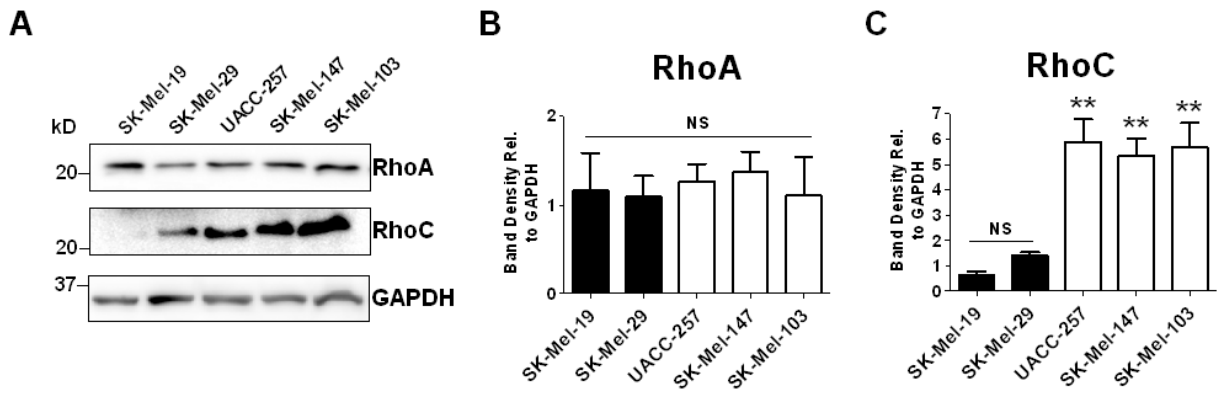

Figure. 4-3. Aggressive melanomas selectively overexpress RhoC but not RhoA.

A.) Western blot analysis of RhoA, RhoC, and GAPDH. Each melanoma cell line was starved for 24 hours in 0.5% serum prior to preparation of total protein lysates. Image is representative blot from three separate experiments. B,C.) Quantitative band density analysis was performed for each experiment comparing the intensity of RhoA and RhoC relative to the normalizing protein GAPDH. Results are expressed as the mean (±SEM) of triplicate experiments (** P< 0.01 vs. SK-Mel-19).

RhoC overexpressing, aggressive melanoma lines maintain spontaneously nuclear and active MRTF-A through F-actin stress fiber formation

MRTF localization and activity are regulated by G-actin. Stress fiber formation leads to G-actin depletion and MRTF translocation into the nucleus (9). UACC-257, SK-Mel-103, and SK-Mel-147 (shown) express strong F-actin staining and stress fiber formation in the absence of serum stimulation (Fig. 4-4A). By comparison SK-Mel-19 (shown) and SK-Mel-29 show reduced F-actin staining and very little stress fiber formation. Consistent with the actin-based mechanism governing MRTF localization and activity, the aggressive melanomas also exhibited spontaneously nuclear MRTF-A under these conditions (Fig. 4-4A). To show that MRTF-A localization was dependent on F-actin dynamics, we stimulated SK-Mel-19 with 20% FBS to induce stress fiber formation which induced MRTF-A nuclear localization (Fig. 4-5). We also treated SK-Mel-147 with latrunculin B which inhibits F-actin formation (26) and MRTF-A relocated to the cytosol (Fig. 4-5). Along with localization, MRTF activity is regulated by the relative levels of G-actin (27). To measure MRTF activity we determined the mRNA expression of three known Rho/MRTF target genes, myosin regulatory light chain 9 (MYL9), cysteine-rich angiogenic inducer 61 (CYR61), and connective tissue growth factor (CTGF). Consistent with the predominantly nuclear MRTF-A, the three aggressive lines (UACC-257, SK-Mel-147, and SK-Mel-103) have dramatically increased expression of these three Rho/MRTF-regulated genes compared to that in the other two lines (Fig. 4-4B). Along with being MRTF target genes, MYL9, CYR61, and CTGF play important roles in cellular migration and metastasis (11,28,29).

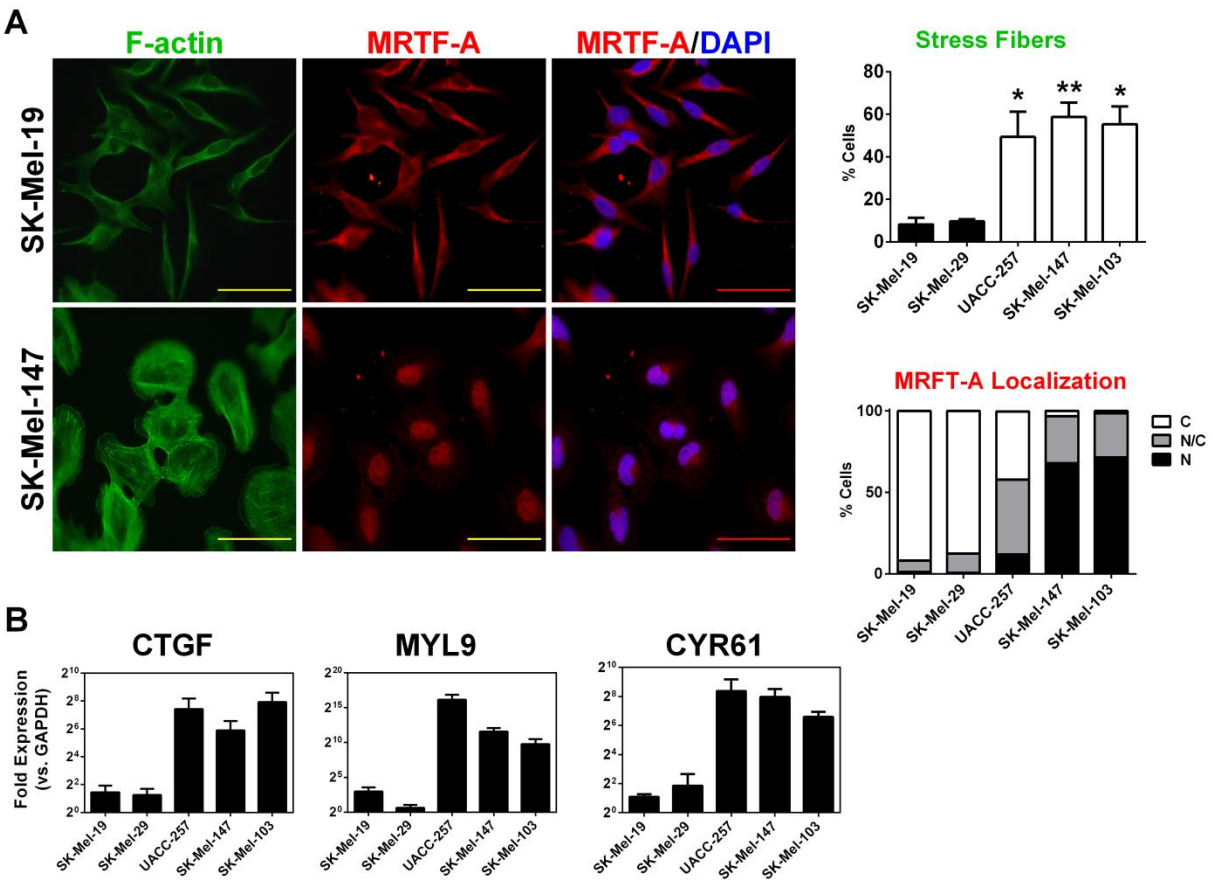

Figure. 4-4. MRTF-A localization and activity is increased with F-actin stress fiber formation in aggressive melanoma cells.

A.) Cellular localization of MRTF-A observed with immunocytochemistry in starved (0.5% FBS, 24 hours) melanoma cells. Images were quantified by scoring an individual cell as predominantly nuclear, cytosolic, or even distribution of MRTF-A. F-actin staining was also performed in the same cells using fluorophore-conjugated phalloidin toxin. Counts are from three independent experiments with at least 100 cells scored for each condition. For stress fiber quantification, only cells expressing prominent stress fiber bundles were determined to be "stress fiber positive". Results are expressed as the mean (±SEM) of triplicate experiments (* $P< 0.05$, ** $P< 0.01$ vs. SK-Mel-19) Scale bar shown represents 200µm B.) Expression of MRTF-A target genes known to be regulated by Rho/MRTF activity and involved in cancer migration; myosin regulatory light polypeptide (MYL9), cysteine-rich angiogenic inducer 61(CYR61), and connective tissue growth factor (CTGF), are quantified by qPCR. Results are expressed as the mean (±SEM) of triplicate experiments.

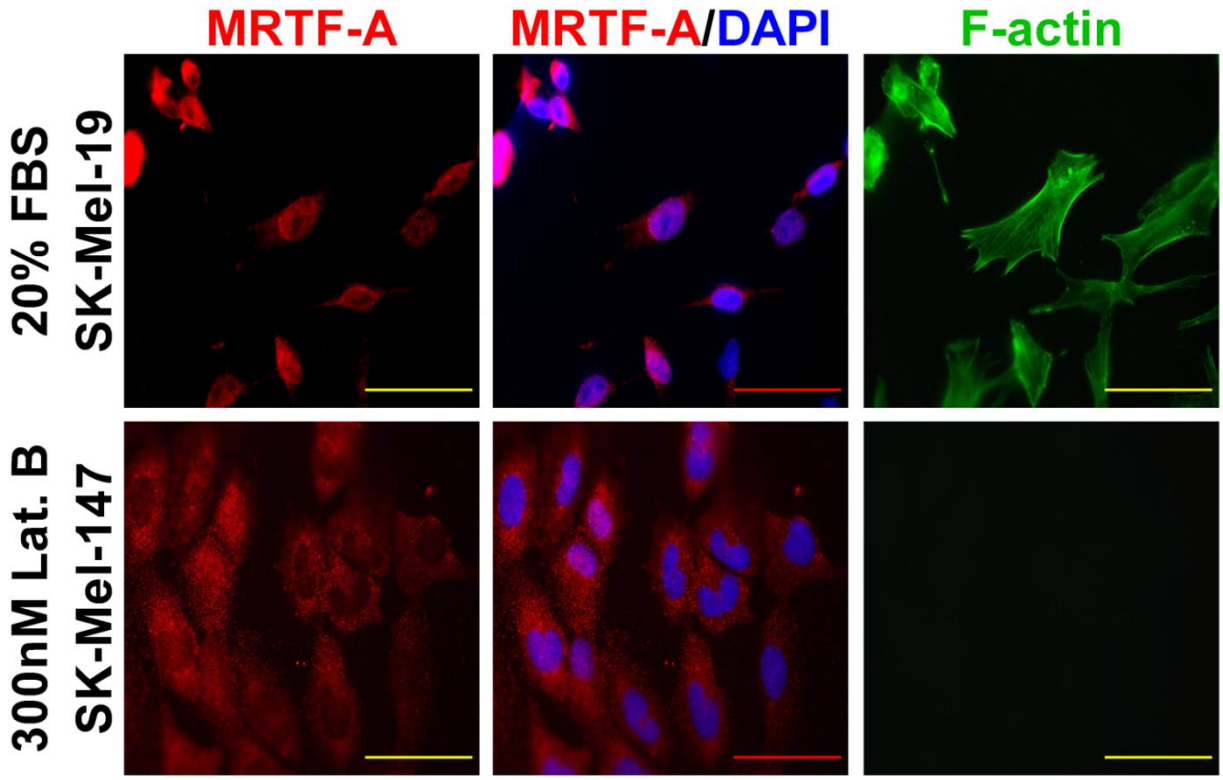

Figure. 4-5. Regulation of MRTF-A localization in serum-starved melanomas is determined by actin dynamics.

Cellular localization of MRTF-A is observed with immunocytochemistry. Top, SK-Mel-19 cells, which exhibit almost exclusively cytosolic MRTF-A in the absence of serum were starved for 23.5 hours in 0.5% FBS DMEM and then stimulated with 20% FBS for 30 minutes before fixation and staining for MRTF-A and F-actin. Bottom, SK-Mel-147 cells, which exhibit nuclear MRTF-A under starved conditions were starved for 23.5 hours in 0.5% FBS DMEM and then treated with 300nM latrunculin B for 30 minutes before fixation and staining for MKL1 and F-actin. Latrunculin B is a natural toxin which blocks F-actin formation. Scale bar shown represents 200µm. Shown are representative examples from triplicate experiments.

MRTF pathway inhibitor CCG-203971 blocks MRTF-A nuclear accumulation and transcription activity

We next wanted to assess the potential for using a novel small-molecule inhibitor of the Rho/MRTF pathway to block *in vitro* and *in vivo* models of melanoma metastasis. In order to assess transcriptional activity of MRTF, we performed luciferase assays with a modified serum response element promoter (SRE.L) that is selective for MRTF (12). CCG-203971 inhibits RhoC-induced SRE-Luciferase expression in SK-Mel-147 cells with an IC_{50} of ~6 μM. Importantly, CCG-203971 does not cause cellular toxicity up to 100 μM using the WST-1 viability assay (Fig. 4-6A). As previously reported by others (30) for compounds in this series, CCG-203971 reduces the nuclear localization of MRTF-A in SK-Mel-147 cells in a concentration dependent manner (Fig. 4-6B). CCG-203971 also reduces the expression of endogenous MYL9, CYR61, and CTGF in SK-Mel-147 cells (Fig. 4-6C) at low μM concentrations.

CCG-203971 inhibits cellular migration and invasion

To determine if inhibition of MRTF localization and activity altered phenotypes of the aggressive melanoma lines, we investigated the influence of CCG-203971 at the cellular level. Using transwell migration and label-free Matrigel invasion assays we found that 10 μM CCG-203971 inhibited cellular migration (Fig. 4-7A) and invasion (Fig. 4-7B) of the aggressive, RhoC overexpressing melanoma SK-Mel-147. Equally interesting, CCG-203971 has no effect on SK-Mel-19, which does not display nuclear MRTF-A under these conditions (Fig. 4-4A).

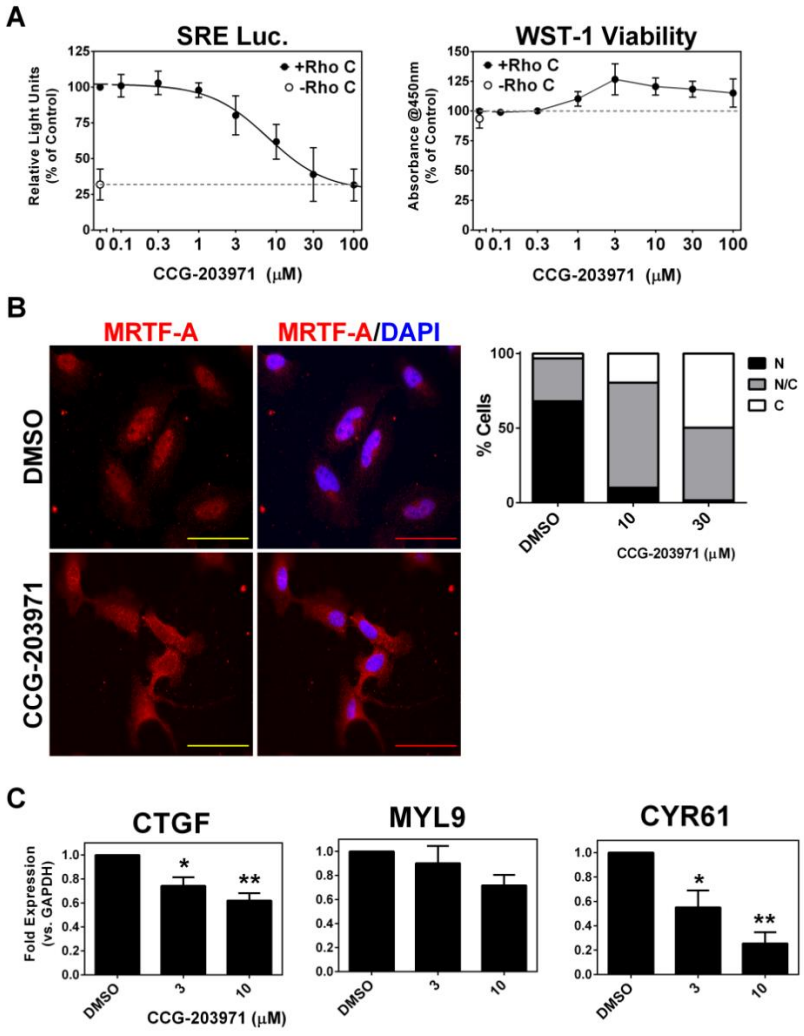

Figure. 4-6. CCG-203971 regulates cellular localization and blocks MRTF target gene expression.

A.) SK-Mel-147 cells were cotransfected with RhoC expression plasmid along with SRE.L reporter plasmid as described in Materials and Methods. Cells were treated with the indicated concentrations of CCG-203971 overnight after transfection before lysis and reading luminescence in the plate reader. Data are graphed as a percentage of the DMSO-negative control. B.) Immunocytochemistry was performed along with the indicated concentrations of CCG-203971 on SK-Mel-147 cells which under starved conditions (0.5% FBS, 24 hours) maintained nuclear MRTF-A. As described previously, individual cells were determined to express predominately nuclear, cytosolic, or even distribution of MRTF-A. Data are the averages of three independent experiments with at least 100 cells counted for each condition. Scale bar shown represents 200μm. C.) CCG-203971 effect on gene expression of CTGF, MYL9, and CYR61. SK-Mel-147 cells were starved in 0.5% media for 24 hours in the presence of the indicated concentration of CCG-203971 or DMSO before isolation of RNA for qPCR analysis. Results are expressed as the mean (±SEM) of triplicate experiments (* $P < 0.05$, ** $P < 0.01$ vs. DMSO control).

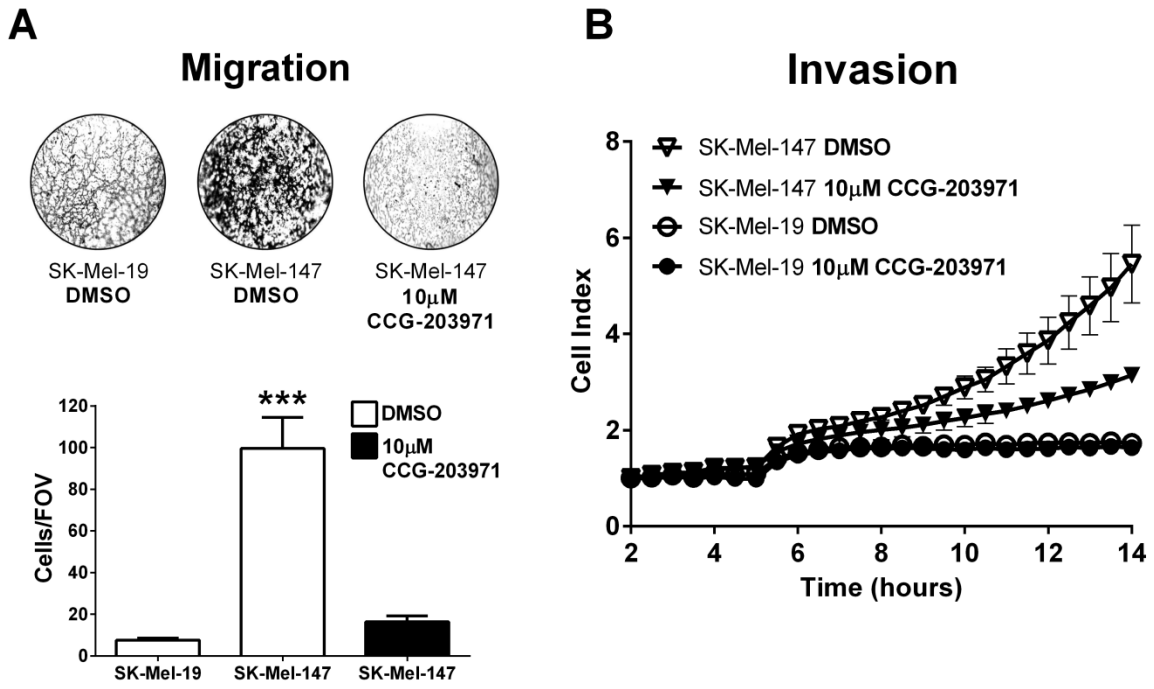

Figure. 4-7. CCG-203971 inhibits cellular migration and invasion.

A.) CCG-203971 blocks melanoma migration. Cells were seeded into the top of a transwell migration chamber with 0.5% on top and bottom to measure basal migration of SK-Mel-19 and SK-Mel-147. CCG-203971 (10μM) blocked SK-Mel-147 migration. Shown on the left are images at 4X magnification using a bright field microscope after six hours of migration. On the right four random fields of view at 20X magnification are quantified for the number of cells which migrated through the membrane. Results are expressed as the mean (±SEM) of triplicate experiments. B.) CCG-203971 inhibits invasion in aggressive melanoma. Real-time Analysis of cellular invasion was analyzed using the xCELLigence label-free system. SK-Mel-147 and SK-Mel-19 were each treated with 10μM CCG-203971 or DMSO control and allowed to invade through Matrigel™ in RPMI containing 0.5% FBS. Shown is a representative figure of the change in cell index (±SEM) from one experiment performed in triplicate. For each condition at least two independent experiments were performed.

CCG-203971 blocks melanoma lung metastasis

There are very few clinically available, effective therapeutics for metastatic melanoma. To determine the potential for MRTF pathway inhibitors as metastasis-targeting therapeutics, we treated mice with CCG-203971 (100 mg/kg BID) or vehicle control for 18 days following tail vein injection of GFP-expressing SK-Mel-147 cells. To compare the *in vivo* effects to the cellular phenotypes we observed in the *in vitro* assays, we also injected mice with GFP-expressing SK-Mel-19 cells. The RhoC overexpressing SK-Mel-147 cells readily formed lung metastases following I.V. injection (Fig. 4-8A). The SK-Mel-147 injected mice not only displayed more metastatic nodules (~3X) but the tumors were much larger (~5X greater area) than the SK-Mel-19 injected mice (Fig. 4-8B). This difference was compounded when considering the total tumor burden (~15X more). The CCG-203971 treated group contained about half as many tumors which were also about 1/4 the size. This resulted in a final tumor burden around 7X lower than in the vehicle treated group (Fig. 4-8B).

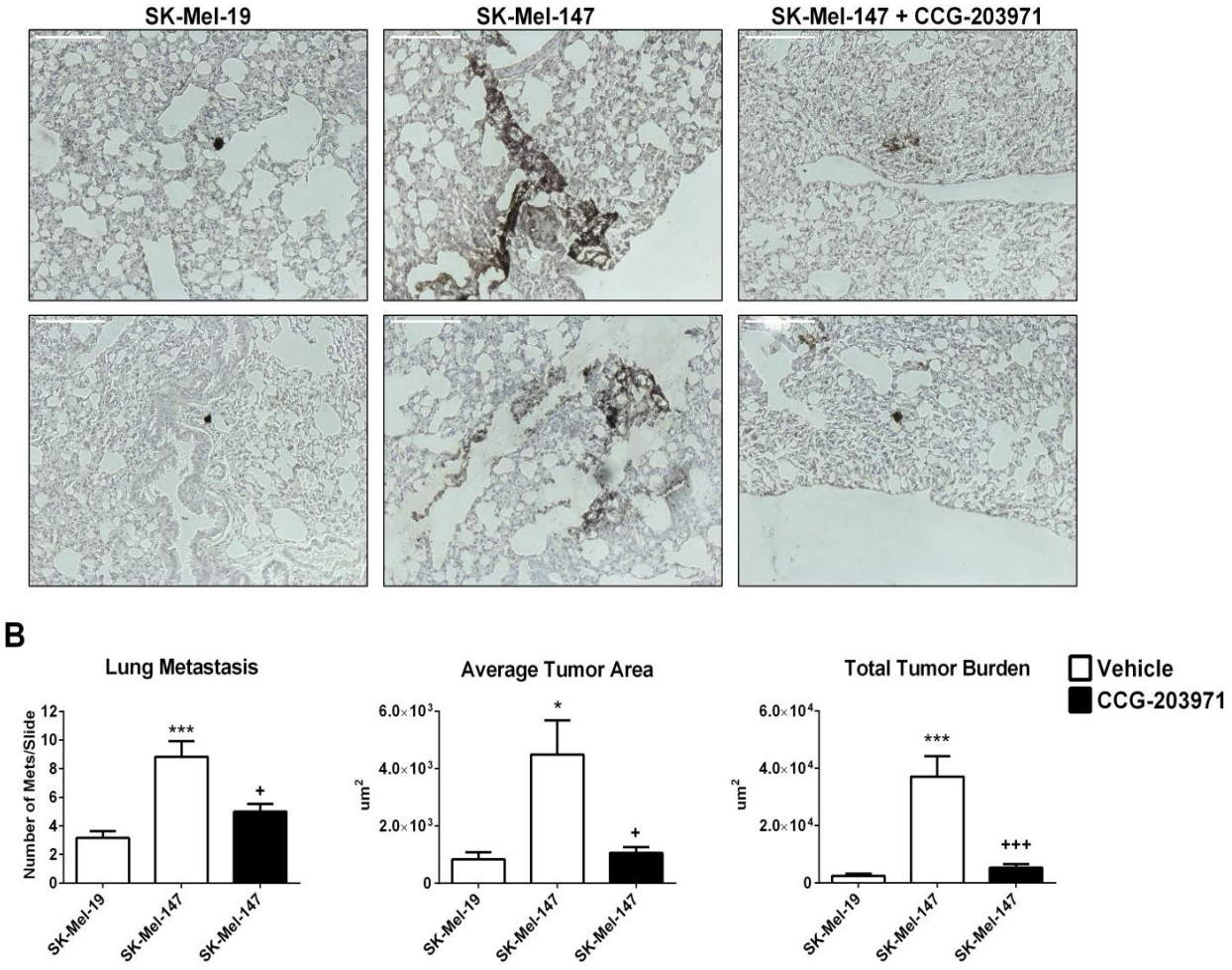

Figure. 4-8. Rho/MRTF pathway effect on experimental lung metastasis

Immunocompromised mice were separated into three groups. One group received tail vein injection of GFP expressing SK-Mel-19 ($2X10^6$ cells). The other two groups were injected with GFP expressing SK-Mel-147 ($2X10^6$ cells). Following tail vein injection the mice began twice daily I.P. injection of 100mg/kg CCG-203971 or 50µL DMSO (vehicle control). After 18 days the mice were euthanized and lungs were collected for histological analysis. Sections from each lung were immunohistologically probed for GFP. Images were taken at 20X magnification, shown are two representative images of metastatic colonies from each group. Scale bar represents 400µm. Each slide was visually scanned for total number of lung colonies, and the average tumor area was determined using image analysis software. The total tumor burden was calculated by adding together the total cross-sectional area of all colonies identified within each mouse. Data is represented as the mean (±SEM) of n=6 (SK-Mel-19+DMSO and SK-Mel-147+DMSO) and n=5 (SK-Mel-147+CCG-203971). (* P< 0.05, *** P< 0.001 vs. SK-Mel-19+DMSO). (+ P< 0.05, +++ P< 0.001 vs. SK-Mel-147+DMSO).

Discussion

Mutations in BRAF and NRAS, leading to constitutive activation of the mitogen-activated protein kinase (MAPK) pathway, are found in nearly ~60-70% of primary human cutaneous melanomas (31,32). However, these driver mutations do not appear to govern the propensity for metastasis; BRAF vs. NRAS mutation status does not predict patient overall survival (33-36). Consequently, it would be important to better understand factors that drive aggressiveness and metastasis of human melanomas. Based on the role of RhoC and MRTF-regulated gene transcription in genetic studies in mouse B16F2 melanoma and breast cancer models (2, 4, 11), we wanted to explore the role of those mechanisms in human metastatic melanoma.

Among 5 human cell lines derived from metastatic cutaneous melanomas, two distinct biological phenotypes were observed. The three melanoma lines (UACC-257, SK-Mel-103, and SK-Mel-147) that behaved aggressively *in vitro* (clonogenicity, migration, invasion) showed strong over-expression of RhoC protein and activation of MRTF-regulated gene expression even in low serum conditions. Furthermore, Sk-Mel-147 which has high RhoC/MRTF activity exhibited numerous lung metastases after tail vein injection in immunocompromised (NOD/SCID) mice while SK-Mel-19, which had low RhoC/MRTF activity, did not. The RhoC/MRTF mechanism is relevant to the biological aggressiveness of the three lines since the phenotypes were reversed by the small molecule inhibitor (14) of MRTF-regulated gene transcription, CCG-203971.

While mutations in Rho proteins are rare, review of cancer genomic information through cBioPortal, (37,38) showed that 31% of cutaneous melanomas had amplification or mutation of RhoA/C, MKL1/2 (gene names for MRTFA/B) or upstream activators (GNA12, GNA13, GNAQ, GNA11 or ARHGEF11). Furthermore, an outlier analysis of melanoma in Oncomine, (39) showed that 5-20% of melanomas across several studies had marked up-regulation of RhoC at the transcriptional level. Mechanisms driving this are not known but could include regulation by the ETS-1 transcription factor (40,41). Loss of E-cadherin in melanoma leads to ETS-1 activation and enhanced RhoC expression (40). RhoC induces c-Jun expression (likely through MRTF/SRF mechanisms) which contributes to cell survival (40). This could partially explain the increased clonogenicity observed in the three RhoC overexpressing melanomas as well as the increased lung colonization by SK-Mel-147.

In light of the multiple genes and pathways that can lead to activation of Rho and MRTF-regulated transcription, inhibition at a downstream step in the pathway would be essential to disrupt the plethora of potential activation mechanisms (42,43). Our compound, CCG-203971 prevents the nuclear accumulation of MRTF potentially by directly binding to MRTF (19) or by modulating intranuclear actin regulation by MICAL2 (20). Previous work has already provided genetic validation of this approach as a means of suppressing metastasis for both melanoma and breast cancer (11). Here we demonstrate the potential for an anti-metastatic small molecule therapeutic that targets this gene transcription mechanism by showing marked suppression of SK-Mel-147 lung metastasis with *in vivo* treatment with CCG-203971. While it has been argued that antimetastatic therapies are not useful or are difficult to test clinically, there is increasing recognition that this approach has value (44). Continued efforts to optimize MRTF-transcription inhibitors like CCG-203971 will be needed. In particular enhancing potency with reduction of

acute toxicity (13,14) is required for chronic treatments that would be required for anti-metastasis therapies. Furthermore, improved bioavailability and pharmacokinetics would facilitate both preclinical and potentially clinical studies.

In addition to melanoma, spontaneous nuclear localization of MRTF-A has been reported in MDA-MB-231 breast cancer cells (11). The MDA-MB-231 cells are often used as a model of aggressive breast cancer cells. Intriguingly they also harbor a Ras mutation (KRAS) (45). Of the three melanomas with enhanced RhoC expression and spontaneous MRTF-A nuclear localization, two had NRAS mutations. Since latrunculin was able to redistribute MRTF into the cytoplasm it appears that there is not a change in the transcription factor itself but in the actin mechanisms (potentially upstream RhoC signaling) that govern its localization.

Rho GTPases and their downstream pathways have also been recognized as drug targets for several years. Virtual screening approaches recently led to the development of small-molecules which inhibit the interaction between RhoA and its GEFs (46,47). These compounds produce *in vitro* efficacy but have not shown effects *in vivo*, potentially due to limited potency and pharmacokinetic issues. Another common approach is to target the Rho kinase (ROCK). ROCK inhibitors block cellular invasion of melanoma cells and reduce tumor volume *in vivo* (48). However their maximal capacity for inhibition of the MRTF transcription mechanism is less than that of CCG-203971 (12), perhaps in part due to parallel pathways and homologous kinases that can activate MRTF/SRF (12,14). So targeting at the MRTF level may be a more effective approach.

Thus Rho-regulated, MRTF-mediated gene transcription signaling appears to play an important role in migration, invasion, and metastasis of human cutaneous melanoma. Expression

levels of RhoC and MRTF target genes may provide useful biomarkers to identify cancers with propensity for metastasis as well as for targeted therapies by this approach. Small molecule inhibitors of this pathway, such as enhanced CCG-203971 analogs, represent an exciting class of pharmacological probes and potential future therapeutics.

References

1. Vega, F. M., and Ridley, A. J. (2008) *FEBS Lett* 582, 2093-2101

2. Hakem, A., Sanchez-Sweatman, O., You-Ten, A., Duncan, G., Wakeham, A., Khokha, R., and Mak, T. W. (2005) *Gene Dev* 19, 1974-1979

3. Jaffe, A. B., and Hall, A. (2005) *Annu Rev Cell Dev Biol* 21, 247-269

4. Clark, E. A., Golub, T. R., Lander, E. S., and Hynes, R. O. (2000) *Nature* 406, 532-535

5. Ridley, A. J., and Hall, A. (1992) *Cell* 70, 389-399

6. Ishizaki, T., Maekawa, M., Fujisawa, K., Okawa, K., Iwamatsu, A., Fujita, A., Watanabe, N., Saito, Y., Kakizuka, A., Morii, N., and Narumiya, S. (1996) *EMBO J* 15, 1885-1893

7. Ishizaki, T., Naito, M., Fujisawa, K., Maekawa, M., Watanabe, N., Saito, Y., and Narumiya, S. (1997) *FEBS Lett* 404, 118-124

8. Palazzo, A. F., Cook, T. A., Alberts, A. S., and Gundersen, G. G. (2001) *Nat Cell Biol* 3, 723-729

9. Miralles, F., Posern, G., Zaromytidou, A. I., and Treisman, R. (2003) *Cell* 113, 329-342

10. Wang, D. Z., Li, S., Hockemeyer, D., Sutherland, L., Wang, Z., Schratt, G., Richardson, J. A., Nordheim, A., and Olson, E. N. (2002) *Proc Natl Acad Sci U S A* 99, 14855-14860

11. Medjkane, S., Perez-Sanchez, C., Gaggioli, C., Sahai, E., and Treisman, R. (2009) *Nat Cell Biol* 11, 257-268

12. Evelyn, C. R., Wade, S. M., Wang, Q., Wu, M., Iniguez-Lluhi, J. A., Merajver, S. D., and Neubig, R. R. (2007) *Mol Cancer Ther* 6, 2249-2260

13. Evelyn, C. R., Bell, J. L., Ryu, J. G., Wade, S. M., Kocab, A., Harzdorf, N. L., Hollis Showalter, H. D., Neubig, R. R., and Larsen, S. D. (2010) *Bioorg Med Chem Lett* 20, 665-672

14. Bell, J. L., Haak, A. J., Wade, S. M., Kirchhoff, P. D., Neubig, R. R., and Larsen, S. D. (2013) *Bioorganic & Medicinal Chemistry Letters* 23, 3826-3832

15. Sandbo, N., Kregel, S., Taurin, S., Bhorade, S., and Dulin, N. O. (2009) *Am J Resp Cell Mol* 41, 332-338

16. Sandbo, N., Lau, A., Kach, J., Ngam, C., Yau, D., and Dulin, N. O. (2011) *Am J Physiol-Lung C* 301, L656-L666

17. Johnson, L. A., Rodansky, E. S., Haak, A. J., Larsen, S. D., Neubig, R. R., and Higgins, P. D. R. (2014) *Inflammatory Bowel Diseases* 20, 154-165

18. Haak, A. J., Tsou, P. S., Amin, M. A., Ruth, J. H., Campbell, P., Fox, D. A., Khanna, D., Larsen, S. D., and Neubig, R. R. (2014) *J Pharmacol Exp Ther*

19. Hayashi, K., Watanabe, B., Nakagawa, Y., Minami, S., and Morita, T. (2014) *Plos One* 9

20. Lundquist, M. R., Storaska, A. J., Liu, T. C., Larsen, S. D., Evans, T., Neubig, R. R., and Jaffrey, S. R. (2014) *Cell* 156, 563-576

21. Jin, W., Goldfine, A. B., Boes, T., Henry, R. R., Ciaraldi, T. P., Kim, E. Y., Emecan, M., Fitzpatrick, C., Sen, A., Shah, A., Mun, E., Vokes, V., Schroeder, J., Tatro, E., Jimenez-Chillaron, J., and Patti, M. E. (2011) *J Clin Invest* 121, 918-929

22. Bell, J. L., Haak, A. J., Wade, S. M., Sun, Y., Neubig, R. R., and Larsen, S. D. (2013) *Beilstein J Org Chem* 9, 966-973

23. Suzuki, N., Nakamura, S., Mano, H., and Kozasa, T. (2003) *P Natl Acad Sci USA* 100, 733-738

24. Ni, W., Geddes, T. J., Priestley, J. R., Szasz, T., Kuhn, D. M., and Watts, S. W. (2008) *Br J Pharmacol* 154, 663-674

25. Karlsson, R., Pedersen, E. D., Wang, Z., and Brakebusch, C. (2009) *Bba-Rev Cancer* 1796, 91-98

26. Wakatsuki, T., Schwab, B., Thompson, N. C., and Elson, E. L. (2001) *J Cell Sci* 114, 1025-1036

27. Vartiainen, M. K., Guettler, S., Larijani, B., and Treisman, R. (2007) *Science* 316, 1749-1752

28. Sun, Z. J., Wang, Y., Cai, Z., Chen, P. P., Tong, X. J., and Xie, D. (2008) *Br J Cancer* 99, 1656-1667

29. Muehlich, S., Cicha, I., Garlichs, C. D., Krueger, B., Posern, G., and Goppelt-Struebe, M. (2007) *Am J Physiol Cell Physiol* 292, C1732-1738

30. Jin, W. Z., Goldfine, A. B., Boes, T., Henry, R. R., Ciaraldi, T. P., Kim, E. Y., Emecan, M., Fitzpatrick, C., Sen, A., Shah, A., Mun, E., Vokes, M., Schroeder, J., Tatro, E., Jimenez-Chillaron, J., and Patti, M. E. (2011) *J Clin Invest* 121, 918-929

31. Colombino, M., Capone, M., Lissia, A., Cossu, A., Rubino, C., De Giorgi, V., Massi, D., Fonsatti, E., Staibano, S., Nappi, O., Pagani, E., Casula, M., Manca, A., Sini, M., Franco, R., Botti, G., Caraco, C., Mozzillo, N., Ascierto, P. A., and Palmieri, G. (2012) *J Clin Oncol* 30, 2522-2529

32. Ekedahl, H., Cirenajwis, H., Harbst, K., Carneiro, A., Nielsen, K., Olsson, H., Lundgren, L., Ingvar, C., and Jonsson, G. (2013) *Brit J Dermatol* 169, 1049-1055

33. Long, G. V., Menzies, A. M., Nagrial, A. M., Haydu, L. E., Hamilton, A. L., Mann, G. J., Hughes, T. M., Thompson, J. F., Scolyer, R. A., and Kefford, R. F. (2011) *J Clin Oncol* 29, 1239-1246

34. Ellerhorst, J. A., Greene, V. R., Ekmekcioglu, S., Warneke, C. L., Johnson, M. M., and Cooke, C. P. (2011) *Clin Cancer Res* 17, 1641-1641

35. Menzies, A. M., Haydu, L. E., Visintin, L., Carlino, M. S., Howle, J. R., Thompson, J. F., Kefford, R. F., Scolyer, R. A., and Long, G. V. (2012) *Clin Cancer Res* 18, 3242-3249

36. Houben, R., Becker, J. C., Kappel, A., Terheyden, P., Brocker, E. B., Goetz, R., and Rapp, U. R. (2004) *J Carcinog* 3, 6

37. Cerami, E., Gao, J., Dogrusoz, U., Gross, B. E., Sumer, S. O., Aksoy, B. A., Jacobsen, A., Byrne, C. J., Heuer, M. L., Larsson, E., Antipin, Y., Reva, B., Goldberg, A. P., Sander, C., and Schultz, N. (2012) *Cancer Discov* 2, 401-404

38. Gao, J. J., Aksoy, B. A., Dogrusoz, U., Dresdner, G., Gross, B., Sumer, S. O., Sun, Y. C., Jacobsen, A., Sinha, R., Larsson, E., Cerami, E., Sander, C., and Schultz, N. (2013) *Sci Signal* 6

39. Rhodes, D. R., Yu, J., Shanker, K., Deshpande, N., Varambally, R., Ghosh, D., Barrette, T., Pandey, A., and Chinnaiyan, A. M. (2004) *Neoplasia* 6, 1-6

40. Spangler, B., Kappelmann, M., Schittek, B., Meierjohann, S., Vardimon, L., Bosserhoff, A. K., and Kuphal, S. (2012) *Int J Cancer* 130, 2801-2811

41. Bellovin, D. I., Simpson, K. J., Danilov, T., Maynard, E., Rimm, D. L., Oettgen, P., and Mercurio, A. M. (2006) *Oncogene* 25, 6959-6967

42. Juneja, J., and Casey, P. J. (2009) *Br J Pharmacol* 158, 32-40

43. Barrio-Real, L., and Kazanietz, M. G. (2012) *Sci Signal* 5, pe43

44. Marino, N., Woditschka, S., Reed, L. T., Nakayama, J., Mayer, M., Wetzel, M., and Steeg, P. S. (2013) *Am J Pathol* 183, 1084-1095

45. Koffa, M., Malamoumitsi, V., Agnantis, N. J., and Spandidos, D. A. (1994) *Int J Oncol* 4, 573-576

46. Shang, X., Marchioni, F., Sipes, N., Evelyn, C. R., Jerabek-Willemsen, M., Duhr, S., Seibel, W., Wortman, M., and Zheng, Y. (2012) *Chem Biol* 19, 699-710

47. Shang, X., Marchioni, F., Evelyn, C. R., Sipes, N., Zhou, X., Seibel, W., Wortman, M., and Zheng, Y. (2013) *P Natl Acad Sci USA* 110, 3155-3160

48. Routhier, A., Astuccio, M., Lahey, D., Monfredo, N., Johnson, A., Callahan, W., Partington, A., Fellows, K., Ouellette, L., Zhidro, S., Goodrow, C., Smith, A., Sullivan, K., Simone, P., Le, L., Vezuli, B., Zohni, M., West, E., Gleason, D., and Bryan, B. (2010) *Oncol Rep* 23, 861-867

CHAPTER V

CONCLUSIONS AND FUTURE DIRECTIONS

Scleroderma and metastatic melanoma remain debilitating and deadly diseases (1,2). Previous evidence suggests the Rho small GTPase modulation of gene expression through the MRTF/SRF transcription pathway plays a significant role in the initiation, stabilization, and progression of these diseases (3-7). The goal of my research was to understand the signaling mechanisms where by Rho activation leads to MRTF/SRF regulated transcription in these diseases, and to determine efficacy of small-molecule inhibitors of this pathway in pre-clinical models of scleroderma and melanoma. An overall goal of my work is to promote the development of targeted therapeutics, which blocks the Rho/MRTF pathway to treat these aggressive diseases.

In Chapter II, I focused on understanding how TGFβ ligand stimulation leads to activation of Rho/MRTF regulated transcription. One of the major challenges in developing targeted therapeutics for scleroderma and other fibrotic diseases is the multitude of receptor signaling mechanisms which appear to play a role in these diseases (8,9). This is supported by multiple clinical trials for IPF and scleroderma which have been terminated early due to lack of efficacy (8). Based on our results in Chapter II, TGFβ and Rho GTPase participate in a variety of cross-talk mechanisms. To further complicate resolving these pathways, it has recently been shown that TGFβ stimulates nuclear accumulation of MRTF where it forms a transcriptional

complex with SMAD3 (10). This adds a new level of complexity to our model of the mechanism whereby TGFβ activates MRTF. MRTF nuclear localization in the context of TGFβ is dependent on Rho activation as we hypothosize and is supported in Chapter II, (10), however, our experiments did not investigate the nuclear complex partners (SRF or SMAD3) which interacted with MRTF after TGFβ or LPA ligand stimulation. Co-immunoprecipitation experiments with MRTF, SRF, and SMAD3 following early and late TGFβ treatment could provide some interesting insight around these questions.

As shown in Chapter II, the ROCK inhibitor clearly supported categorizing specific profibrotic genes as being SMAD or MRTF targets, however, in this same experiment, treatment with CCG-203971 in Chapter III, non-selectively blocked stimulated expression of all profibrotic genes. One major difference in these compounds is where in the pathway they inhibit MRTF-regulated transcription. ROCK stimulates actin stress fibers through phosphorylation of multiple downstream targets leading to F-actin formation and stabilization (11). Inhibition of ROCK leads to decreased stress fibers and MRTF nuclear accumulation and activity. Interestingly we have previously found ROCK inhibitors to only have partial efficacy for the inhibition of MRTF, depending on where the pathway is stimulated (12),(13). CCG-203971 and related compounds however target downstream of F-actin formations and have been shown to bind and inhibit a nuclear actin modifier protein MICAL2 (14) and also MRTF itself (15). Through either mechanism, compounds from this series have been shown to block nuclear accumulation of MRTF. Although there are many potential reasons for these differences observed between these compounds, the step in the pathway where they inhibit could play a significant role. There is obvious cross-talk between TGFβ/SMAD and Rho/MRTF (10), by blocking upstream of MRTF using a ROCK inhibitor could allow for expression of SMAD target genes independent of

MRTF, however by blocking very downstream in the pathway using CCG-203971 SMAD target genes may have become MRTF dependent leading to the inhibition we observed in this assay. Further understanding the molecular target of CCG-203971 and related compounds could support, or oppose this hypothesis.

We also found that TGFβ target genes EDN1 (Endothelin) and CTGF are able to stimulate Rho/MRTF when added exogenously to fibroblasts, and inhibition of these mediators with an endothelin receptor type A antagonist and a CTGF neutralizing antibody is able to block TGFβ induced activation of actin stress fibers and activity of MRTF. This outlines a mechanism where TGFβ stimulates rapid expression of endothelin and CTGF which then autocrine signal back onto the cells to stimulate Rho GTPase and expression of pro-fibrotic genes through MRTF. This model mostly focuses on the signaling pathways after TGFβ, however, equally interesting was the role of LPA in the subtle activation (~20%) of MRTF/SRF activity observed in the absense of serum or TGFβ. To add to this, we found that TGFβ treatment caused a rapid reduction in the expression of the gene encoding autotaxin, the enzyme which synthesizes LPA. This leads to a hypothesis where TGFβ potentially shifts MRTF/SRF activity from being driven by LPA to one driven by CTGF and ET-1. This could further be supported by determining the level of released LPA into the medium of TGFβ stimulated cells. Another intesting experiment would be analyzing the profibrotic, MRTF and SMAD target genes following LPA, CTGF, and ET-1 treatment to determine if there is specificity between these ligands or if they just combine for additive activation.

In Chapter III, we shifted focus onto the small-molecule MRTF pathway inhibitors developed in our lab, in pre-clinical models of scleroderma. From a mechanistic perspective, the nonspecific inhibtion of profibrotic genes with CCG-203971 observed in Chapter III were not as

clean as what we obrserved with the ROCK inhibitor, they did suggest the potential for exciting efficacy against a fibrotic disease like scleroderma. Consistant with the idea that the Rho/MRTF pathway is activated in scleroderma patient fibroblasts vs. normal healthy donor fibroblasts, CTGF, ACTA2, and COL1A2 were all elevated in the scleroderma patient derived fibroblasts. In these patient samples CCG-203971 was able to block gene expression at low micromolar concentrations. We also tested the efficacy of pirfenidone to block expression of these genes in the scleroderma patient samples. At the time of this study prifenidone was approved for the use of IPF in Asia, Europe, and Canada but still awaiting approval in the United States, however in October, 2014 pirfenidone (trade name Esbriet®) was approved for use against IPF by the US FDA. Similar to CCG-203971, pirfenidone does not have a known molecular target. It has been shown to redeuce production of inflammatory cytokines TNF-α and TGFβ (16,17). Pirfenidone may also block TGFβ induced transcription as it was found to inhibit nuclear localization of SMADs (18). Importantly it should be noted that pirfenidone is used at extremely high doses and concentrations, similar to the 300μM *in vitro* concentrations used in our experiments. We also performed a simple cellular proliferation experiment comparing these cells. We found scleroderma patient samples displayed slightly elevated growth rates compared to the normal donor samples. Most interestingly high cencentation treatment (30μM) with CCG-203971 selectively blocked the enhanced proliferation of the scleroderma cells while not affecting the normal samples. Transformed myofibroblasts are resistant to apoptosis (19,20) and designing therapies which can resensitize myofibroblasts to apoptosis is a current focus of novel therapeutics (21). The assay we performed here measured activity of cellular reductases and nondescriptively determines relative viable cells. Based off of the results here, CCG-203971 is reducing the total number of viable cells by selectively targeting the activated myofibroblast

cells for apoptosis, or by converting them back to more quiescent fibroblasts. Further analysis of the mechanism whereby CCG-203971 reduces the total number of viable cells is a crucial next step. Apoptosis assays measuring caspase activation or cell cycle analysis of scleroderma derived fibroblasts or TGFβ stimulates normal donor fibroblasts in the presenence of CCG-203971 could begin to answer these questions. In our next experiments we focused on α-SMA as a marker of a transformed myofibroblast. CCG-203971 was able to block α-SMA expression in TGFβ stimulated normal donor fibroblasts as well as, and most significantly, constituative α-SMA expression observed in unstimulated sclerderma patient derived fibroblasts. This was significant because blocking TGFβ stimulated transformation of healthy donor fibroblasts can be viewed as a "prevention" study, where as reversing scleroderma transformation, or enriching for a population of non-transformed cells can be viewed as a "treatment" study. This is especially signifiant because our in vivo study was a prevention protocol. There are multiple in vivo models of scleroderma, but the two main revolve around bleomycin induced injury or the genetic Tsk/+ (tight skin) mouse model (22). Although both models have their flaws, bleomycin depends heavily on inflammation, while Tsk/+ is independent of inflammation, both models to offer insight into potential efficacy of novel therapeutics. In our bleomycin prevention, study mice were treated with 100mg/kg CCG-203971 BID, I.P. for two weeks. At the end of the study skin samples were obtained for trichrome staining and hydroxyproline analysis. The CCG-203971 treated group not only had significantly thinner dermal layers than the control, bleomycin group, their skin collagen content was also reduced. Efficacy of CCG-20371 against in vitro and in vivo models of scleroderma provided evidence that these compounds have potential for treating providing proof of concept to treat diseases where the Rho/MRTF pathway is implicated. These

results also push towards developing more potent, metabolically stable analogs of this compounds series, which will be discussed at the end of this chapter.

In Chapter IV, we investigated the role of Rho GTPases and MRTF transcription in metastatic melanoma, and again look at efficacy of CCG-203971 in this disease. In the past decade, evidence has highlighted the similarities and consistencies between profibrotic diseases and cancer. Broadly, both diseases are marked with, and driven by abnormal genetic and epigenetic changes, irregular response to regulatory mechanisms, and activation of stimulatory signaling pathways (23). Genetically, IPF patient derived fibroblasts are scattered with mutations in multiple cancer-associated genes including p21Waf1/Cip1/Sdi1 and p53, with the latter observed with heterogeneous point mutations in 80% of IPF samples tested (24,25). Many cell-signaling pathways, which are activated in cancer, are also stimulated in fibrotic diseases. TGFβ signaling, which has been discussed throughout these studies, also plays important roles in tissue invasion in lung cancer, melanoma, and breast cancer (26). Significant to our work Rho/MRTF signaling also plays major importance to cancer metastasis. Despite recently approved targeted therapeutics, melanoma remains a very deadly disease (27). One of the major problems in melanoma cellular biology is understanding the mechanisms and markers which will drive an aggressive, metastatic disease. Although exclusive mutations in BRAF and NRAS combine to be present in over 75% of tested human melanomas they do not predict a clinical prognosis (28). We found, within out panel of five melanomas, the invasive and metastatic cells displayed constitutive nuclear localization of MRTF-A. A very translational next experiment would be to investigate the localization of MRTF-A in a panel of melanoma patient samples and correlate prognosis, potential for metastasis, response to therapeutics, and survival.

In our experiments with melanoma we also found the cells which overexpressed RhoC and displayed nuclear localization of MRTF-A also expressed high levels of CYR61 and CTGF (the genes which encode proteins CCN1 and CCN2). These matricellular proteins can signal through multiple mechanisms to regulate cell adhesion, migration, proliferation, differentiation, and apoptosis (29). Although plenty of evidence exists for the role of CTGF in cancer progression and tissue fibrosis, CYR61 has mostly been discussed in cancer metastasis for its ability to stimulate angiogenesis (30,31). There is evidence however, for a role of CYR61 in fibrosis, during the process of wound healing CYR61 regulates matrix deposition and survival of myofibroblasts (32). Based on what were learned from the melanoma experiments about CYR61 being regulated by MRTF and CCG-203971, it would be important to identify its role in our fibrosis experiments

To move into an *in vivo* model of melanoma metastasis, we injected melanoma cells into the tail-vein of immunocompromised mice. CCG-203971 reduced the total number of lung colonies at the end of this experiment, as well as the cross sectional area of the colonies. This combined for a very dramatic reduction in the calculated total tumor burden. Within a tumor mass, malignant cancer cells are minority. The bulk of a tumor is made up of nonmalignant cells, mesenchymal cells, immune cells, vasculature, and extracellular matrix components (33-36). One of the major contributors to tumor biology are localized fibroblasts which can stimulate collagen production, stabilizing the tumor microenvironment, or also involved in invasion and metastasis where transformed fibroblasts are found at the leading end of invading melanomas (37). Evidence suggests malignant cancer cells release TGFβ onto the local fibroblasts, activating them into myofibroblasts which can then assist in survival, invasion, migration, proliferation, and ECM synthesis (38). In Chapter II and Chapter III we showed that TGFβ feeds into the Rho

GTPase/MRTF transcriptional pathway, and that CCG-203971 is able to block these mechanisms in immortalized mouse fibroblasts, and human dermal fibroblasts. We also however showed in Chapter IV that CCG-203971 blocks melanoma cellular migration and invasion, independent of fibroblast involvement. In our *in vivo* metastasis study CCG-203971 was given systemically, so lung fibroblasts and the injected melanoma cells were treated. Based on these experiments, and prior evidence, this suggests that the efficacy of CCG-203971 in our metastasis study could be a result of the compound effecting the cancer cells themselves, and also the compound blocking the involvement of local fibroblasts in aiding lung colonization. One very clear experiment to begin answering these questions would be to perform tri-chrome staining on the lung sections from our mouse metastasis study and determine if CCG-203971 reduced the amount of fibrotic tissue within, and surrounding the melanoma metastatic colonies.

Some of the major drawbacks of our current lead compound, CCG-203971 are the potency (5-10μM), the solubility, and the rapid metabolism/clearance of this compound. Using *in silico* prediction models of P450 metabolism (SMARTCyp) multiple metabolic sites on CCG-203971 were predicted (Fig. 5-2A). Based off these results, multiple new analogs of CCG-203971 were synthesized with the goal of increasing compound half-life. One of these analogs, CCG-222740, a 5, 5-difluoropiperidine substitution into CCG-203971 actually ended up being dramatically more potent than CCG-203971 (~600nM vs. ~8uM) in the MRTF dependent SRE-Luciferase assay and is currently being tested in in vivo disease models and metabolic stability studies.

In these studies, we have identified mechanisms for MRTF activation in both fibroblasts and metastatic melanoma. TGFβ stimulated ET-1 and CTGF activate F-actin stress fibers and MRTF in fibroblasts, and RhoC overexpression leads to constitutively nuclear, active MRTF in

metastatic melanoma. We have also shown efficacy for our current lead small molecule inhibitor of this pathway, CCG-203971, in *in vitro* and *in vivo* models of tissue fibrosis and metastatic melanoma. Interestingly, throughout the timeline of my thesis work both of these diseases have had exciting therapeutic developments; Vemurafenib for the treatment of BRAF mutant metastatic melanoma, and very recently, pirfenidone for the treatment of IPF. Although both of these therapies leave much work to be done, they do represent a very dynamic time to study these diseases. Combined this work promotes further understanding pathological signaling mechanisms which stimulate MRTF/SRF gene transcription, and additional work into the development of novel therapeutics which target this pathway.

References

1. Barsotti, S., Bellando Randone, S., Guiducci, S., and Della Rossa, A. (2014) *Clin Exp Rheumatol* **32 Suppl 86**, 194-205

2. Rastrelli, M., Tropea, S., Rossi, C. R., and Alaibac, M. (2014) *In Vivo* **28**, 1005-1011

3. Small, E. M., Thatcher, J. E., Sutherland, L. B., Kinoshita, H., Gerard, R. D., Richardson, J. A., Dimaio, J. M., Sadek, H., Kuwahara, K., and Olson, E. N. (2010) *Circ Res* **107**, 294-304

4. Luchsinger, L. L., Patenaude, C. A., Smith, B. D., and Layne, M. D. (2011) *J Biol Chem* **286**, 44116-44125

5. Sakai, N., Chun, J., Duffield, J. S., Wada, T., Luster, A. D., and Tager, A. M. (2013) *Faseb J* **27**, 1830-1846

6. Medjkane, S., Perez-Sanchez, C., Gaggioli, C., Sahai, E., and Treisman, R. (2009) *Nat Cell Biol* **11**, 257-268

7. Leitner, L., Shaposhnikov, D., Mengel, A., Descot, A., Julien, S., Hoffmann, R., and Posern, G. (2011) *J Cell Sci* **124**, 4318-4331

8. Tsou, P. S., Haak, A. J., Khanna, D., and Neubig, R. R. (2014) *Am J Physiol Cell Physiol* **307**, C2-13

9. Lafyatis, R. (2006) *Endocr Metab Immune Disord Drug Targets* **6**, 395-400

10. Morita, T., Mayanagi, T., and Sobue, K. (2007) *J Cell Biol* **179**, 1027-1042

11. Amano, M., Nakayama, M., and Kaibuchi, K. (2010) *Cytoskeleton (Hoboken)* **67**, 545-554

12. Evelyn, C. R., Wade, S. M., Wang, Q., Wu, M., Iniguez-Lluhi, J. A., Merajver, S. D., and Neubig, R. R. (2007) *Mol Cancer Ther* **6**, 2249-2260

13. Bell, J. L., Haak, A. J., Wade, S. M., Kirchhoff, P. D., Neubig, R. R., and Larsen, S. D. (2013) *Bioorg Med Chem Lett* **23**, 3826-3832

14. Lundquist, M. R., Storaska, A. J., Liu, T. C., Larsen, S. D., Evans, T., Neubig, R. R., and Jaffrey, S. R. (2014) *Cell* **156**, 563-576

15. Hayashi, K., Watanabe, B., Nakagawa, Y., Minami, S., and Morita, T. (2014) *Plos One* **9**, e89016

16. Grattendick, K. J., Nakashima, J. M., Feng, L., Giri, S. N., and Margolin, S. B. (2008) *Int Immunopharmacol* **8**, 679-687

17. Iyer, S. N., Gurujeyalakshmi, G., and Giri, S. N. (1999) *J Pharmacol Exp Ther* **291**, 367-373

18. Choi, K., Lee, K., Ryu, S. W., Im, M., Kook, K. H., and Choi, C. (2012) *Mol Vis* **18**, 1010-1020

19. Wynn, T. A., and Ramalingam, T. R. (2012) *Nat Med* **18**, 1028-1040

20. Horowitz, J. C., Ajayi, I. O., Kulasekaran, P., Rogers, D. S., White, J. B., Townsend, S. K., White, E. S., Nho, R. S., Higgins, P. D., Huang, S. K., and Sisson, T. H. (2012) *Int J Biochem Cell Biol* **44**, 158-169

21. Hinz, B., and Gabbiani, G. (2010) *F1000 Biol Rep* **2**, 78

22. Artlett, C. M. (2010) *Curr Opin Rheumatol* **22**, 677-682

23. Vancheri, C. (2013) *Eur Respir Rev* **22**, 265-272

24. Kuwano, K., Kunitake, R., Kawasaki, M., Nomoto, Y., Hagimoto, N., Nakanishi, Y., and Hara, N. (1996) *Am J Respir Crit Care Med* **154**, 477-483

25. Hojo, S., Fujita, J., Yamadori, I., Kamei, T., Yoshinouchi, T., Ohtsuki, Y., Okada, H., Bandoh, S., Yamaji, Y., Takahara, J., Fukui, T., and Kinoshita, M. (1998) *Eur Respir J* **12**, 1404-1408

26. Massague, J. (2008) *Cell* **134**, 215-230

27. Mrazek, A. A., and Chao, C. (2014) *Surg Clin North Am* **94**, 989-1002, vii-viii

28. Ekedahl, H., Cirenajwis, H., Harbst, K., Carneiro, A., Nielsen, K., Olsson, H., Lundgren, L., Ingvar, C., and Jonsson, G. (2013) *Br J Dermatol* **169**, 1049-1055

29. Jun, J. I., and Lau, L. F. (2011) *Nat Rev Drug Discov* **10**, 945-963

30. Babic, A. M., Kireeva, M. L., Kolesnikova, T. V., and Lau, L. F. (1998) *Proc Natl Acad Sci U S A* **95**, 6355-6360

31. Fataccioli, V., Abergel, V., Wingertsmann, L., Neuville, P., Spitz, E., Adnot, S., Calenda, V., and Teiger, E. (2002) *Hum Gene Ther* **13**, 1461-1470

32. Wynn, T. A. (2008) *J Pathol* **214**, 199-210

33. de Visser, K. E., Eichten, A., and Coussens, L. M. (2006) *Nat Rev Cancer* **6**, 24-37

34. Mantovani, A., Allavena, P., Sica, A., and Balkwill, F. (2008) *Nature* **454**, 436-444

35. Hughes, C. C. (2008) *Curr Opin Hematol* **15**, 204-209

36. Ronnov-Jessen, L., Petersen, O. W., and Bissell, M. J. (1996) *Physiol Rev* **76**, 69-125

37. Li, G., Satyamoorthy, K., Meier, F., Berking, C., Bogenrieder, T., and Herlyn, M. (2003) *Oncogene* **22**, 3162-3171

38. Bremnes, R. M., Donnem, T., Al-Saad, S., Al-Shibli, K., Andersen, S., Sirera, R., Camps, C., Marinez, I., and Busund, L. T. (2011) *J Thorac Oncol* **6**, 209-217